ktu kaunas university of technology 1922

17th International Conference on Global Research and Education

(Inter-Academia 2018)

September 24 – 27, 2018
Kaunas, Lithuania

Programme and abstracts

Kaunas, 2018

Conference Chairman

Giedrius Laukaitis, KTU, Faculty of Mathematics and Natural Sciences, Department of Physics, Kaunas

17th International Conference on Global Research and Education, Inter-Academia is organized by

Kaunas University of Technology and Department of Physics (KTU)

International Advisory Conference Committee:

Annamária R. Várkonyi-Kóczy (Óbuda University, Hungary)
Arturs Medvids (Riga Technical University, Latvia)
Gheorghe Popa (Prof-Emeritus, Alexandru Ioan Cuza University, Romania)
Evgenia Benova (Sofia University, Bulgaria)
Dumitru Luca (Prof-Emeritus, Alexandru Ioan Cuza University, Romania)
Hidenori Mimura (Shizuoka University, Japan)
Hiroshi Mizuta (University of Southampton, England)
Kenji Murakami (Shizuoka University, Japan)
Leonid Poperenko (Taras Shevchenko National University of Kyiv, Ukraine)
Lucel Sirghi (Alexandru Ioan Cuza University, Romania)
Masaaki Nagatsu (Shizuoka University, Japan)
Masashi Kando (Prof. Emeritus, Shizuoka University, Japan)
Michiharu Tabe (Prof. Emeritus, Shizuoka University, Japan)
Kazuhiko Hara (Shizuoka University, Japan)
Nobuyuki Araki (Prof. Emeritus-Shizuoka University, Japan)
Noriko Matsuda (Shizuoka University, Japan)
Nicoleta Dumitrascu (Alexandru Ioan Cuza University, Romania)
Ryszard Jablonski (Warsaw University of Technology, Poland)
Jan Maciej Kościelny (Warsaw University of Technology, Poland)
Małgorzata Kujawińska (Warsaw University of Technology, Poland)
Sergiusz Łuczak (Warsaw University of Technology, Poland)
Roman Szewczyk (Warsaw University of Technology, Poland)
Adam Woźniak (Warsaw University of Technology, Poland)
Sergei Khakhomov (Gomel State University, Belarus)
Stefan Matejcik (Comenius University, Slovakia)
Valdis Kokars (Riga Technical University, Latvia)
Giedrius Laukaitis (Kaunas University of Technology, Lithuania)
Maxim M Sychov (Saint Petersburg State Institute of Technology, Russia)
Volodymyr Gnatyuk (National Academy of Sciences of Ukraine)
Yoshimasa Kawata (Shizuoka University, Japan)
Jun Kondoh (Shizuoka University, Japan)

Organizing committee:

Giedrius Laukaitis (KTU, Faculty of Mathematics and Natural Sciences, Department of Physics)
Kristina Bočkutė (KTU, Faculty of Mathematics and Natural Sciences, Department of Physics)
Vytautas Kavaliūnas (KTU, Faculty of Mathematics and Natural Sciences, Department of Physics)
Mantas Sriubas (KTU, Faculty of Mathematics and Natural Sciences, Department of Physics)
Živilė Rutkūnienė (KTU, Faculty of Mathematics and Natural Sciences, Department of Physics)

17th International Conference on Global Research and Education (Inter-Academia 2018)

Hotel EUROPA ROYALE Kaunas, Miško str. 11, Kaunas

Conference Programme

Monday, September 24, 2018

8:00 – 9:00	Registration	
9:00 – 9:30	Opening Ceremony	
	Session 1 (Hall 1) **Session Chairs:** **Kazuhiko Hara**, Shizuoka University **Giedrius Laukaitis**, Kaunas University of Technology	
9:30 – 10:00	**MO-1 (Invited) Recent Progress of Micro Field Emitters** Hidenori Mimura, Shizuoka University, Japan	
10:00 – 10:30	**MO-2 (Invited) Ultrasonic measurement and non-destructive techniques for extreme conditions and non-conventional applications** Renaldas Raišutis, Kaunas University of Technology, Lithuania	
10:30 – 10:50	*Coffee break*	
	Session 2 (Hall 1) **Session Chairs:** **Hidenori Mimura**, Shizuoka University **Volodymyr Gnatyuk**, National Academy of Sciences of Ukraine	**Session 2 (Hall 2)** **Session Chairs:** **Maxim Sychov**, Russian Academy of Sciences **Nugzar Gomidze**, Batumi Shota Rustaveli State University
10:50 – 11:10	**MO-3 Chemical vapor deposition of GaN films using gallium vapor as a gallium source on a c-plane sapphire substrate** Kazuhiko Hara, Shizuoka University, Japan	**MO-8 Evaluation of deterioration of engine oil using shear horizontal surface acoustic wave sensor based on acoustoelectric interaction** Jun Kondoh, Shizuoka University, Japan
11:10 – 11:30	**MO-4 Comparable Analyze of TiO_2 Properties on Ti Formed by Laser Radiation, Sol-Gel, Electrochemical Anodization and Magnetron Sputtering** Arturs Medvids, Riga Technical University, Latvia	**MO-9 Multiple-valued computing by photon-coupled, photoswitchable proteins** Balázs Rakos, Budapest University of Technology and Economics, Hungary
11:30 – 11:50	**MO-5 Photocatalytic activity of unbiased and biased TiO_2-WO_3 bilayers** Marius Dobromir, Alexandru Ioan Cuza University of Iasi, Romania	**MO-10 A Hybrid Machine Learning Approach for Daily Prediction of Solar Radiation** Amir Mosavi, Obuda University, Hungary
11:50 – 12:10	**MO-6 XPS study of the In/CdTe interface modified by nanosecond laser irradiation** Kateryna Zelenska, Shizuoka University, Japan	**MO-11 A Nanoantenna - MIM Diode - Lens Device Concept for Infrared Energy Harvesting** Muhammad Fayyaz Kashif, Budapest University of Technology and Economics, Hungary
12:10 – 12:30	**MO-7 Monolayer PMMA template with close packed structure on large scale** Sridevi Meenachisundaram, Shizuoka University, Japan	**MO-12 Vehicle detection using aerial images under disaster situations** Ayane Makiuchi, Shizuoka University, Japan
12:30 – 12:35	**Conference photo**	
12:35 – 13:30	*Lunch*	

	Session 3 (Hall 1) Session Chairs: **Kenji Murakami**, Shizuoka University **Yasunori Okano**, Osaka University	Session 3 (Hall 2) Session Chairs: **Arturs Medvids**, Riga Technical University **Sakai Katsuhiko**, Shizuoka University
13:30 – 13:50	**MO-13 Remote Detection of Holes Generated by Impact Ionization** Yukinori Ono, Shizuoka University, Japan	**MO-17 Electromotive force of n-type Si wafer connected to piezoelectric device with its vibration under temperature gradient** Hiroya Ikeda, Shizuoka University, Japan
13:50 – 14:10	**MO-14 Normal and axial mode of operation of human sweat duct in sub-terahertz frequency region** Saroj Tripathi, Shizuoka University, Japan	**MO-18 Gamma-ray spectroscopic performance of large-area CdTe-based Schottky diodes** Volodymyr Gnatyuk, V.E. Lashkaryov Institute of Semiconductor Physics of the National Academy of Sciences of Ukraine, Ukraine
14:10 – 14:30	**MO-15 A Study of Single-Electron Tunnelling in 1D Distributed Arrays of Donor Quantum Dots** Daniel Moraru, Shizuoka University, Japan	**MO-19 Correlation Between Optical, Morphological and Compositional Properties of GeSn Epitaxial Layers Irradiated by Nd:YAG Laser Radiation** Pavels Onufrijevs, Riga Technical University, Latvia
14:30 – 14:50	**MO-16 Low-Voltage Multifunctional Graphene Nanoelectromechanical Devices** Manoharan Muruganthan, Japan Advanced Institute of Science and Technology, Japan	**MO-20 Synthetic light interference image analysis algorithm in wedge interferometer** Jakub Mruk, Warsaw University of Technology, Poland
14:50 – 15:00	*Bus*	
15:00 – 17:30	*Excursion to SANTAKA Integrated Science, Studies and Business Centre (Valley), K. Barsausko str. 59, Kaunas, Lithuania*	
18:00 – 20:00	*Dinner*	

Tuesday, September 25, 2018

9:00 – 9:30	Registration	
	Session 4 (Hall 1) **Session Chairs:** **Ryszard Jablonski**, Warsaw University of Technology **Jun Kondoh**, Shizuoka University	
9:30 – 10:00	**TU-1 (Invited) Multimodal Unobtrusive Devices for Chronic Disease Monitoring** Vaidotas Marozas, Kaunas University of Technology, Lithuania	
10:00 – 10:30	**TU-2 (Invited) Properties of polymer based gels for radiation sensors** Diana Adlienė, Kaunas University of Technology, Lithuania	
10:30 – 10:50	*Coffee break*	
	Session 5 (Hall 1) Session Chairs: **Daniel Moraru**, Shizuoka University **Yukinori Ono**, Shizuoka University	Session 5 (Hall 2) Session Chairs: **Hiroya Ikeda**, Shizuoka University **Balázs Rakos**, Budapest University of Technology and Economics
10:50 – 11:10	**TU-3 Effect of damage introduction and He existence on D retention by high flux D plasma exposure** Yasuhisa Oya, Shizuoka University, Japan	**TU-8 Numerical Simulation of Shaking Optimization in a Suspension Culture of iPS Cells** Yasunori Okano, Osaka University, Japan
11:10 – 11:30	**TU-4 Mechanical properties of cellular structures with Shwartz Primitive topology** Maxim M. Sychov, Russian Academy of Sciences, Russia	**TU-9 Re-examination of the concept of "Primary Energy" and problems on the introduction system of renewable energies in Japan** Satoshi Matsuda, Shizuoka University, Japan

11:30 – 11:50	**TU-5 Deuterium removal efficiency in tungsten as a function of hydrogen ion beam fluence and temperature** Mingzhong Zhao, Shizuoka University, Japan	**TU-10 To the Problems of Detecting Signals Passing Through a Random Phase Screen** Nugzar Kh. Gomidze, Batumi Shota Rustaveli State University, Georgia
11:50 – 12:10	**TU-6 The numerical study of co-existence effect of thermal and solutal Marangoni convections in a liquid bridge** Chihao Jin, Osaka University, Japan	**TU-11 Full dynamics and optimization of a controllable minimally invasive robot for soft tissue surgery and servicing the artificial organs** Grzegorz Ilewicz, University of Bielsko - Biała, Poland
12:10 – 12:30	**TU-7 Recovery of the workpiece material in ECM of sintered carbide** Sicong Wang, Shizuoka University, Japan	**TU-12 Feasibility study of a neutron detector made of boron-doped diamond using Monte Carlo simulation** Taku Miyake, Shizuoka University, Japan
12:30 – 13:30	*Lunch*	
	Session 6 (Hall 1) **Session Chairs:** **Saroj Tripathi**, Shizuoka University **Lucel Sirghi**, Alexandru Ioan Cuza University	**Session 6 (Hall 2)** **Session Chairs:** **Satoshi Matsuda**, Shizuoka University **Grzegorz Ilewicz**, University of Bielsko- Biała
13:30 – 13:50	**TU-13 A Statistical Study on the Origin of Dopant Clusters in Highly-Doped Si Nanoscale *pn* Tunnel Diodes** Daniel Moraru, Shizuoka University, Japan	**TU-16 An Application of The Nash Equilibrium to an Experimental Setting: The Real Meaning of the Sacrifice Move in Board Games** Valerie A. Wilkinson, Shizuoka University, Japan
13:50 – 14:10	**TU-14 Photoconversion efficiency in solar cells based on heterostructures ITO-Si with Au nanoparticles** Anastasiia Mykytiuk, Taras Shevchenko National University of Kyiv, Ukraine	**TU-17 Assessment of renewable energy systems in northern Philippines using geospatial toolkit** Carlos Pascual, Mariano Marcos State University, Philippines
14:10 – 14:30	**TU-15 Photocatalytic activity of ZnO-loaded titania nanotube arrays: structural, morphological and compositional effects** Marius Dobromir, Alexandru Ioan Cuza University of Iasi, Romania	**TU-18 A Parallel Fuzzy Filter Network for Pattern Recognition** Balázs Tusor, Obuda University, Hungary
14:30 – 15:00	*Bus*	
15:00 – 19:00	*Excursion Kaunas at a glance*	
19:00 – 21:00	*Dinner*	

Wednesday, September 26, 2018

9:00 – 9:30	Registration
	Session 7 (Hall 1) **Session Chairs:** **Yasuhisa Oya**, Shizuoka University **Mashiko Takashi**, Shizuoka University
9:30 – 10:00	**WE-1 (Invited) Research on Functional Materials for Energy Conversion Devices: Photovoltaics and Mechanoluminescence** Kenji Murakami, Shizuoka University, Japan
10:00 – 10:30	**WE-2 (Invited) Modeling of properties of single chamber fuel cell components** Arvaidas Galdikas, Kaunas University of Technology, Lithuania
10:30 – 10:50	*Coffee break*

Session 8 (Hall 1) **Session Chairs:** **Adam Wozniak**, Warsaw University of Technology **Valerie A. Wilkinson**, Shizuoka University		
10:50 – 12:30	**Special Poster Session for iA Young Researchers (iAY) – 5 min oral communication**	**WE-3 Characterization of thermoelectric generation in Si-wire thermopile structure** Khotimatul Fauziah, Shizuoka University, Japan
		WE-4 Ellipsometric diagnostic of anisotropy properties of surface layer of silicon after laser treatment Iryna Yurgelevych, Taras Shevchenko National University of Kyiv, Ukraine
		WE-5 Single molecule force spectroscopy on collagen deposited on hydroxylated silicon substrate Alexandra Besleaga, Alexandru Ioan Cuza University of Iasi, Romania
		WE-6 Ellipsometry of nanostructured Si wafers after femtosecond laser processing Dmytro Gnatyuk, Taras Shevchenko National University of Kyiv, Ukraine
		WE-7 Low-k sol-gel coating for surface planarization at integrated circuit production Vasili Vaskevich, F. Scorina Gomel State University, Belarus
		WE-8 Instability of CdTe radiation detector characterized by carrier transport properties Hisaya Nakagawa, Shizuoka University, Japan
		WE-9 Investigation of X-ray attenuation properties in water solutions of sodium tungstate dihydrate and silicotungstic acid Laurynas Gilys, Kaunas University of Technology, Lithuania
		WE-10 Formation of Alumina and Alumina-Zirconia coatings employing Plasma Spraying Jakob S. Mathew, Kaunas University of Technology, Lithuania
		WE-11 Activation of water by surface DBD micro plasma in atmospheric air Alexandra Besleaga, Alexandru Ioan Cuza University of Iasi, Romania
		WE-12 Modification of optical properties of amorphous metallic mirrors due to impact of deuterium plasma Iryna Yurgelevych, Taras Shevchenko National University of Kyiv, Ukraine
		WE-13 Lead ferrite doped chrome thin films synthesis by reactive magnetron sputtering and investigation Benas Beklešovas, Kaunas University of Technology, Lithuania
		WE-14 Influence of deposition parameters on the structure of TiO_2 thin films prepared by reactive magnetron sputtering technique Vytautas Kavaliūnas, Kaunas University of Technology, Lithuania
		WE-15 Formation and investigation of doped cerium oxide thin films formed using e-beam deposition technique Nursultan Kainbayev, Kaunas University of Technology, Lithuania
		WE-16 Investigation of deposition parameters influence on the properties of doped diamond-like carbon films Vilius Dovydaitis, Kaunas University of Technology, Lithuania
		WE-17 Aerial image registration for grasping road conditions Kyoji Ogasawara, Shizuoka University, Japan
		WE-18 Up-Conversion Nanosized Phosphors Based Fluoride For Photodynamic Therapy Of Malignant Tumors Anastasiia Dorokhina, Saint-Petersburg State Institute of Technology, Russia
12:30 – 13:30	*Lunch*	

Session 9 (Hotel lobby) **Session Chairs:** **Živilė Rutkūnienė**, Kaunas University of Technology **Kristina Bočkutė**, Kaunas University of Technology	
13:30 – 15:30	Poster session
Session 10 (Hall 1)	
15:30 – 16:00	Conference closing

16:00 – 17:00	iA Committee Meeting

19:00 – 22:00	*Gala Dinner*

Thursday, September 27, 2018	
9:00 – 20:00	*Conference Excursion*

Poster Session Programme

A poster board will be provided in the poster presentation area. The board's segments will measure approximately 1.0 m high x 0.7 m wide and will be set up vertically. On your designated board, you will find all the materials needed for mounting your poster. Poster numbers will be in the upper corner of each poster board and this number corresponds with the number assigned to each poster in the conference program.

Presenters are encouraged to mount their poster in the morning and remove them at the end of the day. Authors must remain with their posters for the duration of their scheduled session, as indicated in the conference program. All posters must remain up until the session ends and then must be removed within one hour.

Wednesday, September 26, 2018	
	Poster Session, 13:30 – 15:30 **Session Chairs:** **Živilė Rutkūnienė**, Kaunas University of Technology **Kristina Bočkutė**, Kaunas University of Technology
P1	**Characterization of thermoelectric generation in Si-wire thermopile structure** Khotimatul Fauziah, Shizuoka University, Japan
P2	**Ellipsometric diagnostic of anisotropy properties of surface layer of silicon after laser treatment** Iryna Yurgelevych, Taras Shevchenko National University of Kyiv, Ukraine
P3	**Single molecule force spectroscopy on collagen deposited on hydroxylated silicon substrate** Alexandra Besleaga, Alexandru Ioan Cuza University of Iasi, Romania
P4	**Ellipsometry of nanostructured Si wafers after femtosecond laser processing** Dmytro Gnatyuk, Taras Shevchenko National University of Kyiv, Ukraine
P5	**Low-k sol-gel coating for surface planarization at integrated circuit production** Vasili Vaskevich, F. Scorina Gomel State University, Belarus
P6	**Instability of CdTe radiation detector characterized by carrier transport properties** Hisaya Nakagawa, Shizuoka University, Japan
P7	**Investigation of X-ray attenuation properties in water solutions of sodium tungstate dihydrate and silicotungstic acid** Laurynas Gilys, Kaunas University of Technology, Lithuania
P8	**Formation of Alumina and Alumina-Zirconia coatings employing Plasma Spraying** Jakob S. Mathew, Kaunas University of Technology, Lithuania
P9	**Activation of water by surface DBD micro plasma in atmospheric air** Alexandra Besleaga, Alexandru Ioan Cuza University of Iasi, Romania
P10	**Modification of optical properties of amorphous metallic mirrors due to impact of deuterium plasma** Iryna Yurgelevych, Taras Shevchenko National University of Kyiv, Ukraine
P11	**Lead ferrite doped chrome thin films synthesis by reactive magnetron sputtering and investigation** Benas Beklešovas, Kaunas University of Technology, Lithuania
P12	**Influence of deposition parameters on the structure of TiO_2 thin films prepared by reactive magnetron sputtering technique** Vytautas Kavaliūnas, Kaunas University of Technology, Lithuania
P13	**Formation and investigation of doped cerium oxide thin films formed using e-beam deposition technique** Nursultan Kainbayev, Kaunas University of Technology, Lithuania
P14	**Investigation of deposition parameters influence on the properties of doped diamond-like carbon films** Vilius Dovydaitis, Kaunas University of Technology, Lithuania
P15	**Aerial image registration for grasping road conditions** Kyoji Ogasawara, Shizuoka University, Japan

P16	**Up-Conversion Nanosized Phosphors Based Fluoride For Photodynamic Therapy Of Malignant Tumors** Anastasiia Dorokhina, Saint-Petersburg State Institute of Technology, Russia
P17	**Structure and mechanical properties of gradient metal-carbon films** Alexander V. Rogachev, Francisk Skorina Gomel State University, Belarus
P18	**Synthesis of $BiFeO_3$-Powders and Films by Sol-Gel Process** Alina Semchenko, Francisk Skorina Gomel State University, Belarus
P19	**Android Botnet Detection Using Soft Computing Methods** Amir Mosavi, Obuda University, Hungary
P20	**A Hybrid Neuro-Fuzzy Algorithm for Estimation of Reference Evapotranspiration** Amir Mosavi, Obuda University, Hungary
P21	**On the Role of Shaped Noise Visibility for Post-Compression Image Enhancement** Damon M. Chandler, Shizuoka University, Japan
P22	**TiO_2 Formation on Ti Substrate by Plasma Immersion Ion Implantation: Morphology, Photocatalytic and Optical Properties** Edvins Letko, Riga Technical University, Latvia
P23	**A Comparison of an Execution Efficiency of the Use of a Skip List and Simple List in a .NET Application** Igor Košťál, University of Economics in Bratislava, Slovakia
P24	**Design and creation of metal-polymer absorbing metamaterials using the vacuum-plasma technologies** Igor Semchenko, Francisk Skorina Gomel State University, Belarus
P25	**Investigation of X-ray attenuation properties in 3D printing materials used for development of head and neck phantom** Jurgita Laurikaitienė, Kaunas University of Technology, Kaunas
P26	**Application of artificial neural networks to the analysis of alcohol addiction** Krzysztof Urbaniak, Politechnika Warszawska, Poland
P27	**Two-photon fluorescent microscopy for 3D dopant imaging in wide bandgap semiconductors** Ryszard Jablonski, Warsaw University of Technology, Poland
P28	**Re-examination of the concept of "Primary Energy" and problems on the introduction system of renewable energies in Japan** Satoshi Matsuda, Shizuoka University, Japan
P29	**Ion Mobility Spectrometry detection of corona discharge decomposition of phthalates** Štefan Matejčik, Comenius University, Slovakia
P30	**Thermal convection of a phase-changing fluid** Takashi Mashiko, Shizuoka University, Japan
P31	**Automatic identification of the kidney shape in CT images** Tomasz Les, Warsaw University of Technology, Poland
P32	**The Flip-Side of Academic English (AE)** Valerie A. Wilkinson, Shizuoka University, Japan
P33	**ZnO/Me Sol-Gel Film for Solar Cells and Photodetectors** Vitali Sidsky, Francisk Skorina Gomel State University, Belarus

Recent Progress of Micro Field Emitters

H. Mimura*
Research Institute of Electronics, Shizuoka University
3-5-1 Johoku Naka-ku Hamamatsu 432-8011
*mimura.hidenori@shizuoka.ac.jp

Vacuum devices are dominant in high power and high frequency. Though thermal cathodes are widely used in vacuum devices, if the thermal cathodes are replaced with field emitters (FEs), more superior devices are expected. The conventional FEs with an electron extraction gate, however, have two big problems such as current fluctuation and beam divergence. The current fluctuation is suppressed when the FE is operated in ultra-high vacuum or connected in series to a constant current source such as a field effect transistor. [1, 2] For the beam divergence, though the double–gated FE with both an electron extraction gate and a focus gate was proposed, the electron emission current was significantly reduced when the electron beam was focused. Recently, we have developed the volcano-structured double-gated field emitter (VDG-FE). [3, 4] The VDG-FE can focus electron beam without decrease of the emission current. By using the VDG-FE, we are developing the compact image pickup tube which is applicable a radiation tolerant image sensor. [5] In the presentation, I introduce recent progress of micro-field emitters.

[1] G. Hashiguchi, H. Mimura and H. Fujita, Jpn. J. Appl. Phys. 35 (1996) L84.
[2] H. Shimawaki, K. Tajima, H. Mimura and K. Yokoo, IEEE Trans. Electron Devices 49 (2002) 1665.
[3] Y. Neo, H. Mimura et al., App. Phys. Express. 1 (2008) 053001.
[4] Y. Neo, H. Mimura et al., J. Vac. Sci. Technol. B 27 (2009) 701.
[5] Y. Honda, H. Mimura et al., J. Vac. Sci. Technol. B 34 (2016) 05220.

Notes:

Ultrasonic measurement and non-destructive techniques for extreme conditions and non-conventional applications

R.Raišutis*, R.Kažys, L.Mažeika, E.Žukauskas, R.Šliteris
Ultrasound Institute, Kaunas University of Technology, Lithuania
*renaldas.raisutis@ktu.lt

The main area of interest covers development of new advanced ultrasonic measurement, imaging and non-destructive techniques for extreme conditions (high temperatures, strong radioactive radiation, high pressure, aerospace and chemical activity) and non-conventional applications of NDT, monitoring, diagnostic and quality control. These techniques are oriented to solve the complicated questions related to the construction safety, environment safety and human health. The results presented cover application of non-invasive ultrasonic measurement and imaging technologies in process control and nuclear industry. Also, application of ultrasonic non-destructive and diagnostics technologies for inspection of modern composite materials in aeronautics sector. The illustrative examples of objects under investigation and obtained results are presented.

Notes:

Chemical vapor deposition of GaN films using gallium vapor as a gallium source on a c-plane sapphire substrate

K. Hara[1,2,*], Y. Masuda[3], W. Kunieda[3], H. Kominami[3]
[1]*Graduate School of Science and Technology, Shizuoka University, 3-5-1 Johoku, Naka-ku, Hamamatsu, 432-8011, Japan*
[2]*Research Institute of Electronics, Shizuoka University, 3-5-1 Johoku, Naka-ku, Hamamatsu, 432-8011 Japan*
[3]*Graduate School of Integrated Science and Technology, Shizuoka University, 3-5-1 Johoku, Nakaku, Hamamatsu, 432-8561 Japan*
[*]*hara.kazuhiko@shizuoka.ac.jp*

GaN-based materials have been recognized as key materials in the present semiconductor industry due to their excellent optical and electronic properties. Such an amazing development has relied on the improvement of thin film growth techniques for these materials like metalorganic chemical vapor phase epitaxy. On the other hand, in recent years, in order to further improve the device performance, the importance to use GaN substrates for thin film growth has increased. Currently, for the fabrication of GaN substrates, high-speed crystal growth by chemical vapor deposition (CVD) using GaCl and NH3 gases as gallium and nitrogen sources is mainly utilized [1]. However, it is difficult to grow continuously for a long term due to the formation of NH_4Cl as a solid byproduct. On the contrary, we have paid an attention to CVD using Ga vapor as a Ga source, in which a GaN film is formed by the reaction, $Ga + NH_3 \rightarrow GaN + 3/2\ H_2$. The merit of this method is that any solid byproduct is not generated during the reaction, which lead us to expect to reduce the maintenance of equipment used for growth. In this paper, aiming to develop a new technique for the fabrication of GaN substrates, we carried out the growth of GaN thin films on c-plane sapphire substrate by CVD using Ga vapor and NH3 gas.

The growth was carried out under atmospheric pressure by using an apparatus consisting of a horizontal reactor tube made of alumina ceramics and a tubular furnace. Ga metal, which was placed in another alumina tube assembled in the reactor, was heated at 1300 °C. Thus, generated Ga vapor was carried by an N_2 flow of 1.0 slm to a c-plane sapphire substrate, and then reacted with NH_3 gas introduced separately in the reactor. After thermal cleaning in an H_2 flow at 1050 °C, a buffer layer was first grown at a substrate temperature of about 600 °C for 10 min, which was followed by film growth at 1100 °C for 120 min. NH_3 supply rates were 1.5 and 0.5 slm for the low- and high-temperature growths, respectively. We also investigated the effect of pre-growth surface treatments in different atmospheres on the growth without a low-temperature buffer layer.

First, it was found that the thin film with a flat surface was epitaxially grown on the low-temperature buffer layer whereas the growth directly on the substrate yields columnar or polycrystalline GaN. The photoluminescence (PL) property was also improved for the sample grown on the buffer layer. These results indicate that the effectiveness of the low-temperature buffer layer holds for the source combination of this study. However, the growth process employing the buffer layer is complicated. In order to explore the alternative method to solve this issue, we grew GaN films following the heat treatments for the substrate surface in a flow of NH_3 or Ga vapor. In the former case, the grown sample consisted of randomly-oriented columnar grains. In contrast, the lateral growth was enhanced by employing the later process, resulting in the film growth with an improved PL property. This comparison suggests the possibility to grow high quality GaN films directly on sapphire substrates.

Keywords: gallium nitride, chemical vapor deposition, gallium vapor, x-ray diffraction, photoluminescence.

[1] T. Yoshida, Y. Oshima, T. Tsuchiya, and T. Mishima, Phys. Stat. Sol. (c), 8, 2110 (2011).

Notes:

Comparable Analyze of TiO_2 Properties on Ti Formed by Laser Radiation, Sol-Gel, Electrochemical Anodization and Magnetron Sputtering

A. Medvids[1*], P. Onufrijevs[1], E. Letko[1], S. Gaidukovs[2], A. Knoks[1], R. Eglitis[3], I. Skadins[4], S. Varnagiris[5], M. Milčius[5] A. Zunda[6], J. Padgurskas[6], H. Mimura[7]

[1]*Institute of Technical Physics, Faculty of Materials Science and Applied Chemistry, Riga Technical University, P. Valdena 3/7, Riga LV-1048, Latvia*

[2]*Institute of Polymer Materials, Faculty of Materials Science and Applied Chemistry, Riga Technical University, P. Valdena 3/7, Riga LV-1048, Latvia*

[3]*Institute of Silicate Materials, Faculty of Materials Science and Applied Chemistry, Riga Technical University, P. Valdena 3/7, Riga LV-1048, Latvia*

[4]*Department of Biology and Microbiology, Riga Stradins University, 16 Dzirciema Street, Rīga, LV 1007, Latvia*

[5]*Center for Hydrogen Energy Technologies, Lithuanian Energy Institute, 3 Breslaujos St., Kaunas, Lithuania*

[6]*Aleksandras Stulginskis University, Institute of Power and Transport Machinery Engineering, Lithuania*

[7]*Research Institute of Electronics, Shizuoka University, 3-5-1, Johoku, Naka-ku, Hamamatsu 432- 8011 Japan*

[*]*medvids@latnet.lv*

It is well known that TiO_2 is one of prominent materials, which can be applied as a catalyst in hydrogen fuel production, biodegradation, environmental cleaning, etc. Every application requires precise controllability of synthesis and polymorph phase. TiO_2 can be obtained by various methods, however, each of them has some limitations in specific applications. The aim of the study is the comparison of chemical, mechanical and catalytic properties of TiO_2 layers formed by different methods for applications in medicine, chemistry and physics. The result of the investigation is the knowledge about best parameters of these TiO_2 coatings on Ti, including recommendations for applications in each of the fields. In the investigation of TiO_2 layers on Ti substrate formed by laser irradiation, sol-gel, electrochemical anodization and magnetron sputtering methods were studied. The topics covered by the study are following: 1. The developed new technologies and TiO_2 coatings, obtained by these technologies within the study, are products with increased added value; 2. The TiO_2 layer with optimized and stable catalytic properties is very important for energy sector, since it has an important application in hydrogen energetics; 3. TiO_2 is well known catalyst, used in waste water purification, therefore, optimization of its catalytic properties is very important for nature and environment protection; 4. TiO_2 coatings on Ti are used in medicine because of their antibacterial properties. Testing and optimization of these properties are thus related to the public health.

As a result of comparable analyze of TiO_2 layer formed on Ti substrate, properties were found: the mechanical properties (adhesion and brittleness) of the structure are the best for laser processing; antibacterial properties is better for sol-gel methods, which was determined by colonization of Ps. Aeruginosa and S. Epidermidis bacteria; photocatalytic study revealed that the TiO_2 layers formed by magnetron sputtering method has shown that decomposition velocity is the best using methylene blue solution.

Notes:

Photocatalytic activity of unbiased and biased TiO_2-WO_3 bilayers

M. Dobromir[1,*], C.T. Teodorescu-Soare[2], R. P. Apetrei[2], V. Pohoaţă[2], D. Luca[2]
[1]*Department of Research, Faculty of Physics, Alexandru Ioan Cuza University of Iasi, 11 Carol I Blvd., 700506, Iasi, Romania;*
[2]*Faculty of Physics, Alexandru Ioan Cuza University of Iasi, 11 Carol I Blvd., 700506, Iasi, Romania*
[*]*marius.dobromir@uaic.ro*

The technology of photocatalytic materials is one of the effective ways for solving the issues of energy crisis and environmental pollution [1]. TiO_2-based semiconductor oxide materials have been intensely investigated during the latest decades, due their high oxidation capacity, low cost, nontoxicity and chemical stability. When used in photocatalytic materials field, the relatively high recombination rate of the electron-hole pairs in the bulk leads to a rather low quantum yield and poor durability performance [2]. To improve the photocatalytic activity of TiO_2 based materials, heterojunction structures of titania with WO_3 films/nanoparticles were proposed [3] as a variant to improving the photo-generated charge carrier's lifetime, and thus the catalyst performance. This can be achieved by coupling a wider band gap semiconductor (TiO_2, with Eg = 3.2 eV) with a lower band gap material (WO_3 with Eg = 2.8 eV), a net charge transfer is ensured inside the formed junction, which reduces the recombination probability of the electron-hole pairs.
In our contribution, we introduce new results of our recent investigations related to the synergic effect of the presence of heterojunctions with the presence of an additional external electric field, for charge separation. TiO_2/WO_3 (labeled as ATW) and WO_3/TiO_2 (AWT) heterostructures were deposited by RF magnetron sputtering on Al_2O_3 substrates on top of an Au interdigital electrode layer. For reference, TiO_2 (AT) and WO_3 (AW) single layers were deposited on the same type of substrate and characterized in a similar manner. The thickness of the investigated layers was 30 nm (Au) and 250 nm (TiO_2 and WO_3).
The photocatalytic activity of the samples was evaluated using spectrophotometric measurements to monitor the degradation rate of a methylene blue (MB) solution (0.1M) in distilled water, under UV light irradiation, at room temperature. The experiments were carried out in the absence and in the presence of the external electrical field (using a value of 0.5 V for the inter-electrode bias). For the unbiased case, the MB degradation rate constants of the AWT and ATW structure were 0.83×10^{-2} min^{-1} and 0.78×10^{-2} min^{-1}, respectively. An increase in the rate constant of MB degradation by a factor of (2.1 and 1.3) was noticed for the sample biased at - 0.5 V and by a factor of (3.7 and 5.8) for the sample biased at 0.5 V, with respect to the unbiased samples. A further comparison with the references samples (AT and AW) and a more detailed interpretation of the current results will be given in the full-length manuscript.

Keywords: TiO_2/WO_3, WO_3/TiO_2, RF magnetron sputtering, photocatalytic activity.

[1] X.B. Chen, S.H. Shen, L.J. Guo, S.S. Mao, Chem. Rev. 110 (2010), 6503–6570.
[2] W. Zhu, X. Liu, H.Q. Liu, D.L. Tong, J.Y. Yang, J.Y. Peng, J. Am. Chem. Soc. 132 (2010), 12619–12626.
[3] Z. T. Kwon, K. Y. Song, W. I. Lee, G. J. Choi, Z. R. Do, J. Catal. 191 (2000), 192-199.

Notes:

XPS study of the In/CdTe interface modified by nanosecond laser irradiation

K.S. Zelenska[1,2,*], V.A. Gnatyuk[1,3], H. Nakajima[4], W. Pecharapa[5]

[1]*Research Institute of Electronics, Shizuoka University, 3-5-1 Johoku, Naka-ku, Hamamatsu 432-8011, Japan*

[2]*Faculty of Physics, Taras Shevchenko National University of Kyiv, Prospekt Akademika Glushkova 4, Kyiv 03127, Ukraine Kyiv, Ukraine*

[3]*V.E. Lashkaryov Institute of Semiconductor Physics of the National Academy of Sciences of Ukraine, Prospekt Nauky 41, Kyiv 03028, Ukraine*

[4]*Synchrotron Light Research Institute, 111 University Avenue, Muang District, Nakhon Ratchasima 30000, Thailand*

[5]*College of Nanotechnology, King Mongkut's Institute of Technology Ladkrabang, 1 Thanon Chalong Krung, Ladkrabang, Bangkok 10520, Thailand*

[*]*czelenska@gmail.com*

High-resistivity CdTe semiconductor grown with the traveling heater method (THM) is known as industrial material for high detection efficiency and good energy resolution room-temperature X/γ-ray detectors. Detector-grade Cl-compensated (111) oriented *p*-like CdTe single crystals, manufactured by Acrorad Co. Ltd., are quite uniform with a decreased number of native point and extended defects, low amount of accidental impurities and excellent electrical characteristics. Such crystals have been generally used for fabrication of diode-type detectors implemented as structures either with a *p-n* junction or Schottky barrier. In this case, processing of the CdTe surface plays a key role in the detector performance. Mechanical and chemical polishing, etching with Br-methanol solutions, inorganic acids, ion bombardment or laser radiation are usually involved in semiconductor surface treatments before the formation of surface barrier structures.

Despite the recent advances in fabrication of such CdTe-based diodes with a *p-n* junction developed using chemical etching and nanosecond laser irradiation, many issues still remain unclear or unsolved, particularly with regard to dopant profile in the thin CdTe region near the contact metal-semiconductor interface, concentration and distribution of impurities, component composition of the laser modified layer, etc.

The CdTe (111) crystals with a pre-deposited In dopant (contact) film (300-400 nm) subjected to irradiation with nanosecond laser pulses were studied by X-ray photoelectron spectroscopy (XPS). It was supposed that laser irradiation of the film resulted in In dopant incorporation due to generation of stress and shock waves, barodiffusion and thus, formation of a heavily doped CdTe layer near the metal-semiconductor interface. The XPS spectra of In/CdTe diodes were obtained under irradiation from the In-coated side with a high-spatial resolution X-ray beam of 650 eV using a synchrotron excitation source at the Synchrotron Light Research Institute (Thailand). The In film was repeatedly etched 12 times with an Ar-ion plasma using a gun operating at 3.0 keV and producing a specimen current of ~ 3 μA. The XPS wide-scan spectra study and precise measurements of the selected peaks for the etched samples were carried out after every hour of the sputtering procedure.

The core level, Auger and valence electron peaks of O, In, Cd and Te were used for the detailed analysis of the component composition of the area adjacent to the In/CdTe interface. The distribution of In and Cd atoms with the thickness was estimated. Cd atoms were revealed in the In film superficial layer which was non-contiguous to the CdTe surface. The obtained results can be explained by the process of fast mutual diffusion of Cd atoms from the semiconductor into the adjoined metal film and also by penetration of In impurity atoms into the CdTe crystal. The phenomena of abnormally fast laser-stimulated mass transfer and barodiffusion under stress and shock waves action were discussed as the possible mechanisms of laser-induced doping and migration of In and Cd atoms in the In/CdTe structure.

This work was supported by the NATO Science for Peace and Security Programme (Project SENERA, SfP-984705) and Academic Melting Pot Program at KMITL (Thailand).

Keywords: CdTe crystals, Laser irradiation, Doping, Diffusion, XPS spectra.

Notes:

Monolayer PMMA template with close packed structure on large scale

S. Meenachisundaram[1,6], T. Kawaguchi[2], P.Gangopadhyay[3], N. Sakamoto[2,4], K. Shinozaki[5], M. Chellamuthu[6], S. Ponnusamy[6], H. Suzuki[1,2,4], and N. Wakiya[1,2,4,*]

[1]*Graduate School of Science and Technology, Shizuoka University, 3–5–1 Johoku, Naka-ku, Hamamatsu 432–8561, Japan*

[2]*Department of Electronics and Materials Science, Shizuoka University, 3–5–1 Johoku, Naka-ku, Hamamatsu 432–8561, Japan*

[3]*Indira Gandhi Centre for Atomic Research, Kalpakkam 603 102, Tamil Nadu, India*

[4]*Research Institute of Electronics, Shizuoka University, 3–5–1 Johoku, Naka-ku, Hamamatsu 432–8561, Japan*

[5]*School of Materials and Chemical Technology, Tokyo Institute of Technology, 2–22–1 O–okayama, Meguro–ku, Tokyo 152–8550, Japan*

[6]*Department of Physics and Nanotechnology, SRM University, Kattankulathur 603203, Tamil Nadu, India*

[*]*wakiya.naoki@shizuoka.ac.jp*

Surface patterned micro and nanostructures have found wide range of recent advances in nanoscale research. Highly ordered Two-dimensional (2D) nanostructured arrays have recently received considerable attention because of their wide variety of potential applications related to catalysis[1], gas sensors[2], and biosensors[3]. In this study, we successfully prepared the large-area (>1 mm^2) close-packed shell structure thin film of polymethylmethacrylate (PMMA) monolayer template on Si substrate (Figure 1). In this approach, a close-packed hexagonal array of polymethyl methacrylate spheres (3.5 μm diameter) dispersed at toluene-water interface, followed by dip coating of spheres on a substrate can be used as a template for replicating the novel structures. This technique allows easy control of close-packed structures by varying the 1.5 ml., 2 ml., 2.5 ml. volume of toluene in the monolayer colloidal crystals (MCCs) solution respectively (Figure 1(a)). This route supports the control of PMMA sizes by the original PMMA microsphere sizes. This monolayer template consists of a controlled array of close-packed spherical templates which is controlled by using the 2 ml. volume of toluene at the interface. This 2D arrays are confirmed by scanning electron microscopy for monolayer, close-packed structure and uniform distribution (Figure 1(b)). We further show that the perfection of close-packed structure and uniformity of the polymer spheres can be evaluated from the corresponding FFT pattern (Figure 1(c)). These results should be useful for fabricating new devices requiring 2D periodicity. [4]

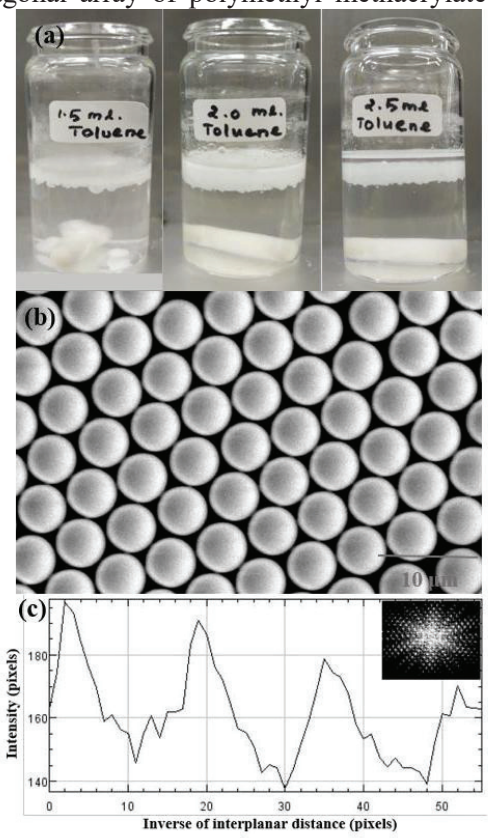

Figure 1. (a) MCCs with different volume of toluene (b) SEM image of PMMA template with close-packed structure (c) Interplanar distance of PMMA spheres and corresponding FFT pattern

Keywords: close-packed structure, monolayer template, 2D periodicity.

[1] C.L.Haynes et al., J. Phys. Chem. B 107(2003)7426.
[2] A.J.Haes et al.,J.Am.Chem.Soc.124(2002)10596.
[3] C.D.Elizabeth et al., Sensors 2(2002)91.
[4] S.Meenachisundaram et al., J. Alloy. Compd. 730 (2018) 369.

Notes:

Evaluation of deterioration of engine oil using shear horizontal surface acoustic wave sensor based on acoustoelectric interaction

S. Kobayashi and J. Kondoh*
Graduate School of Integrated Science and Technology, Shizuoka University, Hamamatsu-shi, Japan
*kondoh.jun@shizuoka.ac.jp

A shear horizontal surface acoustic wave (SH-SAW) device has been widely used in mobile communication system, such as mobile phones, as antenna duplexers and filters [1]. The SH-SAW propagates on a piezoelectric substrate surface and is perturbed by mechanical and electrical changes of an adjacent medium. The electrical perturbation is called an acoustoelectric interaction [2]. In our previous study, we measured an olive oil to discuss the influence of particles in the oil [3]. Also, we compared new and used engine oils, which was extracted from a motorbike. Figure 1 shows the measured results of new and used engine oils based on the acoustoelectric interaction. The reference was an olive oil, which has the almost same viscosity with the engine oil. In the figure, dashed and solid lines indicate the constant conductivity normalized by the frequency and the constant relative permittivity, respectively. The conductivity and relative permittivity of the used engine oil increases. The differences between the both samples cannot be explained on the basis of the results using the olive oil. In this paper, three experimental results are carried out to clarify the deterioration of the engine oil using the SH-SAW sensor.

As particles were observed in the used olive oil, iron and carbon powders were mixed with the new engine oil. Whereas the relative permittivity increases with the amount of the particles, the conductivity was the constant. The influence of the particles are not the main causes. Secondly, the effect of oxidization and heat deterioration was examined. The temperature of the oil increases during the operating engine. The new engine oil was kept at 100 ˚C. Heating times were, 400, 1000, 2000, and 3000 hours. After 3000 hours heating, the color of the sample is similar with the used engine oil. However, the electrical property changes of the heated oils were small. From the results, the difference between the new and used engine oil cannot explain. Third measurement was carried out to discuss the influence of the water. It is necessary to measure the influence of the water contained in the oil. Water was ultrasonically mixed with the new engine oil. Concentrations of water were 1 and 10 wt%. The results are plotted in Fig. 2. The relative permittivity and conductivity increases with the water concentration. From Figs. 1 and 2, it is found that the result of used engine oil almost agrees with the result of 1 wt% water contained oil. Therefore, the mechanism of the deterioration of the engine oil is the influence of the contained water.

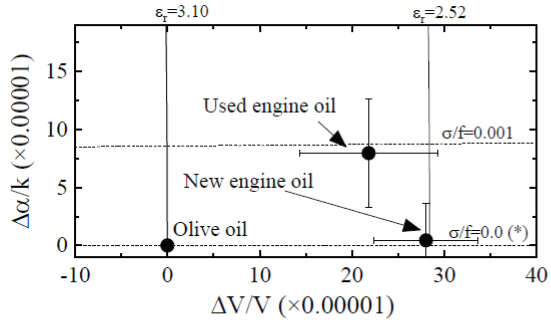

Fig. 1. Experimental results of the new and used engine oils. ε_r: relative permittivity, σ/f: conductivity normalized by frequency, *:$\times 10^{-8}$

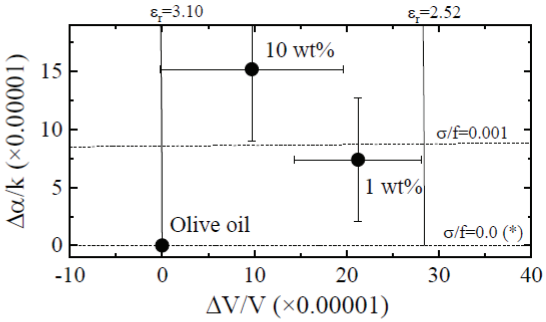

Fig. 2. Experimental results of water contained engine oils. ε_r: relative permittivity, σ/f: conductivity normalized by frequency, *: $\times 10^{-8}$ (S/m)/Hz)

Keywords: SH-SAW sensor, acoustoelectric interaction, engine oil.

[1] C. K. Campbell, “Surface Acoustic Wave Devices for Mobile Communication”, Academic Press, San Diego (1998).
[2] J. Kondoh, Electronics Communication in Jpn. 96 (2013) 02, 41.
[3] S. Kobayashi and J. Kondoh, to be published in Jpn. J. Appl. Phys. 57.

Notes:

Multiple-valued computing by photon-coupled, photoswitchable proteins

B. Rakos*
Department of Automation and Applied Informatics, Budapest University of Technology and Economics, Hungary
MTA-BME Control Engineering Research Group, Hungary
* balazs.rakos@gmail.com

Multiple-valued logic deals with more than two logic values [1,2]. It is a combination of binary logic and analog signal processing, which retains the advantages of both [3], and utilized by various applications [4]. Since present-day technology-related research strives to develop nanometer-size, fast, and low power-consuming electronic devices, elementary building blocks with such properties, applicable for many-valued computations should be explored, as well. Proteins may be promising candidates for this purpose due to their various advantages [5-7]. In two recent studies, we showed that photon pulse-driven, photon-coupled protein arrangements are potentially suitable for terahertz-frequency binary logic computations [8,9]. In this work, we discuss the applicability of such molecules in multi-valued computing circuits. The proposed operational principle is based on photoswitchable proteins, capable of switching between more than two forms when subjected to light with well-defined frequencies. The molecules must be able to emit light with specific frequencies, determined by their forms (e.g. fluorescent photoswitchable proteins) in order to enable photo-coupling between neighboring proteins. According to our considerations such protein arrangements are potentially suitable for the realization of low power-consuming, terahertz-frequency, nanoscale, multiple-valued logic circuits.

Keywords: Multi-valued logic, molecular electronics, logic circuits, photoswitchable protein, photon coupling.

[1] Hayes, B. Third base. Am. Scientist 2001; *89*, 490–494.
[2] Yoeli, M.; Rosenfeld, G. Logical Design of Ternary Switching Circuits. IEEE Transactions on Electronic Computers 1965; EC-14 (1), 19-29.
[3] Current, K.W. Current-mode CMOS multiple valued logic circuits. IEEE J. Solid-State Circuits 1994; 29 (2), 95–107.
[4] Dubrova, E. Multiple-Valued Logic Synthesis and Optimization. The Springer International Series in Engineering and Computer Science 2002; 654, 89-114.
[5] Rakos B. Simulation of Coulomb-coupled, protein-based logic. Journal of Automation, Mobile Robotics & Intelligent Systems 2009; 3(4), 46–48.
[6] Rakos B. Coulomb-coupled, protein-based computing arrays. Advanced Materials Research 2011; 222, 181-184.
[7] Rakos B. Modeling of dipole-dipole-coupled, electric field-driven, protein-based computing architectures. International Journal of Circuit Theory and Applications 2015; 43, 60-72.
[8] Rakos B. Pulse-driven, Photon-coupled, Protein-based Logic Circuits. Advances in Intelligent Systems and Computing 2016; 519, 123-127.
[9] Rakos B. Photon-coupled, photoswitchable protein-based OR, NOR logic gates. Advances in Intelligent Systems and Computing, 2017; 660, 99-103.

Notes:

A Hybrid Machine Learning Approach for Daily Prediction of Solar Radiation

M. Torabi[1], S. Shamshirband[1], M. R. Saybani[1], A. Mosavi[1,*], A. R. Varkonyi-Koczy[1, 2]
[1]*Institute of Automation, Kando Kalman Faculty of Electrical Engineering, Obuda University, Becsi Str. 94-96, 1431 Budapest, Hungary*
[2]*Department of Mathematics and Informatics, J. Selye University, Elektrarenskacesta 2, 945 01 Komarno, Slovakia*
[*]*amir.mosavi@kvk.uni-obuda.hu*

In this paper, we present a Cluster-Based Approach (CBA) which utilizes the support vector machine (SVM) and artificial neural network (ANN) to estimate and predict the daily horizontal global solar radiation. In the proposed CBA-ANN- SVM approach, we first conduct clustering analysis and classify the global solar radiation data into clusters, according to the calendar months. Our approach aims at maximizing the homogeneity of data within the clusters, and the heterogeneity between the clusters. The proposed CBA-ANN- SVM approach is validated using data collected from an Iranian city. The precision of the proposed CBA-ANN- SVM approach is then compared with ANN and SVM techniques. The mean absolute percentage error (MAPE) for the proposed approach is lower than that of ANN and SVM (1.342% vs 1.603% and 1.565%, respectively).

Keywords: Global solar radiation; Cluster-Based Approach; Support Vector Machine (SVM); Machine Learning; Artificial Neural Networks (ANN).

Notes:

A Nanoantenna-MIM Diode-Lens Device Concept for Infrared Energy Harvesting

M.F. Kashif* and B. Rakos
Budapest University of Technology and Economics, H-1117, Budapest, Hungary
**fayyaz.kashif@aut.bme.hu*

The sunlight is a clean and abundantly available energy source. The potential of solar energy is underutilized by the existing photovoltaic (PV) technology. In this paper, we study and propose an antenna-based energy harvesting device for generating electricity from the solar infrared radiation. The proposed device is based on nano-antennas, terahertz rectifying diodes and concentrator lenses fabricated on a single chip.

The idea of collecting energy from solar radiation by the antennas is not new. Since sunlight is basically composed of electromagnetic radiations, it is possible to convert it into electricity by an antenna which is far more efficient than PV cells. With the advent of nanofabrication technologies like electron beam lithography etc., it is now possible to fabricate nano-antennas at large scale. A number of nano-antennas for infrared radiations detection have been actually fabricated and reported [1-3]. A technology for fabricating high-quality micro lenses by high throughput hot embossing techniques was developed in the past years [4]. Spherical and cylindrical lenses of different sizes ranging from ~1 to hundreds of micrometers can be realized with this technology.

We propose an array of nano-antennas connected in series and parallel fashion. Diodes integrated with these antennas can transform the energy of electromagnetic radiations into electricity by rectifying the high frequency currents induced in the antennas. Furthermore, a layer of micro lenses is placed on the chip for focusing the incident radiations on the nano-antennas. We have investigated the conversion efficiency of the proposed device by taking into account the experimental results cited in the technical literature [2], [4]. A conversion efficiency of ~77% is estimated for the 10 μm infrared radiation. From this study, we believe that such devices may be good candidates for future infrared energy harvesting systems.

Keywords: Nano-antenna, MIM diode, energy harvesting, infrared radiation, micro lenses.

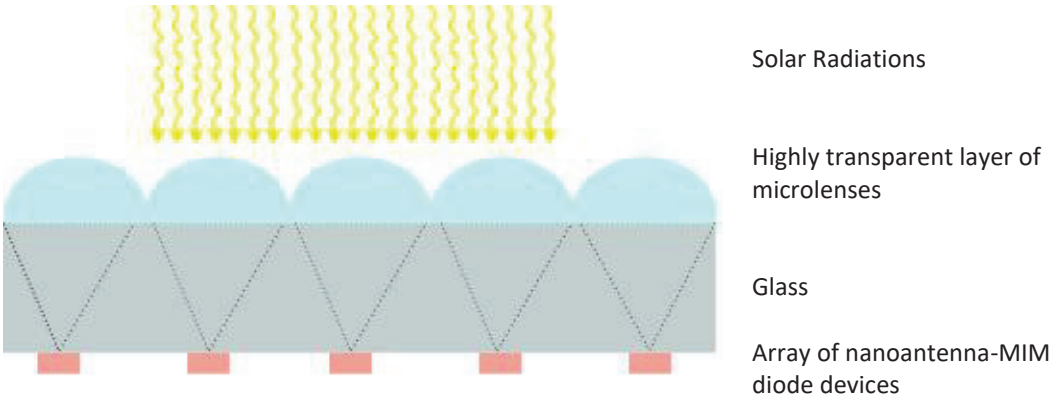

Fig. 1. Conceptual scheme for the infrared energy harvesting device

[1] B.Rakos, H. Yang, J.A.Bean et al, Springer Proceedings in Physics 110 (2006).
[2] J. Bean, Dissertation, University of Notre Dame,USA, (2008).
[3] I. Wilke, W. Herrmann, F.K. Keneubuhl, Appl. Phys. B 58, (1994) 87-95.
[4] M. Tormen, A. Carpentiero, E. Ferrari, D. Cojoc et al, Nanotechnology 18, 385301 (2007).

Notes:

Vehicle detection using aerial images under disaster situations

A. Makiuchi[1], H. Saji[2,*]
[1,2]*Graduate School of Integrated Science and Technology, Shizuoka University, 3-5-1, Johoku, Nakaku, Hamamatsu, Shizuoka, 432-8011, Japan*
[*]*saji@inf.shizuoka.ac.jp*

Under disaster situations, it is necessary to rapidly grasp traffic jams and abandoned vehicles. This is because we can carry out rescue activities efficiently by accurately grasping usable traffic routes. However, it takes time to recognize vehicles and estimate their positions. The purpose of our study is to rapidly detect vehicles and their positions under disasters.
We propose a method of vehicle recognition and position estimation using an aerial image taken from a helicopter and a road map. While such images can be taken locally, Occlusion occurs when buildings are reflected on the road.
In the vehicle recognition, we use shadow correction, asphalt removal by machine learning, and shape analysis. In addition, we use building removal to resolve the occlusion. First, we adjust color of the aerial image by the shadow correction. After that, we remove asphalt areas and building areas on the road, and we extract vehicle areas by using their shape features.
In the vehicle position estimation, we project the road map on the aerial image by the projective transformation. By associating these two images, we mark the position of vehicles in the aerial image on the road map. We extract the road area in the aerial image by the projection before the recognition and improved efficiency of the process.
By our method, we recognized most of the vehicles with different colors from asphalt. Furthermore, we marked position of the vehicle area on the road map. We indicated a possibility of fast detection of vehicles from aerial images under disaster situations.

Keyword: Vehicle recognition, position estimation, aerial image, disaster, image processing.

Notes:

Remote Detection of Holes Generated by Impact Ionization

H. Firdaus, M. Hori, Y. Ono*
Research Institute of Electronics, Shizuoka University, 3-5-1 Johoku, Hamamatsu, 432-8011, Japan
**ono.yukinori@shizuoka.ac.jp*

Energy loss of electrons in nanometer-scaled devices is the critical issue both for classical and quantum circuits. Impact ionization [1,2], or electron-hole pair creation under a high electric field, is one of the main origins of the energy loss of high-energy electrons. In this study, we observe the impact ionization process in silicon, using a novel lateral hot-electron transistor structure. Holes generated by the impact ionization due to high -energy electrons were detected at 6 K by a remote collector, placed at the distance of about 150 nm from the electron emitter. The present results suggest that the detected holes were generated at a place close to the corrector (or far from the emitter), and thus suggest the presence of long-lived high-energy electrons.

The device we used is in effect the lateral hot-electron transistor formed on a silicon-on-insulator (SOI) substrate. It is T-shaped and consists of three n-type leads, which we call emitter, collector and base. The emitter and collector have their own gates so that we can independently control the energy of electrons. Figure 1 explains the detection scheme of holes generated by impact ionization. A negative voltage is applied to the emitter lead so that electrons are injected to the T-branch region. These emitter electrons lose their energy either at the emitter channel underneath the gate or at the T-branch region, and are then drained out to the base. Generated holes, on the other hand, will recombine with electrons either underneath the emitter gate, collector gate, or at the T-branch region.

In the experiments, additional features were observed in the low collector-gate-voltage region when the emitter lead voltage was smaller (negatively larger) than about−1.2 V. This is due to holes trapped at the SOI/buried oxide interface underneath the collector gate [3,4]. The threshold voltage was consistent with the ionization threshold energy reported [5,6], and we therefore ascribe these features to holes generated by the impact ionization.

Since holes generated underneath the emitter gate effectively recombine with electrons there, we anticipated that the detected holes were generated at the T-branch region far from the emitter. Therefore, present results strongly suggest the presence of long-lived high-energy electrons in the T-branch region, and the detected holes were generated by such lucky electrons.

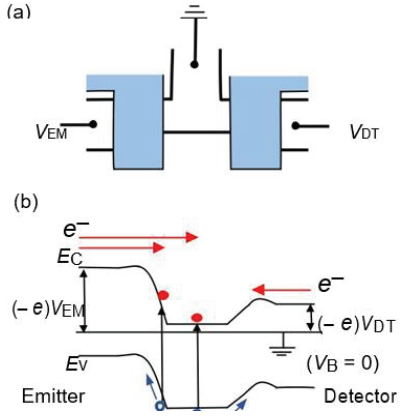

Fig. 1. Detection scheme of impact ionization: (a) top view of the device, (b) band diagram for emitter and collector. High -energy electrons injected towards the T-branch region produce electron hole pairs. Generated Holes generated at T-branch region are expected to be sensed by the corrector current

Keywords: Impact ionization, Silicon, Single holes.

[1] P. A. Wolff, Phys. Rev. 95 (1954) 1415.
[2] W. Shockley, Solid-State Electron. 2 (1961) 35.
[3] A. Fujiwara and Y. Takahashi, Nature (London) 410 (2001) 560.
[4] A. Fujiwara and Y. Takahashi, Jpn. J. Appl. Phys. 41 (2002) 1209.
[5] C. L. Anderson and C. R. Crowell, Phys. Rev. B 5 (1972) 2267.
[6] N. Sano, T. Aoki, M. Tomizawa, and A. Yoshii, Phys. Rev. B 41 (1990) 12122.

Notes:

Normal and axial mode of operation of human sweat duct in sub-terahertz frequency region

S. R. Tripathi[1*], S. Takahasi[1], and K. Kinumura[1]
Department of Mechanical Engineering, Shizuoka University, 3-5-1 Johoku Hamamatsu, Shizuoka 432-8561, Japan
[*]*tripathi.saroj@shizuoka.ac.jp*

Rapid development of optoelectronics and ultrafast technology has enabled the emission and detection of broadband terahertz (THz) waves and the applications of THz waves have expanded into diverse fields such as homeland security, information and communication technology, material characterization and non-destructive testing and analysis [1]. Due to the advancement of such applications, encounters between THz radiation and humans are expected to become common. Therefore, knowledge of the fundamental principles of THz wave interaction with human beings is crucial for understanding the various health consequences [2].
Recently, some studies have demonstrated that the sweat glands present in the human skin play a critical role in THz wave interaction with human beings [3]. It was reported that the sweat ducts act as a low-Q-factor helical antenna due to their helical structure and resonate in the terahertz frequency range. According to the antenna theory, the structural parameters (such as helix diameter and helix length) of the helix plays a key role to determine the frequency of resonance and modes of resonance such as the axial mode (also known as the end-fire mode) and the normal mode (also known as the broadside mode). Therefore, accurate determination of structural parameters of sweat duct is crucially important to obtain both the reliable frequency of resonance and different modes of operation [4].
In this study, we performed the optical coherence tomography (OCT) of human subjects on their palm and foot to investigate the density, distribution and morphological features of sweat ducts. We observed that the density of sweat duct is highest on the tip of fingers. We also found that the average diameter of sweat duct was 95 μm. Along with the structural parameters of sweat duct, the dielectric property of skin in terahertz frequency region plays a crucial role in the determination of frequency of resonance. Here, we used terahertz time domain spectroscopy in reflection geometry to obtain the dielectric properties of skin. Based upon all these information, we found that the sweat duct resonates in 442 GHz in axial mode and 228 GHz in normal mode of operation [5,6].
We believe that these finding will help to further investigate the various effects caused by high frequency electromagnetic wave in the sub-terahertz frequency band. Moreover, this result shows the important criteria to select high frequency electromagnetic wave for the development of biomedical devices and high-speed wireless communication system in sub-terahertz frequency region.

Keywords: Terahertz waves, optical coherence tomography, antenna, helix, resonance frequency.

[1] M. Tonouchi, Nature Photonics. 1 (2007) 2, 97-105.
[2] G. J. Wilmink and J. E. Grundt, J Infrared Millim. THz Waves 32 (2011) 10, 1074–1122.
[3] Y. Feldman, A. Puzenko, P. Ben Ishai, A. Caduff, and A. J. Agranat, Phys. Rev. Lett. 100 (2008) 12, 128102.
[4] C. A. Balanis, Antenna Theory: Analysis and design, 2nd Ed. (2007).
[5] S. R. Tripathi, E. Miyata, P. B. Ishai, K. Kawase, Scientific Reports 5, (2015) 9071, 1- 7.
[6] S. R. Tripathi, P. B. Ishai, K Kawase, Biomedical Optics Express, 9, (2018) 3, 1301-1308.

Notes:

A Study of Single-Electron Tunneling in 1D Distributed Arrays of Donor Quantum Dots

A. Afiff[1,2,3], A. Samanta[4], A. Udhiarto[3], H. Sudibyo[3], D. Hartanto[3], M. Tabe[1], D. Moraru[1,*]
[1]*Research Institute of Electronics, Shizuoka University, 3-5-1 Johoku, Hamamatsu, Japan*
[2]*Graduate School of Integrated Science and Technology, Shizuoka University, Japan*
[3]*Faculty of Engineering, Universitas Indonesia, Depok, Indonesia*
[4]*Indian Institute of Technology (IIT) Roorkee, India*
[*]*moraru.daniel@shizuoka.ac.jp*

One-dimensional (1D) electron transport in semiconductor nanoscale devices offers promising prospects for future CMOS technology. Chains of donor-atoms in Si nano-channel transistors [1,2] can work as a fundamental 1D quantum-dot (QD) array. Individual donor atoms can accommodate and transfer single electrons [3,4] giving rise to a current between the source and drain of such transistors. By strongly coupling several phosphorus (P) donors together, a cluster-donor QD with higher tunnel barriers can be obtained and thermally-activated transport is effectively suppressed [5]. This is done by selectively doping Si nano-channels at a concentration ($N_D \approx 1\times10^{19}$ cm^{-3}) somewhat higher than the metal-insulator transition.

Most importantly, this doping technique allows the formation of a special type of distribution of donor atoms, in which the core several donors are strongly coupled to each other, while the outer donors diffuse towards the leads with weaker and weaker coupling to their neighbors. This kind of distribution can be favorable for applications such as single-electron turnstile, for which an effectively larger QD in the center of the array may be energetically favorable [6].

In this work, we analyze such "distributed" donor-QD arrays by Coulomb blockade simulations in order to clarify their properties as a function of controllable parameters of the distribution (number of donors and coupling strength). We find that even long arrays of donor-QDs can be effectively reduced to simpler structures having a strongly-coupled core and weakly-coupled satellite side QDs. Thus, it is shown that "distributed" donor-QD arrays as obtained by our unique selective-doping technique possess the suitable properties for single-electron transfer applications.

These results can open a versatile range of research that can exploit specific distributions of donor-atoms in 1D arrays for controlling electron transport in time and space at atomic level, with a relatively simple technology.

Keywords: donor-atom, Si nano-transistors, quantum dot, 1D transport.

[1] D. Moraru et al., "Quantized electron transfer through random multiple tunnel junctions in phosphorus-doped silicon nanowires", Phys. Rev. B 76, 075332 (2007).
[2] E. Prati et al., "Band transport across a chain of dopant sites in silicon over micron distances and high temperatures", Sci. Rep. 6, 19704 (2016).
[3] P. M. Koenraad et al., "Single dopants in semiconductors", Nature Mater. 10, 91 (2011).
[4] D. Moraru et al., "Atom devices based on single dopants in silicon nanostructures", Nanoscale Res. Lett. 6, 479-1-9 (2011).
[5] A. Samanta et al., "Single-electron quantization at room temperature in a-few-donor quantum dot in silicon nano-transistors", Appl. Phys. Lett. 110, 093107 (2017).
[6] K. Yokoi, D. Moraru, M. Ligowski, and M. Tabe, "Single-gated single-electron transfer in nonuniform arrays of quantum dots", Jpn. J. Appl. Phys. 48, 024503 (2009).

Notes:

Low-Voltage Multifunctional Graphene Nanoelectromechanical Devices

M. Muruganthan[1,*], H. Van Ngoc[1], J. Kulothungan[1], M. E. Schmidt[1], and H. Mizuta[1, 2]
[1]*Japan Advanced Institute of Science and Technology, 1-1 Asahidai, Nomi, Ishikawa 923-1292, Japan*
[2]*Hitachi Cambridge Laboratory, J. J. Thomson Avenue, CB3 0HE Cambridge, United Kingdom*
[*]*mano@jaist.ac.jp*

Graphene has an ultra-high Young's modulus of 1 TPa, which makes it a promising candidate for future nanoelectromechanical (NEM) applications. The graphene NEM (GNEM) switches have potential to realize minimized electrical leakage, sharp switching response, low actuation voltage and high on/off ratio. Furthermore, GNEM devices offer a unique platform to realize highly sensitive gas molecule detection due to the exceptionally low electronic noise characteristics of graphene in general, and the suspended nature of graphene channel in these devices.

GNEM switches are fabricated using the bottom-up procedure to obtain suspended graphene with a polymer sacrificial spacer. In these switches, low pull-in voltage of less than 2 V is achieved [1-2]. This pull-in voltage is compatible with the conventional, complementary metal-oxide semiconductor circuit requirements. Double-clamped beam and cantilever GNEM switches are also realized with a local top actuation electrode. Moreover, large-scale GNEM switches are successfully fabricated based on directly deposited nanocrystalline graphene on insulating substrates [3].

Three terminal graphene NEM device was fabricated using the two-dimensional materials, graphene and hexagonal boron nitride. The irreversible stiction issue was avoided by employing the weak graphene–graphene van der Waals interaction between the suspended movement element and the electrode. The drain-source conduction switching between the on- and off-states is controlled via the bottom graphene gate. Gate voltage induces the mechanical deflection of the suspended, moveable drain-graphene into physical contact with the bottom source-graphene electrode to form a conducting channel. Our three terminal graphene NEM switch exhibits remarkable switching characteristics, with a subthreshold slope as small as 11 mV/dec at room temperature.

In order to realize the extreme sensing capability, the suspended bilayer graphene GNEM switches are exploited. The step-like changes in the graphene beam resistance with a quantized value of ~62 Ω are measured when exposed to low CO_2 concentration. These discrete responses are clear evidence of individual CO_2 molecule adsorption onto the slanted graphene beam. In order to enhance the molecular adsorption rate, the electrical field is introduced around the suspended graphene region by applying the back-gate voltage. The first-principles calculations and molecular dynamics simulations elucidate the role of van der Waals interaction between molecules and graphene during detection and the back gate effects on accelerating the molecules adsorption [4-5].

Acknowledgement: This work is supported by Grant-in-Aid for Scientific Research Nos. 25220904, 16K18090, 16K13650, 18H03861 and 18K04260 from Japan Society for the Promotion of Science.

[1] J. Sun, W. Wang, M. Muruganathan, H. Mizuta, Applied Physics Letters, 105 (2014) 3, 033103.
[2] J. Kulothungan, M. Muruganathan, H. Mizuta, Micromachines, 7 (2016) 8, 143.
[3] J. Sun, M. E. Schmidt, M. Muruganathan, H. M. Chong, H. Mizuta, Nanoscale 8 (2016) 12, 6659.
[4] M. Muruganathan, J. Sun, T. Imamura, H. Mizuta Nano Letters, 15 (2015) 12, 8176.
[5] J. Sun, M. Muruganathan, H. Mizuta, Science Advances, 2 (2016) 4, p.e1501518.

Notes:

Electromotive force of n-type Si wafer connected to piezoelectric device with its vibration under temperature gradient

H. Ikeda[1,2,*], K. Naito[1,2], Y. Suzuki[1,2], Y. Hayakawa[1,2], M. Shimomura[2], and K. Murakami[2]
[1]*Research Institute of Electronics, Shizuoka University, Johoku 3-5-1, Naka-ku, Hamamatsu 432-8011, Japan*
[2]*Graduate School of Integrated Science and Technology, Shizuoka University, Johoku 3-5-1, Naka-ku, Hamamatsu 432-8561, Japan*
[*]*ikeda.hiroya@shizuoka.ac.jp*

From the standpoint of energy harvesting, we have investigated the thermoelectric (TE) power generator hybridized with a piezoelectric (PE) device [1]. For this purpose, in the present study, the electromotive force (EMF) of an n-type Si substrate connected to a PE device (THRIVE, KINEZ K7520BP2) was measured with PE-device vibration under temperature gradient.

The n-type Si wafer (0.14-0.21 Wcm) was cut to 1 cm x 5 cm. A commercial PE device was fixed to an Al electrode on the Si sample. Figure 1 shows a schematic diagram of our system for measuring the EMF of the Si sample connected to a vibrating PE device. There are two heat sinks with a space between them. One is underneath a Peltier device for applying temperature difference (DT). The other is attached with a thin insulating tape that electrically separates from the sample but easily passes the heat. T-type thermocouples are used for measuring the temperatures at the high- and low-temperature regions simultaneously together with EMF, using a logger (HIOKI 8430).

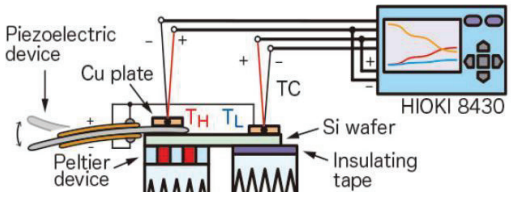

Fig.1: Schematic of measurement system

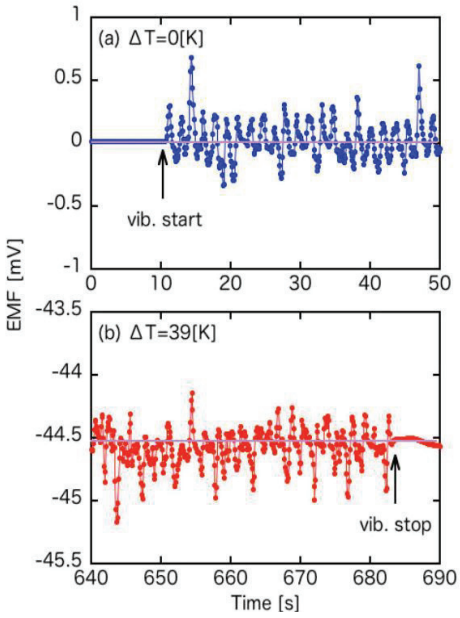

Fig. 2: Time evolution of EMF with PE-device vibration under (a) DT=0K and (b) DT=39K

The time evolution of EMF at DT=0K is shown in Fig. 2(a). It is found that the EMF without vibration (0 mV) seems to exist at the center or lower position of the EMF wave amplitude originating from the PE vibration. On the other hand, in the case of DT=39K shown in Fig. 2(b), the EMF without vibration (-44.5 mV) exists at the higher position of the EMF wave amplitude. This fact indicates that the EMS polarity observed under the PE vibration changes by applying the temperature gradient to Si, suggesting the carrier injection and emission between the PE material and the TE material. This leads to possibility of self-rectification operation.

Keywords: thermoelectric power generator, piezoelectric device, electromotive force.

[1] H. Ikeda, L. Muniraj K. Naito, Y. Hayakawa, M. Shimomura, K. Murakami, Proc. of 2017 Asia-Pacific Workshop on Fundamentals and Applications of Advanced Semiconductor Devices (2017) 364-366.

Notes:

Gamma-ray spectroscopic performance of large-area CdTe-based Schottky diodes

V.A. Gnatyuk[1,2,*], K.S. Zelenska[2,3], V.M. Sklyarchuk[4], W. Pecharapa[5], and T. Aoki[2]
[1]*V.E. Lashkaryov Institute of Semiconductor Physics of the National Academy of Sciences of Ukraine, Prospekt Nauky 41, Kyiv 03028, Ukraine*
[2]*Research Institute of Electronics, Shizuoka University, 3-5-1 Johoku, Naka-ku, Hamamatsu 432-8011, Japan*
[3]*Faculty of Physics, Taras Shevchenko National University of Kyiv, Prospekt Akademika Glushkova 4, Kyiv 03127, Ukraine Kyiv, Ukraine*
[4]*Yuriy Fedkovych Chernivtsi National University, Kotsubynskyi Str. 2, Chernivtsi 58012, Ukraine*
[5]*College of Nanotechnology, King Mongkut's Institute of Technology Ladkrabang, 1 Thanon Chalong Krung, Ladkrabang, Bangkok 10520, Thailand*
[*] *gnatyuk@ua.fm*

Various materials, particularly metals are used for creation of electrical contacts and formation of electrodes in fabrication of CdTe-based X/γ-ray detectors. The application of a certain metal depends on the intention to create a rectifying (blocking, Schottky) or Ohmic contact. Schottky diode detectors have shown great promise in spectroscopic application with In (Al) and Pt (Au), which are commonly used for high-resistivity *p*-like CdTe crystals, to create a rectifying or Ohmic contact, respectively. The choice of Ni for creation of a Schottky contact to such semiconductor in our research was due to the fact that in addition to appropriate electronic characteristics, Ni is a ductile, hard and chemically low-active metal with high corrosion resistivity that advantageously differs from In, which is generally used for Schottky contact formation in the manufacture of CdTe-based diode detectors.
In this study, commercial detector-grade Cl-compensated (111) oriented *p*-like CdTe semiconductor single-crystal wafers with sizes of 10 × 10 × 0.75 mm^3 were used for the diode-type detector fabrication. The γ-ray spectroscopic characteristics of the created Ni/CdTe/Au diode detectors with a high barrier Schottky contact at the Ni-CdTe interface and near Ohmic contact at the Au-CdTe interface were studied. Both the contacts were formed by preliminary chemical etching of the CdTe crystals in a Br-methanol solution and following treatment with an Ar plasma at different regimes (ion energy, beam density, processing duration, etc.) for the *B*- and *A*-faces, respectively. Ni and Au electrodes were placed on the *B*- and *A*-faces of the CdTe(111) crystals by vacuum evaporation and chemical deposition, respectively. The obtained Schottky diodes operated when the Ni contact was positively biased with respect to the Au one (reverse mode) and showed quite low reverse dark currents even at high bias voltages (4-6 nA/cm^2 and 8-12 nA/cm^2 at 500 V and 1000 V, respectively).
The dependencies of the ^{157}Cs radioisotope spectra, obtained with the developed Ni/CdTe/Au Schottky diode detectors, on the distance (10-75 cm) to the γ-ray source, bias voltage applied to the detector (100-1000 V) and also on the operation time (0-280 min) were studied. The spectroscopic characteristics were calculated from the ^{157}Cs radioisotope spectra measured at different parameters indicated above and were analyzed: peak counts, energy resolution (FWHM), peak channel position and peak-to-valley ratio. A few advantageous features of the Ni/CdTe/Au Schottky diode detectors were revealed. Despite the relatively thin CdTe crystals thus, low absorption of high energy radiation (662 keV) and hence low probability of γ-photon capture and generation of electron-hole pairs, the detectors demonstrated quite satisfactory detection efficiency that was due to high rectification properties of the Ni/CdTe Schottky contact allowing to apply high bias voltage (up to 1000 V and higher) and thus, to provide full collection of photogenerated charge carriers. A reduced decrease in the number of counts for the 662 keV peak was observed with an increase the distance between the detector and radiation source. There was a certain optimal bias voltage range for each detector to demonstrate the best values of FWHM (1.0-2.0 %) and peak channel position (662 keV). The detectors showed long-term stability e.g., the detection efficiency (number of counts) decreased only by 40 % and stabilized during quite long operation time (280 min) under γ-ray radiation at room temperature.

This work was supported by the NATO Science for Peace and Security Programme (Project SENERA, SfP-984705) and Academic Melting Pot Program at KMITL (Thailand).

Keywords: CdTe crystals, Schottky diodes, X/γ-ray detectors, Radioisotope spectra.

Notes:

Correlation Between Optical, Morphological and Compositional Properties of GeSn Epitaxial Layers Irradiated by Nd:YAG Laser Radiation

P. Onufrijevs[1,*], A. Medvids[1], P. Ščajev[2], M. Andrulevicius[3], A. Selskis[4], L. Grase[1]
[1]*Institute of Technical Physics, Faculty of Materials Science and Applied Chemistry, Riga Technical University, P. Valdena 3/7, Riga, LV-1048, Latvia*
[2] *Institute of Photonics and Nanotechnology, Vilnius University, Sauletekio al. 3, LT 10257, Vilnius, Lithuania*
[3]*Institute of Materials Science, Kaunas University of Technology, Barsausko str. 59, LT-50131, Kaunas, Lithuania*
[4]*Center for Physical Sciences and Technology (FTMC), Vilnius, Lithuania*

Si-based materials have been the driving force behind the rapid development of revolutionary electronic technology and have dominated the market for the past 40 years. As a parallel effort to advance the reach of group IV technology to mid-infrared range, researchers have strived for years to create group IV-based optical devices that can exploit the benefits of silicon while also being fully compatible with Si electronics.

The all group of IV alloy of germanium-tin (GeSn) based material has shown promising characteristics extending the detection range to long wavelength range, however due to limited Sn atoms solubility, only 4% Sn in alloys with Ge are currently available. Moreover, GeSn is predicted to exhibit an indirect to direct band gap transition at alloy Sn composition of 6.5% [1]. Therefore, we applied pulsed laser radiation to $Ge_{0.96}Sn_{0.04}$ layers epitaxially grown on Si substrates by MBE (molecular beam epitaxy) to redistribute Sn atomic content according to thermogradient effect [2] with the aim to increase Sn content at the surface. We used nanosecond laser radiation (1064 nm wavelength, 6 ns pulse duration) with different intensities in the range I=107.8-463.5 MW/cm^2 to modify GeSn layer. The X-ray photoelectron spectroscopy, Raman and UV reflection spectra confirmed Sn atomic content increase at the surface by order of magnitude. SEM (Fig.1.) and AFM imaging provided evident microstructure changes, while carrier lifetime changes determined by differential transmittivity were not observed, indicating that laser irradiation does not reduce material electronic quality.

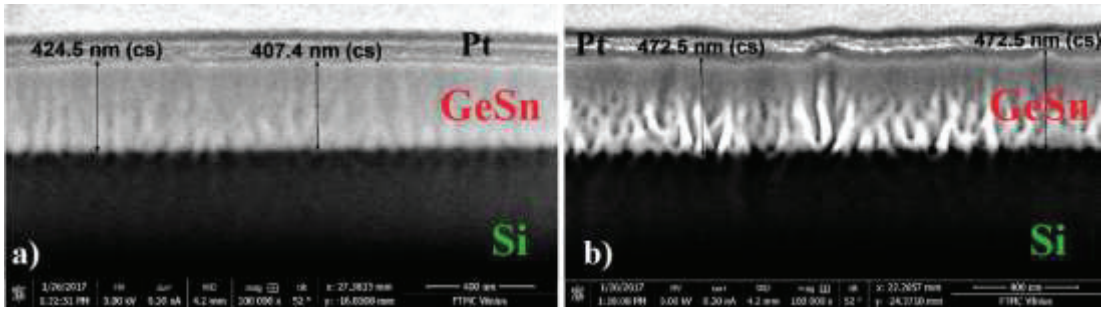

Fig.1 SEM images of FIB cross-section of non-irradiated Pt/Ge0.96Sn0.04/Si structure (a) and irradiated by Nd:YAG laser radiation at I=136.7 MW/cm^2 (b). Pt layer was deposited on the GeSn surface as protective layer for cross-sectioning

The work was supported as part of the Program on Mutual Funds for Scientific Cooperation of Lithuania and Latvia with Taiwan. The authors sincerely acknowledge E. Kasper, K. Lyutovich from University of Stuttgart for provision of the samples.

[1] S. Gupta, B. Magyari-Köpe, Y. Nishi, and K.C. Saraswat, J. Appl. Phys. 113, (2013).
[2] A. Medvid, Defect and Diffusion Forum, 2002, vol. 210–212, pp. 89–102.

Notes:

Synthetic light interference image analysis algorithm in wedge interferometer

J. Mruk[1,*]
Warsaw University of Technology, Faculty of Mechatronics, A. Boboli 8, Warsaw, Poland
*mruk.kuba@gmail.com

This work presents a project of new interference image analysis software. The main idea was to create a new algorithm, that uses the possition of functions local maxima to detect the wedges possition change.
Optical setup consisting of four main elements: source of light (2 laser diodes of diferent wavelenghts, and beamsplitter to join the beams), wedge interferometer (wedge plate mounted on angular table), Mirror reflecting the beam into photodetector, CCD camera working as photodetector. Interference of beams reflected of front and inner surfaces of the wedge was observed.
Interferometer setup genereted interference fringes composition of two different wavelentghts. That allowed to detect local maxima and minima of the periodic function, which modulated the interference fringes[1].
An all-new algorithm analyzes interference image based on density distribution of interference fringes. Software was developed in LabView enviorment.
Alorithm determines possition change of local extremum. Maximum of the function acts as reference point – absolute possition of wedge in relation to the beam. The change of its possition can be calculated into wedge rotation. Fig. 1 shows front panel of the software, with two-beam interference image in the left, intensity distribution in top right corner and intensity histogram in the bottom left corner, which is used to adjust the setup.

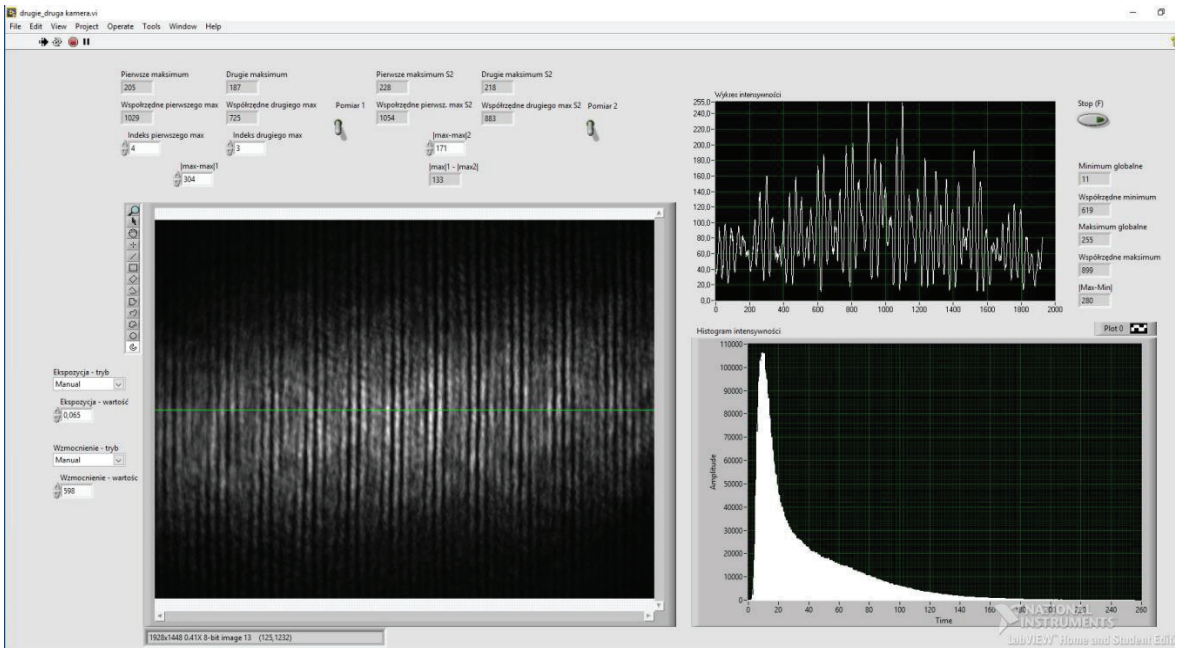

Fig. 1 Front panel – used for the analysis of interference distribution

Keywords: Interference, image, analysis, algorithm, wedge.

[1] O. Iwasińska-Kowalska, M.Dobosz, "A new method of non-contact gauge block calibration using a fringe-counting technique: II. Experimental verification", Optics & Laser Technology 42 (2010) 149-155.

Notes:

Multimodal Unobtrusive Devices for Chronic Disease Monitoring

V. Marozas[1,*], A. Petrėnas[1], S. Daukantas[1], A. Sološenko[1], B. Paliakaitė[1], D. Jegelevičius[1], A. Lukoševičius[1], E. Kaldoudi[2]
[1]*Biomedical Engineering Institute, Kaunas University of Technology, Kaunas, Lithuania,*
[2]*School of Medicine, Democritus University of Thrace, Alexandroupoli, Greece*
**vaimaro@ktu.lt*

We present here several results from the recently finished European Commission supported project "Personalized Patient Empowerment and Shared Decision Support for Cardiorenal Disease and Comorbidities - CARRE" [1]. Two developed devices will be presented: a wrist worn device – for continuous monitoring, and a multiparametric weighing scale – for intermittent health monitoring.
The wrist worn device is intended to be used for unobtrusive and continuous monitoring of paroxysmal atrial fibrillation arrhythmia [2]. It makes use of biooptical signal, i.e., photoplethysmogram for this purpose. Biopotential signal, i.e., electrocardiogram is acquired synchronously and can be used as a reference. The reference channel can be detached from the device in unobtrusive usage scenario. This is in contrast with other commercial devices (e.g., Fitbit Surge, MioAlpha) that are not able to acquire reference data. Moreover, there is no commercial biooptical signal based wrist worn device for arrhythmia monitoring currently on the market. There are two scenarios in which the CARRE wrist worn device can be used: real-time atrial fibrillation arrhythmia monitoring, e.g., during hemodialysis procedure, and long-term, offline atrial fibrillation arrhythmia monitoring, e.g., in rehabilitation settings or at user home.
Weighing scales are actively investigated now as an operator-less device for unobtrusive, intermittent cardiovascular monitoring. We developed a multiparametric scale [3], which is able to acquire 3 leads electrocardiogram (Einthoven's triangle), bioimpedance spectroscopy parameters at 5 frequencies and bioimpedance plethysmogram. Bioimpedance is measured between the subject's feet (lower extremities impedance) and arms (thorax impedance). The electrocardiogram and bioimpedance plethysmogram are combined to estimate pulse arrival time, which is a parameter of arterial stiffness. In addition, electrocardiogram is used for atrial fibrillation arrhythmia detection. A graphical display helps to implement a guided breathing test. Raw multimodal data files are recorded in a standard format for biomedical signals – General Data Format (GDF), therefore the files can be opened with standard GDF viewers (e.g., SigViewer) or the CARRE Multiparametric Scales Data Analyzer. The data files are stored locally and also automatically transferred to the computing server via the embedded WiFi module. Currently, the CARRE Multiparametric scale is being used as a scientific instrument for unobtrusive acquisition of biosignal databases.

Keywords: personal health devices, atrial fibrillation, arterial stiffness, GDF.

[1] CARRE (No. 611140) project, funded by the European Commission Framework Programme 7, https://www.carre-project.eu/.
[2] Paliakaitė, Birutė; Petrėnas, Andrius; Skibarkienė, Jurgita; Mickus, Tomas; Daukantas, Saulius; Kubilius, Raimondas; Marozas, Vaidotas. Towards long-term monitoring of atrial fibrillation using photoplethysmography // BIOSTEC 2017: Proceedings of the 10th International Joint Conference on Biomedical Engineering Systems and Technologies, Porto, Portugal, February 21-23, 2017. Vol. 4: p. 141-146.
[3] Paliakaitė, Birutė; Daukantas, Saulius; Marozas, Vaidotas. Assessment of pulse arrival time for arterial stiffness monitoring on body composition scales // Computers in biology and medicine. Oxford: Pergamon-Elsevier. 2017, vol. 85, p. 135-142.

Notes:

Properties of polymer based gels for radiation sensors

D. Adlienė*
[1] *Physics Department of Kaunas University of Technology, Studentų g.50, LT-51368 Kaunas, Lithuania*
*diana.adliene@ktu.lt

Polymer dose gels are materials which can provide 3D dose distribution after irradiation thus combining properties of radiation sensors and dose phantoms for medical applications.
Optical properties of two most popular normoxic polymer dose gels - nMAG and nPAG modified by different irradiation beams (photons, electrons, protons have been investigated and evaluated using UV-VIS spectroscopy, photoscanning method and Raman spectroscopy.
Mixing composition of basic gels the enhancement of optical gel sensitivity to irradiation by > 10% was achieved . Advanced gels indicated spatial resolution of 0.2 mm.
Aplication of advanced gels for the development of the new type of dose sensors is discussed.

Notes:

Effect of damage introduction and He existence on D retention by high flux D plasma exposure

Y. Oya[1,*], K. Azuma[1], A. Togari[1], M. Nakata[1], Q. Zhou[1] M.Zhao[1], T. Kuwabara[2], N.Ohno[2], M. Yajima[3], Y. Hatano[4], T.Toyama[5]

[1]*Shizuoka University, 836 Ohya, Suruga-ku, Shizuoka, Japan*
[2]*Nagoya University, 1247 Furo-cho, Chikusa-ku, Nagoya, Japan*
[3]*National Institute for Fusion Science, 322-6, Oroshi, Toki, Gifu, Japan*
[4]*University of Toyama, 3190, Gofuku, Toyama, Japan*
[5]*Tohoku University, 2145-2, Narita-cho, Oarai, Ibaraki, Japan*
[*]*oya.yasuhisa@shizuoka.ac.jp*

For the development of future fusion reactor, it is quite important to evaluate the fuel retention, especially tritium, in plasma facing walls to reduce hazard of radiation exposure and control the fuel management. Recently, tungsten (W) is thought to be the best plasma facing material due to higher melting point, lower sputtering yield and lower hydrogen solubility. However, it is known that the radiation damages by energetic hydrogen isotope, helium (He) and neutron, which will be produced by DT fusion reaction, will be introduced into W leading to the formation of stable trapping sites.

Therefore, fuel retention behavior should be evaluated by simulating the actual fusion environment. In our previous fundamental studies, deuterium (D) retention was clearly controlled by damage concentration in W [1]. In addition, the existence of He also change the D retention behavior due to the formation of He bubbles near surface region [2]. In this study, both of damage concentration and He existence effects on D retention behavior were evaluated using high flux divertor plasma exposure device, called Compact Divertor Plasma Simulator (CDPS).

The stress-relieved W was used as samples. To introduce the damages, 6 MeV Fe^{2+} was irradiated into W with the damage concentration of 0.03-0.3 displacement per atom (dpa) at room temperature by 3 MV tandem accelerator, Takasaki Ion Accelerators for Advanced Radiation Application (TIARA) at National Institutes for Quantum and Radiological Science and Technology (QST). For He irradiation, 3 keV He^+ was irradiated at Shizuoka University up to the He fluence of 1.0×10^{21} He^+ m^{-2}. Thereafter, 100 eV D plasma exposure was performed using CDPS at Tohoku University. The thermal desorption spectroscopy was applied to evaluate the D retention behavior after D plasma exposure without air exposure.

The results showed that D desorption was consisted of three desorption stages at 400, 600, 780 K. Comparing to the undamaged W, the D desorption stages were shifted towards higher temperature side and their D desorption rate was quite higher. It can be said that the formation of stable trapping sites by Fe^{2+} irradiation enhances the D trapping in damaged W. For He^+ irradiation, D desorption at lower temperature was enhanced, due to the formation of dense dislocation loops. In case of both sequential Fe^{2+} and He^+ irradiation, D desorption at higher temperature was reduced, comparing to that for only Fe^{2+} damaged W. These facts show that the introduction of He bubbles near surface region refrains D diffusion toward bulk, leading to the reduction of D trapping by voids.

In the presentation, more detail experimental results will be discussed and Hydrogen Isotope Diffusion and Trapping (HIDT) simulation was applied to evaluate D dynamics in damaged W.

Keywords: fuel retention, tritium, plasma exposure, fusion.

[1] Y. Oya et al., J. Nucl. Mater. 461 (2015) 336-340.
[2] Q. Zhou et al., J. Nucl. Mater. 502 (2018) 289-294.

Notes:

Mechanical properties of cellular structures with Shwartz Primitive topology

M. M. Sychov [1,2,*], L. A. Lebedev[1,2], A. A. Evstratov[3], A. Regazzi[3], J. M. Lopez-Cuesta[3]
[1]*Grebenshchikov Institute of Silicate Chemistry, Russian Academy of Sciences, St. Petersburg, Russia*
[2] *St. Petersburg State Technological Institute (Technical University), St. Petersburg, Russia*
[3]*C2MA Ecole des Mines des Ales, Ales, France*
**msychov@yahoo.com*

Cellular structures with triply periodic minimal surface (TPMS) topology are studied in current research work. Previously, it was shown that materials with TPMS topology have a potential as a lightweight material in energy-absorbing systems that can be used in various applications such as protective layer landing pods of spacecraft [1-3].

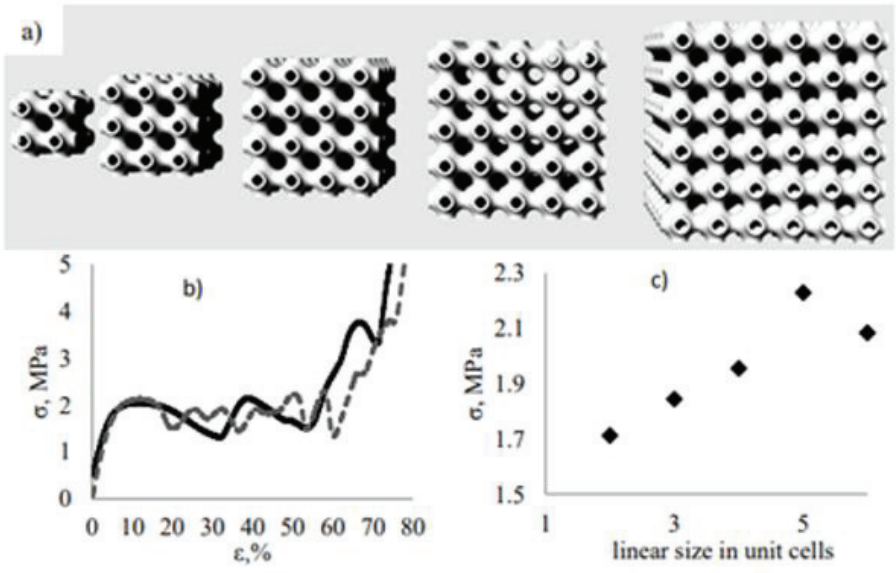

Fig. 1. Schwartz primitive: a) tested samples; b) stress-strain curves; c) stress depending on number of unit cells

In this work Schwartz primitive structure was chosen to study an influence of scale factor and unit number and fill factor on mechanical properties. Samples were made by selective laser sintering process of polyamide powder and tested on Walter+bai ag LFM – 400 kN machine. Example of stressstrain behavior of fabricated samples is shown on the Fig.1.

Keywords: additive manufacturing, TPMS, minimal surface, mechanical properties.

The work was financially supported by the Russian Science Foundation (project no. 17-13-01382).

[1] V.Ya. Shevchenko, M.M. Sychev, A.E. Lapshin, L.A. Lebedev, Glass Physics and Chemistry 43 (2017) 06, 605–607.
[2] V.Ya. Shevchenko, M.M. Sychev, A.E. Lopatin, L.A. Lebedev, A.A. Gruzdkov, A.M. Glezer, Glass Physics and Chemistry 43 (2017) 06, 608–610 [3] M.M.Sychov, L.A.Lebedev,S.V.Dyachenko, L.A.Nefedova, Acta Astronautica (2018), In Press, https://doi.org/10.1016/j.actaastro.2017.12.034.

Notes:

Deuterium removal efficiency in tungsten as a function of hydrogen ion beam fluence and temperature

M. Zhao[1,*], Q. Zhou[2], M. Nakata[3], A. Togari[3], F.Sun[2], Y. Hatano[4], Y. Oya[3]
[1]*Graduate School of Science and Technology, Shizuoka University, Shizuoka, Japan*
[2]*Faculty of Science, Shizuoka University, Shizuoka, Japan*
[3]*Graduate School of Science, Shizuoka University, Shizuoka, Japan*
[4]*Hydrogen Isotope Research Center, University of Toyama, Toyama, Japan*
[*]*zhao.mingzhong.17@shizuoka.ac.jp*

Tritium (T) retention in plasma facing material is an important issue for fusion reactors due to the safety limitation of total T retention and T self-sufficiency. The effective T removal method can prolong the working time of plasma facing component. Hydrogen isotope exchange is considered as one of effective ways to reduce T retention in materials. Various hydrogen isotope exchange experiments using plasma [1] and neutral hydrogen (H) gas [2] have been performed in tungsten (W) which is one of the candidate plasma facing materials for fusion reactor. The results show that deuterium (D) retention in W can be removed by H and the removal efficiency is associated with fluence and temperature. However, the energy of hydrogen isotope particles ranges from several eV to keV in fusion reactor. The formation of defects under energetic hydrogen isotope implantation will complicate the hydrogen isotope exchange behaviour. There are few reports on the hydrogen isotope exchange behaviour in W under the action of energetic hydrogen isotopes.
In this paper, successive 3 keV D and H ion implantation with different fluence and temperature have been performed to obtain the D remove efficiency in W. To understand the hydrogen isotope exchange behaviour, the D signal is measured in situ during H implantation by quadrupole mass spectrometer (QMS). The D retention in W is analyzed by thermal desorption spectroscopy (TDS). The D removal efficiency as a function of depth in W is studied using glow discharge optical emission spectroscopy (GDOES). The deuterium removal efficiency is discussed under various hydrogen implantation parameters.

Keywords: Tungsten, Hydrogen isotope exchange, Ion implantation, Deuterium removal.

[1] T. Watanabe, et al., J. Nucl. Mater., 463 (2015) 1049-1052.
[2] S. Markelj, et al., J. Nucl. Mater., 469 (2016) 133-144.

Notes:

The numerical study of co-existence effect of thermal and solutal Marangoni convections in a liquid bridge

C. Jin[1], A. Sekimoto[1], Y. Okano[1,*], H. Minakuchi[2]
[1]*Dept. of Materials Engineering Science, Osaka University, 1-3, Machikaneyama, Toyonaka, Osaka 560-8531, Japan*
[2]*Dept. of Mechanical Systems Engineering, University of the Ryukyus, 1 Senbaru, Nishihara, Okinawa 903-0213, Japan*
**okano@cheng.es.osaka-u.ac.jp*

Marangoni convection is a flow along the free surface between two fluids due to the variation of surface tension, which is mainly caused by temperature and/or concentration gradients, namely thermal and/or solutal Marangoni convection(s). During the crystal growth, Marangoni convection may induce the striation and affect the quality and purity of growing crystal. Therefore, it is necessary to understand the convective phenomenon and control it. In this study, the floating-zone was considered (Fig.1). A three-dimensional configuration of the half-zone liquid bridge (Fig.2) in the crystal growth of SixGe1-x was selected by establishing the temperature and concentration differences. The equations of continuity, momentum, energy and mass transfer were solved by the PISO algorithm in the OpenFOAM [1]. Thermal and solutal Marangoni convections were set to flow in the opposite direction under zero gravity in the melt with different Marangoni numbers. Fig.3 shows when *Ma*C is larger than -*Ma*T, the flow is steady and axisymmetric, while *Ma*C is smaller than -*Ma*T, the flow is unsteady and irregular. As for the control of Marangoni convection, rotation of top and bottom plane in the liquid bridge was applied in the numerical simulation during the crystal growth. With different rotation speeds and directions, the suppression of Marangoni convection can be effectively realized by the appropriate forced rotation.

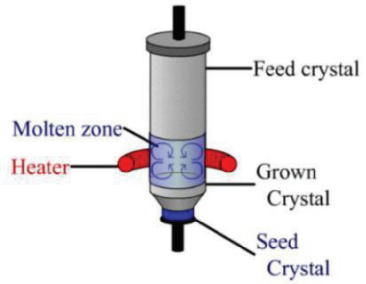

Fig. 1. Floating-zone technology

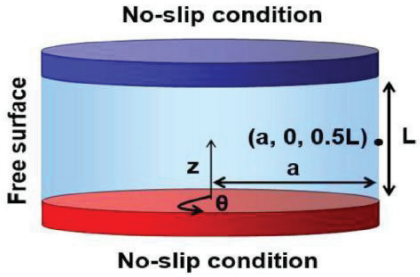

Fig. 2. Schematics of the half-zone liquid bridge [2]

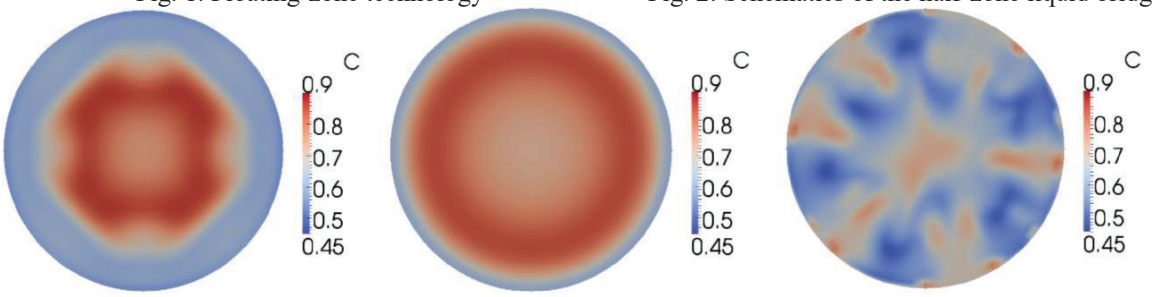

(a)*Ma*T =0, *Ma*C =1072 (b)*Ma*T = -700, *Ma*C =1072 (c)*Ma*T = -1750, *Ma*C =1072

Fig. 3. Concentration distribution at different time with Ma_C =1072 in the *r*-*θ* plane at the height of 0.5L

Keywords: Marangoni convection, Liquid bridge, Opposite direction, Plane rotation.

[1] H. Minakuchi et al., Journal of Crystal Growth, 385(2014), 61-65.
[2] H. Minakuchi et al., Journal of Crystal Growth, 468(2017), 502-505.

Notes:

Recovery of the workpiece material in ECM of sintered carbide

S. Wang[1], A. Goto[2,*], A.Nakata[2], K. Hayakawa[1], K. Sakai[1]
[1]*Shizuoka University, 3-5-1 Johoku, Naka-ku, Hamamatsu, Japan*
[2]*Shizuoka Institute of Science and Technology, 2200-2 Toyosawa,Fukuroi, Japan*
[*]*goto.akihiro@sist.ac.jp*

In this study, authors tried to develop a method to recover the material of ECMed sintered carbide. When workpiece material is dissolved into the electrolyte, it is assumed ECM performance is affected by the change of the electrolyte ingredient. Besides, tungsten and cobalt are precious material. In this report, feasibility of recovery of these two material changing soluble material into insoluble one was investigated, in which process tungsten as calcium tungstate and cobalt as cobalt hydrate. It was found that the tungsten compounds and cobalt compounds could be recycled by these processes.

Keywords: ECM, Sintered Carbide, Recovery.

Notes:

Numerical Simulation of Shaking Optimization in a Suspension Culture of iPS Cells

K. Elvitigala[1], Y. Kanemaru[1], M. Yano[1], A. Sekimoto[1], Y. Okano[1,*] and M. Kino-Oka[2]
[1]*Dept. of Materials Engineering Science, Osaka University, 1-3, Machikaneyama, Toyonaka, Osaka 560-8531, Japan*
[2]*Dept. of Biotechnology, Osaka University, 1-2, Yamadaoka, Suita, Osaka 565-0971, Japan*
**okano@cheng.es.osaka-u.ac.jp*

Researches on induced pluripotent (iPS) cell have attracted attention due to their remarkable progress in regenerative medicine. Cost and quality are two main factors to be considered when using iPS cell in biological applications in a large scale. In this study, suspension culture of iPS cells was numerically simulated in a cylindrical tank under the two-different shaking methods; one-directional rotation and alternate rotation. Computational Fluid Dynamics (CFD) and Discrete Element Method (DEM) were coupled and Volume of Fluid (VOF) method was used to track the free surface. The governing equations; continuity, momentum, energy and mass transfer equations were solved by the PISO algorithm and OpenFOAM open source software [1] was used for the simulation. Because iPS cells differentiate according to the shear stress strength, shear stress was calculated in terms of slip velocity. The average slip velocity of one-directional rotation and alternate rotation were reduced to steady state while oscillating from the point where shaking was initiated (Fig. 1). However, one-directional rotation resulted a lower average slip velocity than that by the alternate shaking. Also, two shaking methods exhibited a significant difference in the average number of cells accumulated in the bottom (R_B). Even though the one-directional rotation method suppressed the shear stress acting on iPS cells, after four seconds it accumulated more cells in the bottom than the alternate rotation method (Fig. 2).

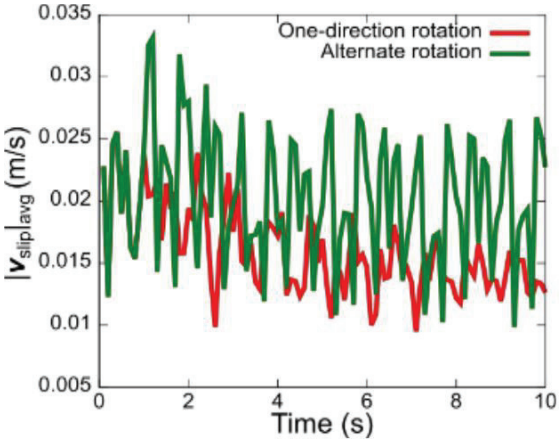

Fig. 1. Time development of average slip velocity

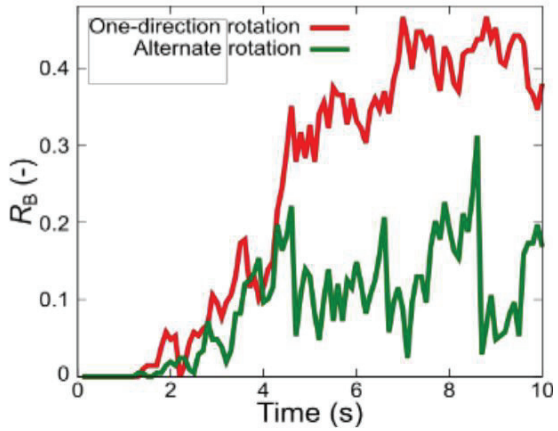

Fig. 2. Average number of cells in the bottom

Keywords: iPS cell, Numerical simulation, Suspension culture.

[1] T. Yamamoto, M. Yano, Y. Okano, M. Kino-Oka, Journal of Chemical Engineering of Japan (2017), Vol. 44, No. 1, pp. 1-7.

Notes:

Re-examination of the concept of "Primary Energy" and problems on the introduction system of renewable energies in Japan

S. Matsuda[1*] and H. Kubota[2]
[1]*Graduate School of Science and Technology, Shizuoka University, Hamamatsu 432-8561, Japan*
[2]*Tokyo Institute of Technology, Tokyo, Japan*
[*]*matsuda.satoshi@shizuoka.ac.jp*

It is important for us to marshal the basic concept for energy issues in order to discuss this problem objectively, quantitatively and logically. For example, the term "primary energy" is always used, but the method of calculation of "primary energy" as an oil-equivalent is not so easy. According to the definition by IEA [1], 1 toe (tonne of oil equivalent) = 41.87 or 42 GJ = 11.63 MWh = 7.11 or 7.33 or 7.4 barrel of oil equivalent, 1 tonne of coal equivalent = 0.7 toe, these values are based on the caloric value of oil. This means 1 MWh = 3.6 GJ = 861 Mcal, which is physically true when electricity is consumed and converted to waste heat. But 1 MWh of electricity can not be generated from 861 Mcal of heat, because the efficiency of electric power generation is never 100 % but 30 to 42 % in most thermal power plants. Thus, the primary energy value of 1 MWh electricity should be 2050 (=861/0.42) to 2870 (=861/0.30) Mcal of oil-equivalent [2]. This is why the energy conversion factor should not be 861 but 2050 to 2870 when we calculate the amount of primary energy (toe) from the electricity consumption (MWh). The situation is more complicated when electricity is generated from renewable energies such as hydro, wind and solar, because these energy sources do not consume fuels(oil, goal or natural gas) which have certain caloric value and can be converted to the primary energy (toe). But an appropriate conversion factor should be decided to estimate the primary energy consumption (toe) in order to analyze the structure of energy demand, supply and consumption quantitatively. In particular, since most energy sources in the "Society independent of fossil fuel" will be renewable energies, a logical methodology of calculating "primary energy" will be important in order to estimate and select a better renewable energy source and secondary energy. In this report, the differences in the values of total primary energy between the IEA and our calculation will be disclosed.
And also, other concepts are valuable such as "net effective energy ratio", "energy yield" to evaluate the effectiveness of renewable energies quantitatively, and "marginal cost of power facility" to introduce renewable energies without FIT(Feed-in Tariff) mechanism [3]. In this report, these concepts will be discussed using concrete model case studies and how to select a better renewable energy can be selected in terms of energy balance and economical point of view.

Keywords: "Primary Energy" concept, energy conversion rate, Oil-equivalent, Renewable energies.

[1] IEA(International Energy Agency). World energy balances: Overview 2017. www.iea.org/publications/freepublications/publication/WorldEnergyBalances2017Overview.pdf
[2] The Energy Data and Modiling Center (in Japan). Handbook of Japan's & World Energy & Economics Statistics, 2017 ver.
[3] S. Matsuda et. al. Advanced Materials Reseadch 1117 (2015), 307-310.

Notes:

To the Problems of Detecting Signals Passing Through a Random Phase Screen

N.Kh. Gomidze, M.R. Khajishvili*, I.N. Jabnidze, K.A. Makharadze, and Z.J. Surmanidze
Batumi Shota Rustaveli State University, Batumi, Georgia
*mirandukht@gmail.com

The goal of the present work is to study the regulations of the changes of the characteristics of high frequency optical signals using both quantitative and qualitative terms, on the basis of changes statistical parameters of turbulent media on the random phase screen model. There is an analytical assessment of statistical moments of laser radiation via random phase screen by numerical modeling and comparison with known experimental results. The object of the study is a random inhomogeneous atmosphere with weak turbulence, as well as optically dense turbulent media. The model of a random phase screen is discussed and the distribution of the statistical moments of scattered laser radiation is studied. The dependence of the effective size of the laser beam and the scintillation index on the correlation radius of the phase screen in the plane of the detector for a random phase screen is estimated.

Let's say, on the $z=0$ plane the primary $u_0=\exp(ikz)$ field statistics (its moments, coherence function) are given. It is necessary to find out how these functions are changing away from the $z=0$ plane (Fig.1), if on the way the field is transformed (for example, the wave is going through a diaphragm, lens or other).

The phase screen is of a small thickness, scattered radiation is registered in the distant zone through the photo detector. The photo detector axis makes θ angle of the laser beam (Fig. 2).

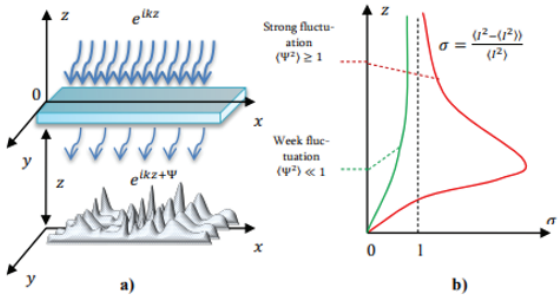

Fig. 1. a) Distribution intensity of wave threw random phase screen. b) Dependence scintillation index on distance from random phase screen for week $\langle\Psi^2\rangle \ll 1$ and strong $\langle\Psi^2\rangle \gg 1$ fluctuation of phase

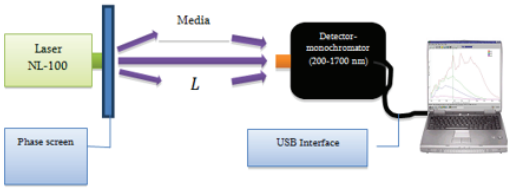

Fig. 2. An experimental device scheme for studying partially coherent laser beam in the free space or in the turbulent media. L>> L_f, L_f – is the distance from diffuser to the detector, the L_f – the focal length of the optical system

The laser beam size, intensity, correlation radius and the expressions of the angle of fluctuations are obtained in the plane of the detector. It is shown that the laser beam size, the correlation radius and the average intensity of the radiation coincide with the classical results. However, the results obtained in the turbulence of the atmosphere somewhat differ from the classical results. The effect of diffusion on the scintillation has been studied. The scintillation index is obtained in the free space of laser beam, as well as in the weak turbulence atmosphere. In case of a strong diffuser, the model shows that the index is close to 1.

Keywords: Random phase screen, Square detector, Fourier transform, Scintillation index.

Notes:

Full dynamics and optimization of a controllable minimally invasive robot for soft tissue surgery and servicing the artificial organs

G. Ilewicz[1,*], A. Harlecki[1]
[1]*Faculty of Mechanical Engineering and Computer Sciences, University of Bielsko- Biała, Bielsko- Biała, ul. Willowa 2, Poland*
[*]*gilewicz@ath.bielsko.pl*

Minimally invasive robots are currently used during operations of human body in the entire world. There are various important mechanical quantities in the designing process of the medical robot structure, such as the dynamic safety factor, which is calculated in this following article. Matlab program was used to calculate the torque in every joint with a DC motor, controlled with PID regulator for a given trajectory.

Fig.1. Mechanical model of the medical robot and steering system with DC motor in Simulink

Trajectory allows the effector to move in the tunnel of tissue inside the patient's chest (tunnel was obtained by using 3D Slicer computer program and CT scan diagnostics). Subsequently, the FEM (finite element method) was applied to calculate transient conditions during the deformation of robots' structure (RRRS). Numerical experiment of multi-objective optimization is presented in the work, where two criteria, during the calculation, are very significant stiffness and mass for multibody effector of medical robot in motion, taking into account the inertia, damping and stiffness reactions.

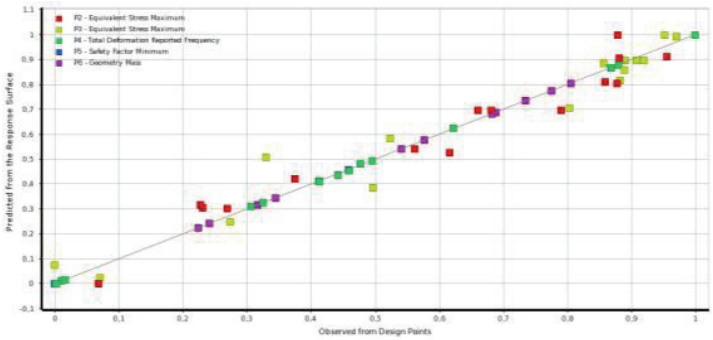

Fig. 2. Goodness of fit of criterions for optimization process

The Pareto optimum for these criteria is calculated by using a genetic algorithm and responce surface. The mini robot effector is finished with a scalpel.

Keywords: medical robot, optimization, genetic alghoritm, PID controller, CT scan.

[1] G. Ilewicz. Multibody model of dynamics and optimization of medical robot to soft tissue surgery, Advances in Intelligent Systems and Computing, vol.393, pp. 129-134, Springer, Switzerland 2016, Inter-Academia 16.
[2] G. Ilewicz. Modeling and controlling medical robot for soft tissue surgery and servicing the artificial organs, Proceedings of the 17th Mechatronika 2016, IEEE, pp.102-107, Prague 2016.
[3] G. Ilewicz. Natural frequencies and multi - objective optimization of the model of medical robot with serial kinematical chain. Advances in Inteligent Systems and Computing vol. 519, pp. 371-379, Springer, Switzerland 2017.

Notes:

Feasibility study of a neutron detector made of boron-doped diamond using Monte Carlo simulation

T. Miyake, T. Masuzawa*, H. Nakagawa, T. Aoki, and H. Mimura
Shizuoka university, 3-5-1 Johoku, Naka-ku, Hamamatsu 432-8011, Japan
** masuzawa.tomoaki@shizuoka.ac.jp*

Neutrons are used in accelerators, nuclear reactors, non-destructive inspections, etc. Neutrons can penetrate through heavy elements, which gamma rays are relatively less permeable. Thus neutron imaging is highly demanded as an image technology complementary to X-ray imaging. Current technical issues of neutron image sensors is that the image sensors tend to be large and hard to move, due to the limited sensitivity.
We propose a solid-state neutron detector using boron (B)-doped diamond. By using boron as neutron-charge converter, large capture cross section of neutron owing to 10B (n, α) is expected. In addition, both B and carbon (C) have relatively small atomic number, reducing noise from unintended gamma-ray capturing. Furthermore, electrical/thermal properties of diamond are attractive for sensor applications, such as wide band gap, high dielectric breakdown voltage, and excellent thermal conductivity.
In previous research, diamond is used for fast neutron detection [1]. In this research, we focus on B-doped diamond for improvement of thermal and epithermal neutron sensitivity.
We have employed a Monte-Carlo simulation to calculate a capture rate when neutron beam is irradiated to B-doped diamond. A simulation code, PHITS, was used for the calculation [2]. Neutron beams and gamma rays were irradiated to the structure in which 4.7% (molar concentration) of B was added to the diamond, and its penetration depth was calculated. The simulation results showed that the capture rate increased drastically as the beam penetrate into the B-doped diamond. At 3 mm from the diamond surface, more than 85% of incident neutrons were captured, whereas γ ray absorption was below 3%. The result confirmed a feasibility of B-doped diamond as a neutron detector material.

[1] T. Shimaoka, J. H. Kaneko, K. Ochiai, M. Tsubota, H. Shimmyo, A. Chayahara, H. Umezawa, H. Watanabe, S. Shikata, M. Isobe, and M. Osakabe, Rev. Sci. Instrum. 87 (2016) 023503.
[2] T. Sato, Y. Iwamoto, S. Hashimoto, T. Ogawa, T. Furuta, S. Abe, T. Kai, P. Tsai, N. Matsuda, H. Iwase, N. Shigyo, L.Silver, K. Niita, J. Nucl. Sci. Technol. 55 (2018) 684-690.

Notes:

A Statistical Study on the Origin of Dopant Clusters in Highly-Doped Si Nanoscale *pn* Tunnel Diodes

G. Prabhudesai[1,2], G. Greeshma [1,2], M. Tabe[1], and D. Moraru[1,*]
[1]*Research Institute of Electronics, Shizuoka University, 3-5-1 Johoku, Hamamatsu, Japan*
[2]*Graduate School of Integrated Science and Technology, Shizuoka University, Japan*
[*]*moraru.daniel@shizuoka.ac.jp*

Band-to-band tunneling (BTBT) is a promising mechanism for tunnel diodes [1,2] and tunnel field-effect transistors (TFETs) [3], structures that can suppress thermally-activated current that hinders the observation of quantum tunneling effect. Furthermore, BTBT mechanism can be enhanced by tunneling via dopant energy states, if available [4]. However, the observation of suitable dopant states at Si *pn* junctions is difficult because of the high built-in electric field. Such dopant states would be suitable if they are deep enough to efficiently mediate BTBT transport.

In this work, we show that such deep dopant states are statistically available at suitable positions in the depletion region of nanoscale (2D) *pn* diodes, doped with high doping concentration (on the order of 1×10^{20} cm^{-3}) with phosphorus (P) as donors and boron (B) as acceptors. Due to proximity of counter-part dopants, a large fraction of the dopants are effectively compensated and their energy states remain shallow. The remaining fraction, however, have a finite probability of coupling to dopants of the same type, giving rise to energy states that are deep enough to appear within the transport window even at small biases. It is in fact expected that the energy levels of such few-dopant clusters can be several hundreds of meV below (above) conduction (valence) band edge [5].

We will discuss the nature of the resulting dopant clusters, their preferential orientation, and transport mechanisms. We will also show experimentally that such dopant states significantly modulate the BTBT transport in nanoscale *pn* tunnel diodes. These results can open a new research pathway toward molecular-level electronics fully utilizing quantum tunneling transport.

Keywords: dopant-atom, *pn* tunnel diodes, band-to-band tunneling, dopant-cluster.

[1] H. Schmid et al., “Silicon nanowire Esaki diodes”, Nano Lett. 12, 699 (2012).
[2] M. Tabe et al., “Atomistic nature in band-to-band tunneling in two-dimensional silicon pn tunnel diodes”, Appl. Phys. Lett. 108, 093502 (2016).
[3] A. M. Ionescu and H. Riel, “Tunnel field-effect transistors as energy-efficient electronic switches”, Nature 479, 329 (2011).
[4] T. Mori et al., “Study of tunneling transport in Si-based tunnel field-effect transistors with ON current enhancement utilizing isoelectronic traps”, Appl. Phys. Lett. 106, 083501 (2015).
[5] B. Weber et al., “Spin blockade and exchange in Coulomb-confined silicon double quantum dots”, Nature Nanotechnol. 9, 430 (2014).

Notes:

Photoconversion efficiency in solar cells based on heterostructures ITO-Si with Au nanoparticles

A.O. Mykytiuk[1,2,*] and S.V. Kondratenko[1]

[1]*Taras Shevchenko National University of Kyiv, Faculty of Physics, Chair of Optics, 64/13 Volodymyrska Str., 01601 Kyiv, Ukraine*

[2]*State enterprise of a special instrumentation "Arsenal", 8, Moskovska Str., 01010 Kyiv, Ukraine*

[*]*mykytiuk_nastya@ukr.net*

Nowadays, solar energy is considered as a promising tool for solving the global energy crisis. Among the technologies aimed at increasing the efficiency of solar cells, two main directions are presented: tandem solar cells and solar cells based on heterojunctions [1,2]. However, often the actual values of the efficiency of such solar cells are much smaller than the theoretical limit. The deposition of nanoparticles of noble metals, e.g. Au, on the surface of solar cells is a promising method for increasing light absorption in the spatial charge due to the excitation of surface plasmons in metallic nanoparticles [3,4].

The aim of our work is to find out the influence of nanostructured Au film on the efficiency of photoconversion and the lifetime of nonequilibrium charge carriers in solar cells based on ITO-Si heterostructures. Our samples were grown by the magnetic sputter deposition method in vacuum. The surface of ITO was covered with a thin layer of Au. To create Au nanoparticles with diameters of 5, 10 or 20 nm the annealing at 300°C was used. The shape of nanoparticles was controlled by means of atomic-force microscope Integra (NT-MDT) with Si tip with radius of 10 nm.

We investigated the spectral dependences of optical absorption of Au-ITO films and photoconductivity of Au-ITO-Si heterostructures and also the kinetics of photovoltage relaxation after photoexcitation with light pulses. Spectral and time dependences of photovoltage were studied at temperatures in the range 80-290 K.

We observed that covering the surface of ITO with a layer of Au nanoparticles leads to increasing of the photovoltage amplitude due to increasing of the potential barrier height in the system. Excitation of the surface plasmons leads to increasing of the efficiency coefficient due to the effects of local amplification.

The short-circuit current of solar cells has been reduced after the deposition of Au films due to the absorption and reflection of a part of the light with Au films. However, in some heterostructures, the optical losses in the Au film were compensated by the effect of plasmon amplification, which determined its highest efficiency.

Also, the deposition of a nanostructured Au film leads to increasing of the lifetime of nonequilibrium charge carriers compared to the initial structure of ITO due to the creation of electrostatic potential variations in the near-surface Si region. At the same time, the effects of plasmon amplification do not affect the observed relaxation times of photovoltage.

Keywords: solar cell, photovoltage, heterostructures ITO-Si, nanoparticles.

[1] W. Shockley and H.J. Queisser, J. Appl. Phys. 32 (1961) 510.
[2] A. Luque and A. Martí, Phys. Rev. Lett. 78 (1997) 5014.
[3] A. Polman, Opt. Express, 16 (2008) 1793.
[4] H.A. Atwater and A. Polman, Nat. Mater. 9 (2010) 205.

Notes:

Photocatalytic activity of ZnO-loaded titania nanotube arrays: structural, morphological and compositional effects

M. Dobromir[1,*], C.T. Teodorescu-Soare[2], R. P. Apetrei[2], V. Pohoață[2], G. Stoian[3], D. Luca[2]
[1]*Department of Research, Faculty of Physics, Alexandru Ioan Cuza University of Iasi, 11 Carol I Blvd., 700506, Iasi, Romania;*
[2]*Faculty of Physics, Alexandru Ioan Cuza University of Iasi, 11 Carol I Blvd., 700506, Iasi, Romania;*
[3]*National Institute of Research and Development for Technical Physics, 47, Dimitrie Mangeron Blvd., 700050, Iasi, România*
[*] *marius.dobromir@uaic.ro*

Titania nanotube materials continue to attract scientific and technological interest, owing to large specific photo-active area and controllability of the physical and chemical characteristics. By using cheap technical means, such as self-organized anodic oxidation, titania nanotube arrays (TNA) were already proposed, among others, as materials for photocatalytic pollutant degradation, solar energy conversion, lithium battery, or bacteria killing [1-3]. The beneficial characteristics of the TNA can be further enhanced via surface modifications, doping or by decorating with suitable oxide or noble metal materials. In line with this latter research direction, we report here on the effects of loading of TNA with ZnO non-contiguous films, on the structure, morphology and composition of the nanotube array. Further on, the effects on the photo-catalytic performance were evaluated during the degradation of a standard pollutant - methylene blue, for which a standard ISO procedure was adopted.
TNA were prepared here by static electrochemical anodization of Ti foils using a NH_4F-glycerine electrolyte in a standard electrochemical cell configuration. ZnO non-contiguous ultra-thin films were deposited on top of TNA by plasma-assisted reactive RF ion sputtering of a Zn target in a discharge in Ar-O_2 gas mixture. By changing the ZnO deposition time, samples with different ZnO coverage were prepared and their characteristics were evaluated vs. the non-modified TNA reference counterpart. Annealing the decorated samples for 1h at 450 °C in air, resulted in a predominant anatase and weak rutile ordering of the samples. While the non-loaded samples reveal the formation of nanotubes with nearly cylindrical openings, 80 - 87 nm in diameter and approx. 1.6 m long, the FESEM images of ZnO-loaded samples show increasing coverage of this material on the TNA layer. The variation in the top surface morphology and the columnar structure of the TNA-loaded samples are reflected in the shape of the UV-Vis light absorption spectra of the MB solution and in its kinetics of degradation. The bleaching rate of the methylene blue is increased by a factor of 1.3 by increasing the ZnO coverage, within our experimental limits. The association of the two oxides and the implications of the oxide coupling are discussed in the full-size manuscript. The current results demonstrate a promising way to design improved photocatalytic performance devices for technological applications in environmental area.

Keywords: TiO_2 nanotube arrays, ZnO, photocatalytic degradation, methytlene blue.

[1] J. M. Macak, H. Tsuchiya, A. Ghicov, K. Yasuda, R. Hahn, S Bauer, P. Schmuki, Curr. Opin. Solid State Mater. Sci. 11 (2007) 3-18.
[2] K. Huo, X. Zhang, H. Wang, L. Zhao, X. Liu, P. K. Chu, Biomaterials, 34(13) (2013) 3467-478.
[3] D. Strbac, C.A. Aggelopoulos, G. Strbac, M. Dimitropoulos, M. Novakovic, T. Ivetic, S. Yannopoulos, Process. Saf. Environ. 113 (2018), 174–183.

Notes:

An Application of The Nash Equilibrium to an Experimental Setting: The Real Meaning of the Sacrifice Move in Board Games

N. Igarashi[1], R. Yamamoto[2], V. A. Wilkinson[1*]
[1]*Shizuoka University, Faculty of Informatics 3-5-1 Johoku, Naka-ku, Hamamatsu, Japan*
[2]*Sanyou-onoda City University 1-1-1 Daigaku-dori, Sanyo Onoda, Yamaguchi, Japan*
[*]*vwilk@inf,shizuoka.ac.jp*

The following is an account of one student's research about the game of shogi. First we explain the context: Faculty of Informatics was a brand new kind of faculty in 1995. The mandate of the founding members was to create an educational environment with requisite variety to nurture undergraduates in science, technology, engineering and mathematics (STEM). The Faculty with two departments, Computer Science (CS) and Information Arts (IA), was also building laboratories for graduates who chose to pursue the master degree. From the beginning, the CS program had a framework and labs for the 60% of undergraduates who chose to continue into graduate school. The IA program, with no such framework, was an innovative mix of languages, social sciences, and media. The whole faculty was a "simulation" for establishing a viable institution of higher learning. Supervision and protocol made it possible for irregular procedures to accommodate the interests of developing CS students. Programming is an essential first class for all CS students; TAs assist large programming classes. Graduate students function as coaches as well as technical assistants, thus developing hierarchical relations. In this context, in July of 2013 a CS student chose IS EVENT/GAME lab for undergraduate graduation preparation. The native speaker of English language, who supervises the lab, has keywords General Systems Theory (GST) experiential learning, game theory (GT) experiential learning and requisite variety, etc. We presented a paper on 1st and 2nd order cybernetics at Iasi 2017 [1]. Educational environment impacts strategic learning [2], at the level of student, faculty and university. The three characters in this narrative are researchers with different ages, grade levels, and keywords.

1. B4 Computer Science (CS) student selects "GT lab" and Nash Equilibrium for research.
2. MS Program (TA) whose programming keyword is educational environment.
3. Communication supervisor (DIR) is doing research in GST, 2nd order cybernetics and GT.

In this research we show how the Nash equilibrium can explain the sacrifice move in a comprehensible setting. The players and stakeholders hold differing roles in the experimental environment: DIR job is to provide a praxis of requisite variety, not only for one undergraduate taking a BS degree in Informatics (CS), but a layered educational environment for STEM students, "freshers" through graduate school. In that sense, the actual, real-life student provides a case study, a "proof of concept" for the total curriculum of Informatics. This story is a kind of parable, a learning story with a template. B4 needed an experimental environment for experiments. B4's main interest is the board game Shogi. We set up a shogi table at the Shizuoka University Festival in our Game Space. We also set up a long term experiment of 6 - 8 weeks of playing the game of Hearts, keeping score sheets. When we evaluated the score sheets, we thought the experiment failed. Reflection showed a clear equilibrium pattern. Level/phase charts, Venn diagrams, and experiment results form part of the planned paper.

Keywords: board-games, sacrifice move, game theory, 2nd order cybernetics, educational environment.

[1] Wilkinson, Valerie. "An Exercise in First and Second Order Cybernetics: the 18th Year of the General Systems Theory (GST) Communication Project." Iasi, Inter-Academia 17. Pp. 334-340.
[2] Young, H. Peyton. Strategic Learning and Its Limits. (1982).

Notes:

Assessment of renewable energy systems in northern philippines using geospatial toolkit

C. Pascual[1,*], M. Delos Santos[2], and M.Valenzuela[3]
[1]*Mariano Marcos State University, Batac City 2906, Philippines*
[2]*MPDO, Dingras, Ilocos Norte*
[3]*MPDO, Adams, Ilocos Norte*
[*]*cmpascual777@gmail.com*

The Philippines Geospatial Toolkit (GsT) is a map-based renewable energy resource data and used geographic information systems (GIS) for energy resource assessment. Such GsT also developed an optimization software HOMER for distributed hybrid power analysis. The new version of the GsT with contained high-resolution remote sensing data, lend more analytical processing time and could explored for assessment of renewable energy systems. Two case studies were presented to explore how the PGsT can be used to assess renewable energy systems in northern part of the country: (1) a site selection for solar panel installation at government buildings in Dingras was conducted for assessing potential solar energy installation from which ideal sites for solar panel placement on building rooftops were determined. Geospatial analysis showed that the average solar energy was 5.25 kW/m² and could generate 4,500 kW on large rooftop buildings; and (2) in town of Adams, the energy power generated from the solar and wind energy was assessed for feasible power plant for the area. Weighted overlaid theme maps of solar power density, slope, landuse and elevation showed varying degrees of suitability of solar energy in the area. On wind energy assessment, overlaid theme maps of wind power density, distance to major road network, distance to inclusionary areas, landuse and slope showed delimitation of suitable areas suited for wind power generation. Using HOMER for optimization of solar-wind hybrid energy systems, revealed shared of 51% for wind and 42% for solar energy production which were feasible with payback periods of 5 years.

Keywords: Geographic information systems, Geospatial Toolkit, HOMER, renewable energy.

[1] Energies. Land Suitability Analysis for Solar Farms Exploitation Using GIS and Fuzzy Analytic Hierarchy Process (FAHP) – A Case Study of Iran. (2016).
[2] Miller, A and R. Li. A Geospatial Approach for Prioritizing Wind Farm Development in Northeast Nebraska, USA https://www.researchgate.net/publication/264040834_A_Geospatial_Approach_for_Prioritizing_Wind_Farm_Development_in_Northeast_Nebraska_USA. (2017).
[3] Meyer, A. 2015. A Case Study: Solar Panels at Boston College by Annie Meyer - httpwww.bc.educontentdamfilesschoolscas_sitesenvstudiespdfStudent%20Research8_Solar_Panels_at_Boston%20College_paper.
[4] NREL. Philippine Geospatial Toolkit. (2016).
[5] NREL, 2010. Geospatial toolkit manual.http://www.nrel.gov/international/geospatial_toolkits.html. (2010).
[6] Noorillahi, Dawud Fadai*, Mohsen Akbarpour Shirazi and Seyed Hassan Ghodsipour. https://www.researchgate.net/publication/306286685_Land_Suitability_Analysis_for_Solar_Farms_Explion_Using_GIS_and_Fuzzy_Analytic_Hierarchy_Process_FAHP_– A_Case_Study_of_Iran.CSP.
[7] Sites Suitability Analysis in the Eastern Region of Morocco by A. Alami Merrounia* , Ab. Mezrhabb, A. Mezrhaba. https://www.sciencedirect.comsciencearticlepiiS1876610214006948. (2015).
[8] USAID. Philippines launches wind energy atlas and geospatial toolkit: A success story. (2015).
[9] USAID. The Geospatial Toolkit: Using Renewable Energy Resource Data and Geospatial Analysis to Explore Clean Energy Opportunities. (2016).
[10] Wang, Q. A GIS-Based Approach in Support of Spatial Planning for Renewable Energy: A Case Study of Fukushima, Japan. https://www.mdpi.com2071-1050642087. (2017)

Notes:

A Parallel Fuzzy Filter Network for Pattern Recognition

B. Tusor[1,2,3,*], A. R. Várkonyi-Kóczy[1,2,3], J. Bukor[3]
[1]*Integrated Intelligent Syst. Japanese-Hungarian Lab*
[2]*Institute of Automation, Óbuda University, Budapest, Hungary*
[3]*Department of Mathematics and Informatics, J. Selye University, Bratislavská Str. 3322, P.O. BOX 54. 945 01, Komárno, Slovakia*
[*]*tusorb@ujs.sk*

Nowadays, pattern recognition is one of the most popular tools to solve classification problems. But as the data for such problems are getting larger, the operational speed of regular classifiers often becomes much slower as well, reducing their efficiency. One solution to this problem is using parallel computing [1] techniques, where the task is divided to smaller processes, which are distributed among multiple devices to be executed at the same time, thus completing the given task in a fraction of the time that is required for the sequential implementation.

In this paper, the parallel improved version of a pattern recognition network is proposed. Its predecessor, the sequential classifier is based on a simple modification [2] of Radial Basis Function Neural Networks [3], where output layer is replaced by an argmax (arguments of the maxima) function, thus changing the functionality from calculating the weighted combination of the hidden layer neurons to finding which neuron is the most similar (its center being the closest) to the input data point. This change essentially turns the network into a fuzzy inference system. The advantage of the system is that it is easy to implement and modify (add or remove rules by adding or removing neurons in the hidden layer), but it is very slow considering higher quantities of training data and problem dimensions. However, it can be parallelized: each neuron (rule) can be processed in parallel.

The training of the classifier is done through parallelized clustering as well: the problem space is divided into labeled areas (i.e. clusters) based on the training data, of which the parameters of each rule are derived. This can be simply done with the combination of circular areas, which should cover as much of the known parts of the problem space as possible. Initially, each training sample is appointed as the center of a cluster (circular area), with its width being half of the distance to the nearest sample that belongs to a different class. The complexity of the calculation of these values sequentially is $O(P^2)$ at best for a training pool of P samples, which is very time consuming for high training data quantities. This, however, can be solved with parallel computing as well: either by using parallel reduction [4] on each sample pairs (which in turn requires a large amount of device memory), or using the heuristics that for each sample only the distance to closest ones need to be regarded, starting from the sample point and gradually extending the search zone. Then the resulting, significantly shorter lists are used for parallel reduction. Finally, clusters that are mostly covered by other clusters are removed, thus reducing the number of insignificant rules.

During the tests, the improved method has demonstrated a much faster operation than its predecessor, without any decrease in classification performance.

Keywords: classification; machine learning; pattern recognition; parallel computing.

[1] D.E. Rumelhart, J. McClelland, Parallel Distributed Processing: Explorations in the Microstructure of Cognition, Cambridge: MIT Press (1986).
[2] B. Tusor, A.R. Varkonyi-Koczy, A Hybrid Fuzzy-RBFN Filter for Data Classification, Advanced Materials Research, 1117 (2015) 261-264.
[3] M.D. Buhmann, Radial Basis Functions: Theory and Implementations, Cambridge University Press (2003) 272.
[4] M. Cole, Bringing skeletons out of the closet: a pragmatic manifesto for skeletal parallel programming, Parallel computing, 30 (2004) 393.

Notes:

Research on Functional Materials for Energy Conversion Devices: Photovoltaics and Mechanoluminescence

K. Murakami*
Department of Engineering, Graduate School of Integrated Science and Technology, Shizuoka University, Naka-ku Hamamatsu, Japan
*murakami.kenji@shizuoka.ac.jp

Energy can be converted from one form into another. Solar cell is a well-known example of the energy conversion device that converts light energy to electrical energy. We have been engaged in the researches on dye-sensitized solar cells and mechanoluminescent materials, the latter is the material which convert mechanical energy to light energy.

In the present talk, I introduce two topics regarding to the title: Firstly, novel transparent conducting oxide (TCO) nanostructures for applying to the dye-sensitized solar cells. Secondly, novel organic mechanoluminescent materials with different color emissions.

Various nanotechnological architectures of the fluorine-doped tin oxide (FTO) layers have been formed on a glass substrate by using an advanced spray pyrolysis deposition (ASPD) technique. This technique allows for the perfect control of morphology of nanotechnological architectures of FTO, which can be achieved simply by controlling spray angle and spray duration. As such, 0-D nanocrystallites, 1-D uncapped nanorods and 1-D capped nanorods; all in 2-D thin layers, and extensively cross-linked 3-D nano-technological architectures of FTO can be prepared, on soda lime glass surfaces. This is the first report on kinetically-controlled growth of different nanotechnological architectures of FTO, using the same technique. Furthermore, the technique is versatile and is not limited only to fabricate FTO nanostructures, but, it can also be used to fabricate thin layers of nano-technological structures of different dimensionalities of various materials on various substrates, which is capable to withstand required pyrolytic temperatures. Aluminum or gallium-doped zinc oxide (AZO or GZO) nanorods are also directly formed on the soda lime or FTO glass surface by using the ASPD technique.

Mechanoluminescence (ML) is a phenomenon that light emission is induced by a mechanical action on a solid. Europium-doped dibenzoylmethide triethylammonium (EuD_4TEA) has been known as an organic ML material. We have succeeded to synthesize EuD_4TEA at a very low temperature of 70 °C using controlled slow cooling method. An addition of polyvinylpyrrolidon has enhanced the emission intensity. Orange light emission (612 nm) is detected by grinding the materials. We have also synthesized new organic mechanoluminescent material based on the phenanthroline, the acetylacetone and triethylamine with terbium (Tb) doping. This material emits the green light (545 nm) by the mechanical action. Co-doping of Tb and dysprosium (Dy) enhances its ML.

Details of properties and structures will be discussed for the synthesized materials.

I am deeply grateful to my all students and co-workers, in particular, Dr. A. Bandara and M. Ranasinghe, Prof. M. Shimomura, Assoc. Prof. M. Okuya, Shizuoka University and Profs. O. Illeperuma and G. Rajapakse, University of Peradeniya, Sri Lanka.

Notes:

Modeling of properties of single chamber fuel cell components

A.Galdikas*, G. Kairaitis, T. Moskaliovienė, K. Bočkutė, D. Virbukas, M. Sriubas, V. Kavaliūnas, M. Kaminskas, G. Laukaitis, K. Petruškevičius

Kaunas University of Technology, Faculty of Mathematics and Natural Sciences, Department of Physics, Studentu g. 50, LT-51368 Kaunas, Lithuania

*arvaidas.galdikas@ktu.lt

Different methods are used for modeling of the properties of single chamber fuel cell components. The morphology and structure of solid electrolyte prepared by electron beam evaporation method is modeled by using Mote Carlo simulations and phase separation modeling based phase filed theory and Cahn-Hilliard equation. Both methods let to model surface roughness of ionic electrolyte which influences ion conductivity. Most convenient way to model surface roughness is by using island film growth model. This model separates adsorption processes on various surface formations and involves island coalescence process, and lets to analyze different modes of film growth from layer by layer till 2-d and 3-d island growth. This method is very useful to analyze the processes of formation of island like electrodes deposited on surface of electrolyte. The Ion conductivity of solid electrolyte is modeled by using so called Brick-Layer model which relates impedance with various kinds of diffusion processes: surface diffusion, bulk diffusion, grain boundary diffusion. The dissociative adsorption and catalysis on the surfaces of cathode and anode is modeled by using mass action law. By combining in one model the different processes such as dissociative adsorption, surface chemical reactions on the surfaces of electrodes with formation of oxygen negative ions on the cathode and water molecules after combining with hydrogen on the anode, surface and bulk diffusion of oxygen ions in electrolyte leading by electric field formed and including grain boundary diffusion and surface diffusion the efficiency of working fuel cell can be analyzed by varying of different properties electrolyte and electrodes. The theoretical simulations and modeling are verified with experimental observations and measurements done by X-ray diffraction, X-ray photoelectron spectroscopy, scanning electron microscopy, atomic force microscopy, impedance measurements and other methods. By fitting of experimental results the various model kinetic and thermodynamic parameters are calculated which late helps to simulate properties of single chamber solid oxide fuel cell components.

This research is funded by the European Regional Development Fund according to the supported activity ‘Research Projects Implemented by World-class Researcher Groups’ under Measure No. 01.2.2-LMT-K-718.

Notes:

Characterization of thermoelectric generation in Si-wire thermopile structure

K. Fauziah[1,2,*], Y. Suzuki[2,3], Y.Narita[2,3], Y. Kamakura[4], T. Watanabe[5], F.Salleh[6], and H. Ikeda[1,2,3]

[1]*Graduate School of Science and Technology, Shizuoka University, 3-5-1 Johoku, Naka-ku, Hamamatsu 432-8011, Japan*
[2]*Research Institute of Electronics, Shizuoka University, 3-5-1 Johoku, Naka-ku,Hamamatsu 432-8011, Japan*
[3]*Faculty of Engineering, Shizuoka University, 3-5-1 Johoku, Naka-ku, Hamamatsu 432-8561, Japan*
[4]*Graduate School of Engineering, Osaka University, Suita, Osaka 565-0871, Japan*
[5]*School of Fundamental Science and Engineering, Waseda University, 3-4-1 Ohkubo, Shinjuku, Tokyo 169-8555, Japan*
[6]*Faculty of Engineering, University of Malaya, Kuala Lumpur 50603, Malaysia*
**khotimatul.fauziah.16@shizuoka.ac.jp*

Introduction of nanowires have been widely studied to enhance the performance of thermoelectric applications, such as infrared photodetector and thermoelectric generator, due to the quantum confinement effect of electrons and the boundary scattering of phonons [1,2]. However, the phonon-drag part in Seebeck coefficient of a Si nanowire is decreased due to boundary scattering in phonon transport. In order to optimize the performance of thermoelectric devices, we have fabricated and characterized the micrometer-scaled Si thermopile preserving the phonon-drag effect. The Si thermopile consists of p-n-wire pairs. On a Si-on-insulator (SOI) wafer, the array of Si wires was patterned with a thickness of 30-40 nm, a width of 10 μm and a length of 1 mm by using lithography (Fig. 1). The p-type wire and n-type wire were prepared by thermal diffusion of B atoms and P atoms alternately with a carrier concentration of $3.6\text{x}10^{17}$ cm^{-3} and $2.0\text{x}10^{19}$ cm^{-3}, respectively. In order to perform the Seebeck coefficient measurement, temperature difference was applied to the sample in plane parallel to the sample surface by a resistive heater and measured by an infrared camera placed over the sample. A couple of probes were directly attached to the sample surface to measure the thermoelectromotive force (TEMF). The Seebeck coefficient was evaluated from the slope of the linear relationship between the measured TEMF and the temperature difference (Fig. 2). The measured Seebeck coefficient of p-type wire was found to be higher than the theoretical value related only to the carrier contribution. Therefore, the measured Seebeck coefficient includes the contribution of the phonon-drag part. However, the phonon-drag contribution was hardly observed in the n-type wire owing to the high carrier concentration. The maximum power output of 3.7 nW/cm^2 was obtained at a temperature difference of 1.9 K. The power output can be increased due to the contribution of phonon-drag part in the n-type wire by adjusting the P concentration.

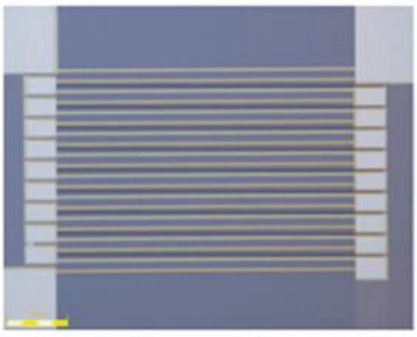

Fig. 1. Optical image of fabricated Si-wire thermopile

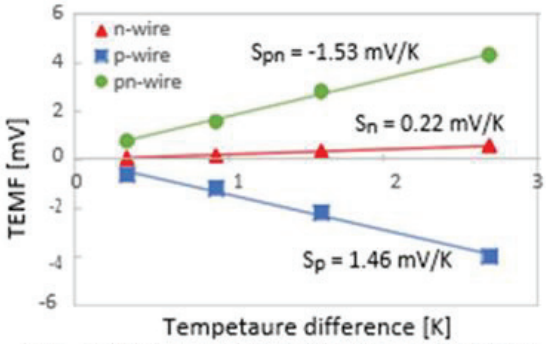

Fig. 2. Thermoelectromotive force of Si-wire thermopile

Keywords: Si, thermopile, Seebeck coefficient, phonon-drag.

[1] A.I. Boukai, Y. Bunimovich, J. Tahir-Kheli, J.-K. Yu, W.A. Goddard, and J.R. Heath, Nature 451 (2008) 168.
[2] E.B. Ramayya, L.N. Maurer, A.H. Davoody, and I. Knezevic, Phys. Rev. B 86 (2012) 115328.

Notes:

Ellipsometric diagnostic of anisotropy properties of surface layer of silicon after laser treatment

T. Aoki[1], D. Gnatyuk[2], L. Melnichenko[2], L. Poperenko[2], I. Yurgelevych[2,*]
[1]*Research Institute of Electronics, Shizuoka University 3-5-1 Johoku, Hamamatsu 432-8011, Japan*
[2]*Faculty of Physics of Taras Shevchenko National University of Kyiv, Academician Glushkov Avenue 2, Building 1, Kyiv 03680, Ukraine*
[*]*vladira_19@ukr.net*

Silicon is still widely used in micro- and nanoelectronics, sensor technology, biomedicine, etc. due to their thermodynamic, physical, chemical and semiconductor properties. Interest in the nanocomposite and nanostructured silicon based structures caused by perspectivity of their use in the creation of silicon photonics devices and nonvolatile memory devices. Promising method to produce nanoparticles of different materials is laser ablation. One characteristic of ablation using high-power pulses of laser light is the formation of different kinds of particles (clusters, droplets or solid fragments). The most widely in recent years, laser ablation is used in the preparation of nanocomposite materials for electronic devices.

Optical properties of non-treated silicon plates and Si plates modified by femtosecond laser irradiation have been investigated by ellipsometry. The samples of the nanostructured silicon as isolated cells were formed on the single-crystal silicon wafers by a method of the laser ablation. The laser source was a home-built Yb-doped fibre laser, operating at a central wavelength of 1060 nm and generating pulses with up to 1 mJ energy at 1 MHz, which can be compressed to 100 fs. The powers incident on the samples ranged from 100 mW to 1 W. The pulse-to-pulse power stability was on the order of 0.05% (measured from 3 Hz to 250 kHz). Laser beam scanning modes provide the synthesis of nanostructured silicon dioxide particles or silicon nanoparticles.

Optical polarization measurements were carried out on laser elipsometer LEF-3M-1 at a wavelength of 632.8 nm within the 15 divided cells on the wafer. The ellipsometric parameters of the samples such as a cos and tg were measured for two mutually perpendicular directions in own plane of the sample for characterization of optical anisotropy of some isolated cells of silicon samples at variation of the angle of light incidence. All angular dependencies of ellipsometric parameters cos and tg of the nanostructured silicon were analyzed and the principal angle of incidence ($\cos\Delta = 0$) and minimal value of the tg are obtained from these dependencies.

It was established that the principal angle of incidence for the nanostructured silicon is significantly reduced in comparison to the one for monocrystalline silicon wafers of 12-21 . Moreover, the essential difference between the values of the $\cos\Delta$ and $tg\Psi$ for two mutually perpendicular directions in own plane of the cell when measured at one taken angle of light incidence $\varphi=53$ was observed. Besides, for single cell it was found that the difference between the significance of the principal angle of incidence and ellipsometric parameter Ψ for two mutually perpendicular directions in own plane of the isolated cell of the nanostructured silicon is essential and equal to about 9° and more than 15° respectively. This means that the formed silicon nanostructures possess great optical anisotropy as a result of deformation influence of laser ablation and appearance of elastic stresses within the surface layer of the nanostructured silicon. The optical anisotropy was not found for silicon areas located between the cells of the nanostructured silicon.

Keywords: nanostructured silicon, laser ablation, ellipsometry, optical anisotropy.

Notes:

Single molecule force spectroscopy on collagen deposited on hydroxylated silicon substrate

A. Besleaga and L. Sirghi*

Iasi Plasma Advanced Research Center (IPARC), Faculty of Physics, Alexandru Ioan Cuza University of Iasi, Blvd. Carol I nr. 11, Iasi 700506, Romania

*lsirghi@uaic.ro

Development of single-molecule force spectroscopy techniques, as atomic force microscopy (AFM), optical tweezers and magnetic tweezers, allows for manipulation of individual molecules and measurements of intermolecular forces with pico Newton resolution. Such investigations have been performed to study the mechanical properties of various biomolecules as DNA, RNA, proteins and polysaccharides. In all these techniques single-molecules are physically or chemically bound to larger bodies, which can be moved with high spatial precision. For the case of AFM technique, one end of a molecule is bound to the tip of an AFM probe and the other end is bound to a flat substrate. To do this, the molecules to be studied are deposited on a substrate where from they are picked up by the AFM tip. The tip and substrate surfaces are chemically functionalized in order to bind the ends of the studied molecules through specific chemical interactions. Nonspecific physical adsorption of molecules on tip and substrate surfaces may be also used to bind molecules. In typical force spectroscopy experiments, the AFM tip is pushed to the sample surface for some time in order to bind the end of a molecule to its surface. Binding of a molecule to the tip is probed by the occurrence of the characteristic entropic force-extension pattern of the molecule on the force-displacement curve observed during the tip retraction form the substrate.

In the present work collagen type I molecules isolated from rat tail (Sigma Aldrich) were deposited on silicon wafers. To enhance formation of hydrogen bonds between collagen molecules and either silicon AFM probes and substrates, the probes and substrates were cleaned and hydroxylated in negative glow plasma of a dc discharge in low-pressure air. Then, the collagen molecules were deposited by imbedding the hydroxylated silicon wafers in aqueous solutions of collagen molecules (10 g/ml) for 2 hours. AFM images of dried collagen samples showed a complete coverage of substrates with a thick layer of collagen molecules. The collagen samples were loaded on liquid cell of the AFM apparatus for force spectroscopy measurements, which showed typical characteristic entropic force-extension pattern that is described well by the worm like chain model of molecules. Single molecule stretching experiments were made on large numbers of molecules and results were statistically analyzed to determine the most probable values of molecule bounding force, contour length and persistence length.

Keywords: single-molecule force spectroscopy, collagen type I, atomic force microscopy, plasma hydroxylation.

Notes:

Ellipsometry of nanostructured Si wafers after femtosecond laser processing

D. Gnatyuk, I. Yurgelevych, L. Melnichenko, and L. Poperenko
Taras Shevchenko National University of Kyiv, Faculty of Physics, Academician Glushkov Ave. 4, Kyiv 03127, Ukraine
*dimamid@i.ua

Optical methods were used to study thin layer of different plots of monocrystalline silicon, formed by nonlinear laser lithography with femtosecond pulses with wavelength λ = 1.06 μm and intensity I =1012 W/cm^2 [1]. Particularly, multiple-angle-of-incidence ellipsometry was applied to measure the nanostructures in four orientations. The ellipsometric parameters (phase shift between the orthogonal components of polarization vector) and Ψ (azimuth of restored linear polarization) were measured by a laser ellipsometer ЛЕФ-3М-1 with λ = 632.8 nm at several light incidence angles from 50° to 69° angular degrees for four orientations in own plane of the sample, which corresponds to angular positions 0° (p-plane), 45°, 90° (s-plane), -45°. The angular dependencies of ellipsometric parameters and Ψ of thin films were analyzed and the principal angle φ_0 (= 90°) and minimal value of the azimuth Ψ_{min} were obtained from these dependences.

It was established that the principal angle of incidence for nanostructured silicon is significantly reduced as compared with the one for monocrystalline silicon wafers of 12-21°. The essential difference between the values of the cos and tg Ψ for two perpendicular directions in own plane of the sample when measured at one angle of incidence φ = 53° was observed too. The formed silicon nanostructures possess great optical anisotropy because of deformation influence on surface structure and appearance of elastic stresses on the surface layer of the nanostructured silicon.

It was found that polar diagrams of ellipsometric parameters and Ψ are represented by not-circle second order curves, which indicate optical anisotropy of the structure, created by action of a powerful laser.

Principal angles and tg Ψ at these angles for different cells 1 and 2 for Si sample for four orientations in its own plane.

Cell number	3				10			
	0°	45°	90°	135°	0°	45°	90°	135°
Principal angle, φ_0	54°	57°	63°	59°	55°	58°	64°	60°
tg Ψ	0,093	0,158	0,488	0,243	0,086	0,151	0,469	0,205

Keywords: Nanostructured silicon, laser ablation, ellipsometry, optical properties.

[1] B. Öktem, I. Pavlov, S. Ilday, H. Kalaycıoğlu, A. Rybak, S. Yavaş, M. Erdoğan, Ö. Ilday "Nonlinear laser lithography for indefinitely large-area nanostructuring with femtosecond pulses", Nature Photonics 7 (2013), 897–901.

Notes:

Low-k sol-gel coating for surface planarization at integrated circuit production

V. Vaskevich[1,*], D. Kovalenko[1], V. Gaishun[1], S. Khakhomov[1], A. Demidov[2], S. Mhin[3]
[1]*F. Scorina Gomel State University, Sovetskaya str. 104, 246019, Gomel, Republic of Belarus*
[2]*Bryansk State Technical University, Bul. 50-letiya Oktyabrya 7, 241035, Bryansk, Russia*
[3]*Korea Institute of Industrial Technology, 113-58, Seohaean-ro, 15014, Seoul, Republic of Korea*
[*]*vaskevich@gsu.by*

The modern development of capacitor and transistor elements of integrated circuits requires the introduction of new thin-film materials into the microelectronic industry. Thus, to increase the number of transistor structures without changing the technological processes, it is possible to obtain multilevel systems. For those purposes, coatings are required to ensure smoothing of the surface of the finished integrated circuit in order for it to form another integral layer. Such coatings should provide a smoothing of the surface from 1 μm to 100-150 nm, and at the same time, to reduce the time delay in integrated circuits with multi-level systems, to have a low dielectric constant.

The paper presents coatings on the surface of the integrated circuit obtained by the sol-gel method from solutions based on the organic compound of silicon. To ensure the necessary smoothing of the surface, two-layer coatings of a total thickness of about 0.6 μm were obtained. The AFM method established that the obtained coatings make it possible to smooth the surface of the integrated circuit from 1 μm to 150 nm (Fig. 1).

Investigation of the electrophysical properties of the obtained two-layer coatings shows that the average value of the permittivity of the dielectric layer is ε = 1.9, which for this thickness of the dielectric is close to the dielectric constant of thermal silicon dioxide. The value of the leakage current through the resulting coating at a voltage of +5 V is 0.9 nA and is retained in this case when the voltage is increased to +100 V. The TPI results show that the value of the voltage shift of the flat zones is Udf = 1.2 V, which corresponds to a change in the density of the effective charge at the interface, that is a small and admissible value.

Thus, developed sol-gel coatings can be used as an interlayer low-k dielectric in the production of multilevel integrated circuits.

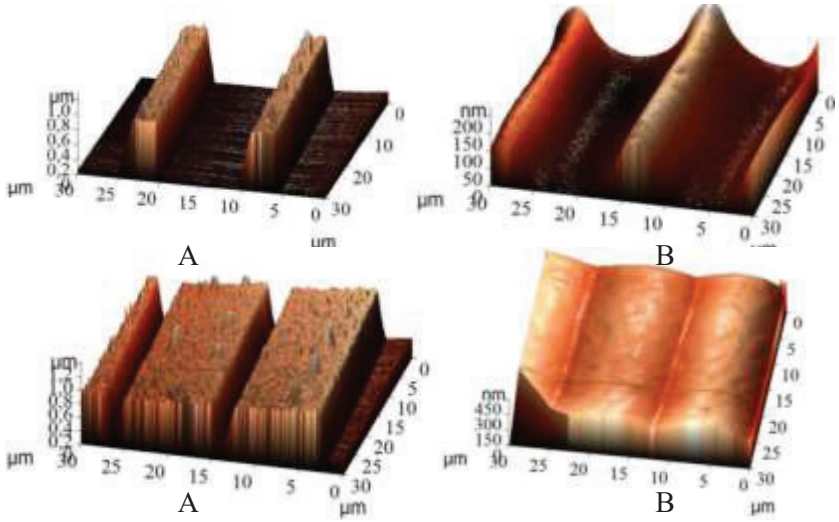

Fig. 1. 3D AFM image (A) without coating, (B) with sol-gel coating

Notes:

Instability of CdTe radiation detector characterized by carrier transport properties

H. Nakagawa[1,*], K. Sakaida[2], T. Terao[1], T. Masuzawa[3], T. Ito[3], A. Koike[4], H. Morii[4], and T, Aoki[3,4]

[1]*Graduate School of Science and Technology, Shizuoka Univ., 3-5-1 Johoku Nakaku, Hamamatsu, Japan*
[2]*Graduate School of Integrated Science and Technology, Shizuoka Univ., 3-5-1 Johoku Nakaku, Hamamatsu, Japan*
[3]*Reserch Institute of Electronic, Shizuoka Univ., 3-5-1 Johoku Nakaku, Hamamatsu, Japan*
[4]*ANSeeN Inc., 3-5-1 Johoku Nakaku, Hamamatsu, Japan*
[*]*nakagawa.hisaya.14@shizuoka.ac.jp*

Cadmium Telluride (CdTe) semiconductor have been used in for some application of X-ray and gamma-ray detection. CdTe detectors have good physical properties such as the room temperature operation and high X- and gamma-ray detection efficiency. However, its detectors have a very serious problem of being instability in long term operation. This instability is called polarization, and the spectrum properties with diode type CdTe detector degraded. Therefore, the details of polarization have been still discussed and suggested some mechanisms [1-3]. In this study, we estimated the model of the polarization focused on the carrier transport properties.

CdTe detectors were used Schottky diode based on p-type crystal in this study. The CdTe detector was connected to charge sensitive amplifier (CSA, CLEAR-PULSE Co., LTD. Model 5102) and the output signals from CSA were introduced to a specially designed signal-processing system (ANSeeN Inc. ANS-HSMCA1-2D) which enable to measure both pulse height and pulse rise time. The gamma-rays from ^{241}Am radioisotopes (59.5 keV) were measured at room temperature by irradiating from In-side and Pt-side, respectively.

Fig. 1 shows the rise time of the signal pulses for main peak after each measurement intervals. Here, the transit time designated the rise time of output signal pulse from CSA. In the case of In-side irradiation, the carrier transit time did not change until 120 min. However, the carrier transit time increased after 120 min. As the operation time passed further, the carrier transit time start to decrease. The similar result was obtained in the Pt-side irradiation. The tendency obtained experimental result have the good agreement of the calculated transit time from the previous charge accumulation model [3].

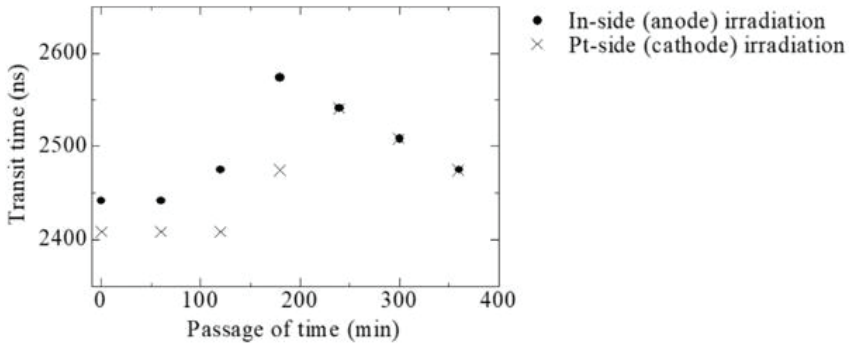

Fig. 1. Transit time by ^{241}Am irradiation from In-side and Pt-side, respectively, with time

Keywords: CdTe, semiconductor detector, radiation detector polarization, instability.

[1] H. L. Malm and M. Martini: IEEE Trans. Nucl. Sci. 21 (1974) 322.
[2] H. Toyama, A. Higa, M. Yamazato, T. Maehara, R. Ohno, and M. Toguchi: Jpn. J. Appl. Phys. 45 (2006) 8842.
[3] R.Grill, E. Belas, J. Franc, M. Bugar, S. Uxa, P. Moravec, and P. Hoschl: IEEE Trans. Nucl Sci. 58 (2011) 3172.

Notes:

Investigation of X-ray attenuation properties in water solutions of sodium tungstate dihydrate and silicotungstic acid

L. Gilys[1,*], D. Adlienė[1][0000-0002-8683-8757], E. Griškonis[2]
[1]*Physics Department of Kaunas University of Technology, Studentų g.50, LT-51368 Kaunas, Lithuania*
[2]*Faculty of Chemical Technology of Kaunas University of Technology, Radvilėnų pl. 19, LT-50254 Kaunas, Lithuania*
[*]*Laurynas.gilys@ktu.edu*

Due to its outstanding photon attenuation features lead (Pb) is the most popular material which is used for radiation shielding and for radiation protection of individuals against ionizing radiation. However, Pb is very toxic and can cause serious health problems. Also recycling of lead containing materials is relative complicated. To overcome Pb related problems researchers are looking for lead free materials possessing similar photon attenuation properties as lead and that can be used for the development and fabrication of radiation shielding elements and radiation protection equipment.
In this paper we discuss the investigation results of two tungsten containing water solutions: sodium tungstate dihydrate ($Na_2WO_4 \cdot 2H_2O$) and silicotungstic acid ($H_4SiW_{12}O_{40} \cdot xH_2O$). Aqueous solutions containing different concentrations of tungsten products were fabricated and their X-ray attenuation properties were investigated. Since these solutions were thought for application as the fillers in aquarium type radiation protection screens their lead equivalent was calculated. Radiation protection screen of this type were developed for application in interventional radiology departments. It was found, that the lead equivalent of investigated solutions was dependent on concentration of tungsten compounds. Solutions containing ≥30% of sodium tungstate and ≥45 % of silicotungstic acid indicated lead equivalent ≥0.25 mmPb, thus meeting the requirements set for radiation protection equipment.

Keywords: lead free materials, X-ray shielding, radiation protection equipment.

Notes:

Formation of Alumina and Alumina-Zirconia coatings employing Plasma Spraying

J. S. Mathew[1,*], L. Marcinauskas[1, 2], M. Milieška[2], M. Kalin[3], R. Kėželis[2], R. Česnavičius[4]
[1]*Kaunas University of Technology, Department of Physics, Studentų str. 50, LT- 51368 Kaunas, Lithuania*
[2]*Lithuanian Energy Institute, Breslaujos str. 3, LT-44403 Kaunas, Lithuania*
[3]*University of Ljubljana, Laboratory for Tribology and Interface Nanotechnology, Bogišićeva 8, 1000 Ljubljana, Slovenia*
[4]*Kaunas University of Technology, Department of Mechanical Engineering, Studentų str. 56, LT-51424 Kaunas, Lithuania*
[*]*jacob.mathew@ktu.edu*

The abrading of alloys such as steel from constant use is a common demerit in industries. A low intrinsic hardness it possesses makes it potentially vulnerable. One of the ways to efficiently protect these surfaces is by coating them with ceramic materials employing the plasma spraying technique [1,2,3]. A commonly used ceramic is alumina, reasons attributing to its merits such as high hardness, good strength and wear-resistant properties [4]. Zirconia is another neat ceramic with outstanding toughness [5]. To put together the properties of both the materials would be to derive a condition of high hardness and strength (alumina) and high toughness (zirconia). We have herein deposited Al_2O_3 and Al_2O_3-10wt.% ZrO_2 on stainless steel substrates to examine its morphological and tribological properties. The torch powers were taken from ~36 to ~42 kW. The surface morphology was investigated by a scanning electron microscope (SEM) Hitachi S-3400N. The elemental composition of the coatings was gauged by energy dispersive X-ray spectroscopy (EDS) Bruker Quad 5040 spectrometer. The surface roughness was determined using a Mitutoyo Surftest-SJ-210-Ver2.00 profilometer. X-ray diffractometry was performed for the structural characterization of the coatings. The tribological properties of the samples were determined using a CETR-UMT-2 ball-on-disc tribometer. With increase in torch power, the surface roughness of Al_2O_3 and Al_2O_3-ZrO_2 coatings had increased. For Al_2O_3-ZrO_2 coatings, there was a significant drop in surface roughness (29-34%). XRD indicated that the dominant phases in the Al_2O_3 coating were α-Al_2O_3 and β -Al_2O_3. For Al_2O_3-ZrO_2, it was t-ZrO_2 (tetragonal) and m-ZrO_2 (monoclinic). At a normal load of 1 N, the friction coefficients of alumina and alumina-zirconia coatings were ~0.75. Wear rates for the alumina coatings were in the range of ~10^{-5} mm^3/Nm whereas with alumina-zirconia, there was insignificant and immeasurable wear due to plastic deformation.

Keywords: Plasma Spraying, Alumina, Zirconia, Coatings, Tribological properties.

[1] W. Deng, S. Li, X. Liu, X. Zhao, Y. An, H. Zhou, J. Chen, Material Letters (2017) 193, 199-202.
[2] S. Wan, D. Li, G. Zhang, A. K. Tieu, B. Zhang, Tribology International (2017) 106, 10-22.
[3] E.P. Georgiu, T. Van Der Donck, M. Peeters, D. Drees, J.-P. Celis, Wear (2016) 368–369, 453–460.
[4] Y. Yang, Y. Wang, W. Tian, D. Yan, J. Zhang, L. Wang, Materials and Design, (2015) 65, 814-822.
[5] R. Younes, M. A. Bradai, A. Sadeddine, Y. Mouadji, A. Bilek, A. Benabbas, The Transactions of Nonferrous Metals Society (2016) 26, 1345–1352.

Notes:

Activation of water by surface DBD micro plasma in atmospheric air

A. Dascalu[1], A. Besleaga[1], K. Shimizu[2], and L. Sirghi[1,*]
[1]*Iasi Plasma Advanced Research Center (IPARC), Faculty of Physics, Alexandru Ioan Cuza University of Iasi, Blvd. Carol I nr. 11, Iasi 700506, Romania*
[2]*Organization for Innovation and Social Collaboration, Shizuoka University, 3-5-1, Naka-ku, Johoku, Hamamatsu, Shizuoka 432-8561, Japan*
[*]*lsirghi@uaic.ro*

Exposure of water to atmospheric discharge plasma in air determines generation of long-living reactive species as hydrogen peroxide H_2O_2, nitrites NO_2^- and nitrates NO_3^- [1]. The water thus treated is called plasma activated water and have applications in medicine [2] and agriculture [3]. In the present work, surface DBD micro plasma working in a closed volume of air at atmospheric pressure is used to treat a small amount of deionized water. The surface DBD plasma was generated on the surface of a device formed by two silver electrodes deposited on the two sides of a thin glass plate. The device was powered by a high voltage amplifier that applied on the electrodes a sinusoidal waveform voltage at a frequency around 10 kHz and peak to peak amplitude of 3.4 kV. Time series of current intensity and voltage values were acquired to determine the power injected into the surface DBD micro plasma. Optical emission spectroscopy was used to get information on reactive species generated by micro plasma in gaseous phase. The reactive species generated in water during the discharge-on and discharge-off periods were investigated by means of UV absorption spectroscopy. The UV absorption spectra were fitted with Gaussian absorption peaks corresponding to absorption of H_2O_2, NO_2^- and NO_3^- reactive species. The measurements showed that the concentration of these reactive species rise not only during the discharge-on time, but also during post discharge-off time for a few tenths of minutes. This observation points towards an optimization scheme of the treatment, which uses discharge on/off steps.

Keywords: dielectric barrier discharge, surface microplasma, plasma activated water.

[1] D. P. Park, K. Devis, S. Gilani, C. A. Alonzo, A. J. Drexel, Current Appl. Phys. 13 (2013) S19-S29.
[2] G. Fridman, G. Friedman, A. Gutsol, A. B. Shekhter, V. N. Vasilets, A. Fridman, Plasma Process. Polym. 5 (2008) 503–533.
[3] L. Sivachandirana, A. Khacef, RSC Adv.7 (2017) 1822–1832.

Notes:

Modification of optical properties of amorphous metallic mirrors due to impact of deuterium plasma

I. Lyashenko[1], V. Konovalov[2], L. Poperenko[1], I. Ryzhkov[2], V.Voitsenya[2], I. Yurgelevych[1,*]
[1]*Faculty of Physics of Taras Shevchenko National University of Kyiv, Academician Glushkov Avenue 2, Building 1, Kyiv 03680, Ukraine*
[2]*Institute of Plasma Physics of NSC KIPT, 1, Akademicheskaya St., Kharkov, 61108, Ukraine*
[*]*vladira_19@ukr.net*

Amorphous metallic alloys (AMA) due to their structural disordering possess properties that make these materials promising for use in different applications.
The optical properties of $Zr_{57}Cu_{15.4}Al_{10}Ni_{12.6}Nb_5$ mirrors subjected to deuterium plasma action have been studied. The face and back surfaces of the pristine sample (AMGN2) and sample treated by deuterium plasma (AMGN1) of $Zr_{57}Cu_{15.4}Al_{10}Ni_{12.6}Nb_5$ alloy were investigated by ellipsometry and atomic force microscopy (AFM). The ellipsometric measurements of the phase shift between the p-and s-components of the polarization vector and the azimuth Ψ of the restored linear polarization for mirrors were obtained as dependences on the light incidence angle φ using a laser ellipsometer LEF-3M-1 with $\lambda = 632.8$ nm. On the basis of the obtained data the principal angles of incidence φ_p ($\cos\Delta = 0$) and the angular position of the minimal value of $tg\Psi_{min}$ for the investigated samples were calculated.
For all mirror samples the values φ_p and $tg\Psi_{min}$ were obtained for two mutually perpendicular directions in own plane of the sample for the purpose of determining the optical anisotropy within surface layer of the mirror. It was established that both values φ_p and $tg\Psi_{min}$ for mutually perpendicular directions coincide within a limits of the error of the determination of these parameters. It means that the optical anisotropy of the samples both in the initial and after treatment in the deuterium plasma was not observed being inherent for amorphous surface layer structures. However, when comparing values φ_p and $tg\Psi_{min}$ of samples AMGN1 and AMGN2, it was observed that for the former sample these parameters are lower than for both sides of AMGN2 sample, which was not exposed in plasma. It means that the roughness of the surface of AMGN1 sample is increased after treatment by deuterium plasma. This fact follows from our previous results [1] where it was found relationship between behavior of absolute values of $tg\Psi_{min}$ and roughness height for the bulk sample of nickel, namely the $tg\Psi_{min}$ decreases whereas roughness increases.
To make sure that the roughness parameters of the mirror surfaces after the action of the deuterium plasma (AMGN1) are changed, in addition to angular ellipsometric measurements we have carried out the diagnostics of surface of both samples by AFM. The AFM results indicate that the impact of deuterium plasma on both surfaces of the AMGN1 sample leads to increasing the roughness parameters such as average roughness, root mean square height, maximum height etc. compared with the AMGN2 sample. For example, the value of root mean square height, Sq equals to 1.66 nm for 5 m x 5 m AFM image of AMGN2 sample and 3.59 nm for 1 m x 1 m AFM image of AMGN1 sample respectively.
Thus, it was found that the treatment of mirror-like surfaces by the deuterium plasma essentially changes the roughness of the surface of the investigated $Zr_{57}Cu_{15.4}Al_{10}Ni_{12.6}Nb_5$ mirror sample, because there are differences in absolute values of $tg\Psi_{min}$ and the magnitudes of deviations in the structure of the microrelief of the pristine and treated surfaces.

Keywords: amorphous metal alloys, deuterium plasma, ellipsometry, roughness.

[1] Poperenko L.V., Stashchuk V.S., Shaykevich I.A. et al., Precision Tools and Devices of Optotechnique, Kyiv, Kyiv University, 2016 (in Ukraine).

Notes:

Lead ferrite doped chrome thin films synthesis by reactive magnetron sputtering and investigation

B. Beklešovas*, V. Stankus
Physics Department of Kaunas University of Technology, Studentų g.50, LT-51368 Kaunas, Lithuania
*benas.beklesovas@ktu.edu

Interest in multiferroic increases rapidly due to its unique properties. These materials combine at least two primary ferroic properties - electron spins controlled by magnetic field and electric dipole moment is switched by external electrical field. Coupling between these properties in the same phase is called magnetoelectric effect. Most appealing aspect of this effect is the posibility to control magnetic properties by external electric field and vice versa. Such unique properties are the base for the novel applications in memory media, sensors, energy harvesting, photovoltaic technologies [1]. FeRAMS technology is beside Flash memory, it offers lower power consumptions, faster read/write process, high durability. Condtition for feroelectricity to occur is an empty d shell (d^0-ness) and for ferromagnetism – partially filled d or f shell. This is the reason why multiferroic materials are rare. Coupling between ferroic properties exists due to complex mechanisms. In perovskites A and B site cations provide different properties, where A site cation is responsible for ferroelectric properties and B site – magnetic. There are many problems to overcome in formation of multiferroic materials – low neel temperature, weak coupling between ferroic properties and etc. [2]
Our research group successfully synthesized lead ferrite ($Pb_2Fe_2O_5$) which showed ferroelectric properties – where sample synthesized at 500 °C temperature on platinized silicon obtained remnant polarization (Pr) ~54 μC/cm^2 and the coercive electric field (Ec) ~68,6 kV/cm. In this work chrome has been chosen for doping. Substitution for Fe site could lead to better saturation of ferroelectric hysteresis loop, lower leakage currents due to decrease of oxygen vacancies and defects. Samples were synthesized on platinized silicon by reactive magnetron sputtering at temperature range from 500 °C to 600 °C. Structural and dielectric measurements were performed and compared with undoped lead ferrite.

Keywords: multeferroics, lead ferrite, reactive magnetron sputtering, thin films, ferroelectric.

[1] Vopson, M.M., Fundamentals of Multiferroic Materials and Their Possible Applications. Critical Reviews in Solid State and Materials Sciences, 2015. 40(4): p. 223-250.
[2] Lawes, G. and G. Srinivasan, Introduction to magnetoelectric coupling and multiferroic films. Journal of Physics D: Applied Physics, 2011. 44(24): p. 243001.

Notes:

Influence of deposition parameters on the structure of TiO_2 thin films prepared by reactive magnetron sputtering technique

V. Kavaliūnas*, A. Šeštakauskaitė, M. Sriubas, and G. Laukaitis
Kaunas University of Technology, Faculty of Mathematics and Natural Sciences, Department of Physics, Studentu g. 50, LT-51368 Kaunas, Lithuania
**vytautas.kavaliunas@ktu.edu*

TiO_2 is well known for its photocatalytic properties and wide range of applications. However, the efficiency of amorphous TiO_2 as photocatalyst is low and deposition of crystal TiO_2 phases is strict to deposition parameters. The TiO_2 phase dependence on temperature, total pressure (p_{tot}) and oxygen partial pressure and total pressure (p_{O2}/p_{tot} [%]) ratio and how this affect growth rate has been studied in this work, TiO_2 thin films were deposited via magnetron sputtering technique using different deposition parameters in order to get TiO_2 either pure anatase or rutile phase. Crystallographic structure and morphology of deposited thin films were analyzed by XRD and SEM/EDS.

During the sputtering deposition temperature, total pressure and p_{O2}/p_{tot} ratio obviously affects the crystallographic structure of thin films. TiO_2 anatase phase depends more on substrate temperature than on p_{O2}/p_{tot} ratio while TiO_2 rutile depends more on p_{O2}/p_{tot} ratio than on substrate temperature. This dependence of rutile structure was, considered to be, caused by the bombardment effect of high-energy particles or migration of Ti atoms on the surface. Anatase dependence on substrate temperature is caused by increased grain size with increase of temperature. Also, need to mention that anatase transforms to rutile at high temperatures (600-800 °C). Thus, could be explained by density of structures knowing that rutile is denser than anatase. Nevertheless, further investigation of thin films deposition needs to be done to get optimal configuration for magnetron sputtering technique in order to get TiO_2 anatase or rutile structure.

This research is funded by the European Social Fund according to the activity ‘Improvement of researchers’ qualification by implementing world-class R&D projects’ of Measure No. 09.3.3-LMT-K-712.

Keywords: TiO_2, TiO_2 characterization, TiO_2 phase dependence.

Notes:

Formation and investigation of doped cerium oxide thin films formed using e-beam deposition technique

N. Kainbayev[1, 2], S. Bolegenova[2], G. Laukaitis[1]
[1] *Kaunas University of Technology, Physics Department, Studentu str. 50, LT-51368, Kaunas, Lithuania*
[2] *Al-Farabi Kazakh National University, Department of Thermal Physics and Technical Physics, 71 al-Farabi Ave, Almaty, Kazakhstan*
[*] *nursultan.kainbayev@ktu.edu*

The investigation of new functional materials (ceramics) based on cerium (IV) oxides is a promising field of scientific research. A wide application in the industry received composite materials based on CeO_2–Gd_2O_3 and CeO_2–Sm_2O_3.
Thin ceramic films were formed on the basis of CeO_2 with 10 mol% Gd_2O_3 (GDC10), CeO_2 with 20 mol% Gd_2O_3 (GDC20), CeO_2 with 15 mol% Sm_2O_3 (SDC15), CeO_2 with 20 mol% Sm_2O_3 (SDC20) using e-beam technique in this work. The deposition rate and temperature of the substrate had influence on the formed doped cerium oxide GDC10, GDC20, SDC15, SDC20 thin films structure. Sm and Gd doped cerium oxide thin films were deposited on SiO_2, Alloy 600 (Fe-Ni-Cr), Si (111), Si (100) and Al_2O_3 substrates. Investigations of the formed thin films were carried out using a Scanning electron microscope (SEM), Electron dispersive spectroscopy (EDS), X-ray diffraction (XRD), and Raman spectroscopy. It has been established that the cerium oxide-based ceramic retains the crystalline structure, regardless of the concentration of the dopant and used substrate type. The most dominant crystallographic orientation of formed thin films was cubic (111). Raman spectroscopy measurements showed the peak (465 cm^{-1}) of pure ceria corresponding to F_{2g} vibrational mode. First-order peaks, inherent to cerium oxide, were shifted to a region of lower wavenumbers and depend on dopant concentration. The peaks for all formed thin films were similar to each other in form but the position, half width and their intensity varied depending on the dopant concentration. Raman peaks position at 550 cm^{-1} and 600 cm^{-1} could be explained as change of oxygen vacancy amount due to the cerium transition between oxidized and reduced forms of $Ce^{3+} \rightleftarrows Ce^{4+}$.

Notes:

Investigation of deposition parameters influence on the properties of doped diamond-like carbon films

V. Dovydaitis[1,*], L. Marcinauskas[1], A. Iljinas[1]
[1]*Department of Physics, Kaunas University of Technology, Studentu str. 50, LT-51368 Kaunas, Lithuania*
[*]*vilius.dovydaitis@ktu.edu*

Diamond-like carbon (DLC) exhibits unique mechanical, chemical, optical and electrical properties. These properties could be achieved by modifying the bonding structure and the ratio of C-C sp^3 and C=C sp^2 bonds by choosing technological parameters accordingly [1,2]. Magnetron sputtering is one of the most promising techniques to produce hydrogen free DLC films in industrial scale due to possibility to coat large surfaces and the easy control of the technological parameters. Desirable sp^3/sp^2 ratio could be obtained by varying sputtering power other deposition parameters [2]. Another possibility to alter bonding structure of DLC films is doping. Doping amorphous carbon films with various transition metals (Ni, Ag, Ti, Cr and etc.) improves coating adhesion due to reduction of residual stresses, also improves tribological properties due to formation of sp^2 sites that cause lubrication [3]. Titanium based or titanium doped materials are getting a lot of interest lately, due to unique set of properties. However, the affinity of titanium for oxygen is high and doping DLC films with titanium might increase oxygen content in the coatings, therefore, the influence of oxygen incorporation into DLC films must be investigated. It has been reported that doping hydrogenated DLC films with oxygen results in increased refractive index and changed other optical properties [4], Also, there are papers that suggest that oxygen incorporation in DLC films might improve mechanical and tribological properties of the film and increase its wettability [3,5].

The doped amorphous carbon films were grown using layer-by-layer direct current magnetron deposition method by sputtering 3 inch graphite target (99.9 at.%) in 2-3 Pa argon environment. Films were deposited using different sputtering currents (1 A, 1.5 A and 2 A for graphite cathode and 1 A for titanium) on Si (100) and glass substrates. Energy dispersive X-ray spectroscopy was used to determine elemental composition of the films. The thickness of films was measured using profiler. Atomic force microscope was used to examine surface morphology and determine surface roughness. Optical properties of the doped DLC films were analyzed by using UV–VIS–NIR spectrophotometer and null-ellipsometer. The optical band gap (Eg) was calculated using Tauc method. MicroRaman spectroscopy was used to examine the bonding structure of carbon films.

It was determined that the increase of the sputtering current from 1 A to 2 A resulted in increase of deposition rate from ~0.22 nm/s to ~0.45 nm/s and increase of the surface roughness from ~1.2 nm to 1.7 nm. The EDX analysis revealed that coating mostly contain carbon, oxygen and titanium but there were some additional elements. The addition of titanium resulted in increased oxygen concentration. Doped DLC films had optical transparency of 60-90 % in the visible range. The water contact angle of the films varied between 85° and 99°, the addition of titanium reduced water contact angle value. The results of Raman spectroscopy indicated that the ID/IG ratio decreased as the sputtering currents increased. Furthermore, the D peak position shifted to lower wavenumbers and the G band became wider. These results suggest that the film deposited at the lowest current had the highest fraction of C=C sp^2 sites. The addition of titanium increased graphitization even further. It was observed that the C=C sp^2 sites concentration affect the Tauc gap and refractive index values of the films.

Keywords: diamond-like carbon, DC magnetron sputtering, oxygen, titanium, thin films.

[1] J. Robertson, Mater. Sci. Eng. R Reports 37 (2002) 129–281.
[2] Ö.D. Coşkun, T. Zerrin, Diam. Relat. Mater. 56 (2015) 29–35.
[3] J.C. Sánchez-López, A. Fernández, Tribol. Diamond-Like Carbon Film. Fundam. Appl. (2008) 311–328.
[4] P. Safaie, A. Eshaghi, S.R. Bakhshi, J. Alloys Compd. 672 (2016) 426–432.
[5] P. Safaie, A. Eshaghi, S.R. Bakhshi, Diam. Relat. Mater. 70 (2016) 91–97.

Notes:

Aerial image registration for grasping road conditions

K. Ogasawara, H. Saji*
Graduate School of Integrated Science and Technology, Shizuoka University, 3-5-1, Johoku Naka-ku, Hamamatsu, Shizuoka, 432-8011, Japan
saji@inf.shizuoka.ac.jp

Grasping road traffic information at the time of a disaster can be used for rescue and recovery activities. Using the aerial image is important for grasping the information because the aerial image is not affected by ground conditions. In particular, aerial images taken from a helicopter can be used for grasping road traffic information and rescue activities. Furthermore, system that transmit images on the ground in real time, such as helicopter television relay system and helicopter satellite communication system, attract attention, and there are also achievements that have played a wide range in the Kumamoto earthquake that occurred in April 2016[1]. However, it is difficult to find the viewing position on the ground from the images. This is because the images are taken obliquely on the ground and the viewing position is away from the shooting position (Fig. 1).

Fig. 1. Oblique aerial image

In this paper, we propose the registration method of the aerial images and the digital map using the GPS information (Fig. 2). Our method can be used for collecting wide area information at the time of the disaster.

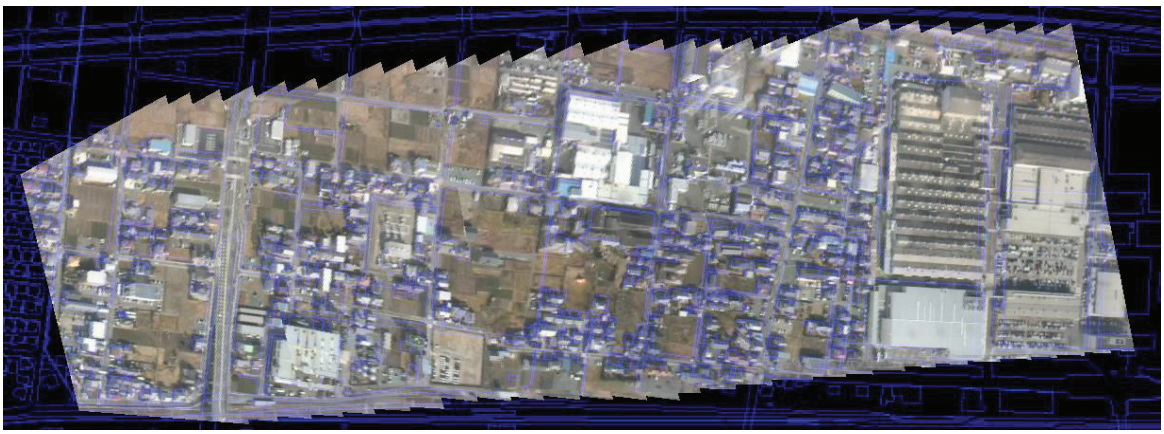

Fig. 2. Registration result

Keyword: aerial image, registration, road, map.

[1] 総務省消防局 Ministry of Internal Affairs and Communications Fire Department, 熊本県熊本地方を震源とする地震（第 38 報）Earthquake with seismic origin in the Kumamoto district (38th report), Kumamoto Prefecture, 2016.

Notes:

Up-Conversion Nanosized Phosphors Based Fluoride For Photodynamic Therapy Of Malignant Tumors

A.M. Dorokhina *, V.V. Bakhmetyev, M.M. Sychov
Saint-Petersburg State Institute of Technology, Moskovsky prospect, 26, St.-Petersburg, Russia
**nastya.dorokhina@mail.ru*

Photodynamic therapy (PDT) is a modern method of treatment for oncological diseases with superficial localization of tumors. To expand the application of PDT to the treatment for tumors with cavitary localization, an approach is suggested based on the use of photosensitizer and special nanophosphors converting infrared radiation easily penetrating into body tissues into visible light required to activate a photosensitizer and destroy tumor cells [1].
The synthesis was carried out by a hydrothermal method [2] since it can produce high-dispersion phosphors suitable for administration to the body (about 100 nm). As raw materials for the synthesis, we used rare earth chlorides prepared by dissolving oxides in hydrochloric acid.
Characterization of the synthesized phosphors were carried out by XRD for structural properties using Rigaku SmartLab 3 X-ray diffractometer and SEM observation for the morphology using TescanVega 3 SBH. The photoluminescence (PL) for phosphors were measured under excitation by infrared semiconductor laser (emission wavelength: 980 nm, output power: 800 mW). That is up-conversion luminescence.
In addition to the particle size, the most important requirement that the phosphor must satisfy for photodynamic therapy (PDT) is the closeness of its luminescence bands to the absorption bands of the photosensitizer. The highest intensity in the spectrum of these samples has a luminescence band with a maximum of 657 nm, related to the electronic transition $^4F9/2 \rightarrow {}^4I15/2$ and practically coinciding with the absorption band of the industrial photosensitizer “Radakhlorin” 660 nm. Thus, in terms of their spectral characteristics, the YF3: Yb^{3+}, Er^{3+} and GdF3: Yb^{3+}, Er^{3+} nanophosphors are most suitable for use in PDT in combination with the “Radachlorin” photosensitizer.
To study the efficiency of generation of active oxygen, a preparation on the basis of bidistilled water, containing a nanophosphor YF3: Yb^{3+}, Er^{3+} at a concentration of 2.0 g/l and a photosensitizer “Radachlorin” at a concentration of 8.75 mg/l was prepared. Sodium lauryl sulfate was used as the stabilizer of the colloid solution. The study of the production of active oxygen was carried out by chemical traps. The efficiency of active oxygen generation with the use of the YF3: Yb^{3+}, Er^{3+} synthesized by us, combined with the “Radachlorin” photosensitizer, is 1.9 μmol/MJ of the energy of the IR laser.

Keywords: photodynamic therapy, nanophosphors, mixed fluorides, hydrothermal synthesis, up-conversion.

[1] Bakhmetyev, V., Sychov, M., Orlova, A., Potanina, E., Sovestnov, A., Kulvelis, Yu.: “Nanophosphors for Photodynamic Therapy of Oncological Diseases” Nanoindustry (8), 46–50 (2013).
[2] Sudheendra L., Das G.K., Li C., Stark D., Cena J., Cherry S., Kennedy I.M. “NaGdF4:Eu3+ Nanoparticles for enhanced x-ray excited optical imaging”, Chemistry of Materials. 2014. V. 26, № 5. P. 1881-1888.

This work was carried out as a result of obtaining support in the form of a grant for young researchers in the framework of the program of the Japan-Russia Youth Exchange (JREX Fellowship).

Notes:

Structure and mechanical properties of gradient metal-carbon films

E.A. Kulesh[1], A. V. Rogachev[1,2,*], D.G.Piliptsou[1,2], A.S Rudenkov[1,2] and J.X. Hong[2]
International Chinese-Belarusian scientific laboratory on vacuum-plasma technology:
[1]*Francisk Skorina Gomel State University, Belarus*
[2]*Nanjing University of Science and Technology, China*
[*]*rogachevav@mail.ru*

Amorphous carbon (a-C) films are widely used as wear-resistant protective films for friction units and tools However, a sudden change the mechanical parameters from substrate to film has many inherent disadvantages, such as the mismatch in properties at the interface between the film and type of substrate can cause stress concentrations to develop during deposition or while in service cause delamination of the film and result in a deterioration of a tool's life, especially in the friction conditions [1]. One way to resolve this problem is to apply gradient metal-carbon films with the improved functional characteristics [2].
Gradient films were obtained as a result of deposition from the combined titanium plasma fluxes of a DC arc discharge and the flow of carbon ions formed by sputtering a graphite target with an impulse arc discharge. The ratio of titanium and carbon atoms in the films was ruled by a change in the frequency of the pulsed arc discharge. To obtain nitride layers (TiN or CN), nitrogen was introduced into the chamber with a pressure of 10^{-1} Pa.
Structure and surface morphology of the Ti/a-C (5…20Hz) and TiN/a-CN(5…20 Hz) films were analyzed by Raman spectroscopy, X-ray photoelectron spectroscopy, atomic force microscopy, and scanning electron microscopy equipped with energy dispersive X-ray spectroscopy. Friction parameters of the films have been studied under the condition of dry sliding using a "sphere-plane" method. The microhardness of the films were studied by the AFFRI DM8 test machine with a Knoop style diamond tip. The microhardness was determined for various burdens on the indenter, which allowed to establish the distribution of hardness along the thickness of the film. The dependence between the carbon concentration in the depth of the studied films and their microhardness has been found out. Raman spectroscopy showed that films with high contents of the sp^3 phase are formed, the presence of titanium atoms leads to a decrease the size of the carbon sp^2 cluster, nitrogen conducts to an increase in the degree of disordering of sp^2 carbon clusters. The N-doping of uplayer of the gradient films leads to a decrease in the friction coefficient and substantial changes in both the phase compositions and surface morphology, which, in turn, reduce the counterbody wear rate and noticeably increase microhardness of these films, due to the formation nitride layers in the volume of film.

Keywords: Carbon films, gradient films, Raman spectroscopy, microhardness, friction and wear.

[1] R. Manaila, A. Devenyi, D. Biro, et al., Surf. Coat. Technol. 21–25 (2002), 151–152.
[2] X. Qiao, Y. Hou, Y. Wu, et al., Surf. Coat. Technol. 131 (2005), 462–464.

Notes:

Synthesis of BiFeO3-Powders and Films by Sol-Gel Process

S.A. Khakhomov[1], V.E. Gaishun[1], D.L. Kovalenko[1], A.V. Semchenko[1,*], V.V. Sidsky[1], W. Strek[2], D. Hreniak[2], A. Lukowiak[2] N.S. Kovalchuk[3], A.N. Pyatlitski[3], V.A. Solodukha[3]
[1]*F. Skorina Gomel State University, Sovetskaya 104, Gomel, 246019, Belarus*
[2]*Institute of Low Temperature and Structures Research PAN, Okolna st. 2, Wroclaw, Poland*
[3]*JSC "INTEGRAL", Korjenevsky str., 12, Minsk, 220108, Belarus*
**semchenko@gsu.by*

The present work aims to design and study novel functional materials with multiferroic properties required in electric applications, such as magnetic and magnetoresistive sensors, actuators, microwave electronic devices, phase shifters, mechanical actuators etc. Complex oxides $BiFeO_3$ for analysis of its ferromagnetic properties were synthesized by sol-gel method as powders and films. The size, shape and degree of crystallinity of the nanoparticles formed by sol-gel method can be controlled by varying of the temperature and the ratio of the concentrations of the initial reactants and the stabilizer. To stop the growth of particles in all cases, it is usually quite to cool quickly the reaction mixture. To isolate the nanoparticles, the precipitating solvent is added, which mixes with the reaction system, but poorly dissolves the "protective shells" of the nanoparticles and, therefore, destabilizes the suspension. As a result, the nanoparticles precipitate as powder, which can be separated by centrifugation. The sol-gel method makes it possible to obtain practically monodisperse nanoparticles of various metals oxides.
The initials for the first way of sol-gel synthesis were salts of metals; ethylene glycol; zitric acid; ethylenediamine. At the beginning, salts of metals was dissolved separately in ethylene glycol without the addition of water. Then, citric acid was added to form metals citrate. After that, the pH of the solution was adjusted to value of 7-8 by neutralizing excess citric acid with ethylenediamine. After homogenization of the resulting mixing solution, ethylene glycol was added thereto. The solution was stirred for 30 minutes and then dried on the vacuum evaporator to form the powder. The reactions take place between the citrates of different metals and ethylene glycol leads in the condensation stage to the formation of a three-dimensional polymer network with uniform distribution of metal ions into the film with homogeneous composition. The mass ratio of citric acid to ethylene glycol was 3:2. Then the samples of $BiFeO_3$ sol-gel materials were annealed at the temperature of 550 ° C for 10 hours (powders) and at the temperature of 800 °C for 20 minutes (films).

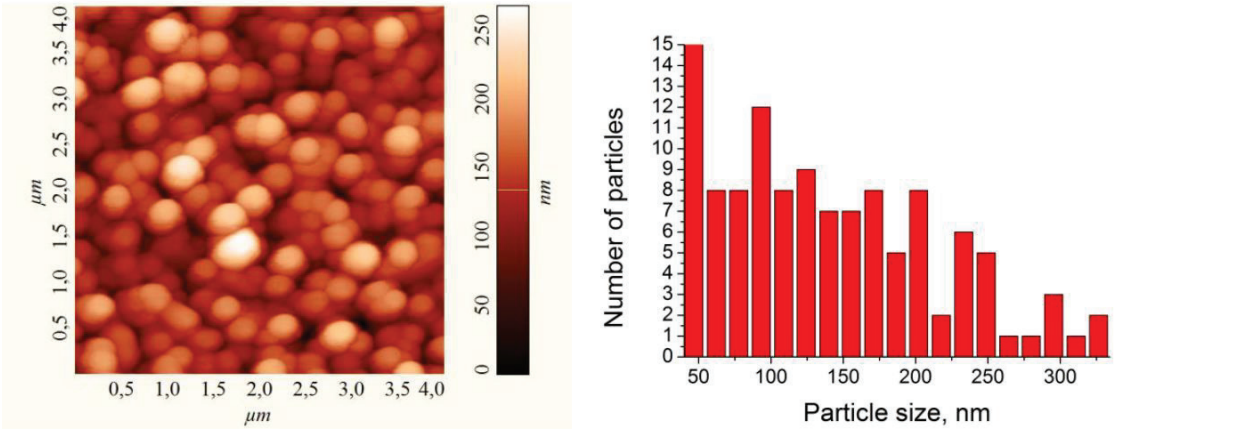

Fig. 1. AFM – image (a) and particle size distributions (b) BiFeO3 sol-gel films

Keywords: sol-gel, film, powder, ferromagnethics.

Notes:

Android Botnet Detection Using Soft Computing Methods

S. Shamshirband[1], A. Mosavi[1,*], A. R. Varkonyi-Koczy[1, 2]
[1]*Institute of Automation, Kando Kalman Faculty of Electrical Engineering, Obuda University, Becsi Str. 94-96, 1431 Budapest, Hungary*
[2]*Department of Mathematics and Informatics, J. Selye University, Elektrarenskacesta 2, 945 01 Komarno, Slovakia*
[*]*amir.mosavi@kvk.uni-obuda.hu*

Android has become a leader in market share of mobile operating systems. In addition, it has attracted attention of attackers more than other operating systems. As a result, Android malware is growing rapidly. In this study, the main focus is on analyzing and detecting botnets that are specific type of malwares. To analyze android botnet detection, it is desirable to select and analyze factors that are highly relevant or most influential to the botnet detection. This procedure usually named variable selection is corresponds to determine a subset of total recorded variables, which provides favorable predictions capability. In this research work, architecture based upon adaptive neuro-fuzzy inference system (ANFIS) is used to model complex systems in function approximation and regression. ANFIS network is employed to perform variable selection for identifying that how the botnet influence the android. After selecting the two most influential parameters, the ANFIS is utilized to create a system for android botnet detection on the basis of the selected parameters.

Keywords: Android, Malware, Neuro-fuzzy, Adaptive neuro-fuzzy inference system (ANFIS).

Notes:

Fuzzy algorithm with particle swarm optimization and principle component analysis for estimation of reference evapotranspiration

S. Shamshirband[1], M. Edalatifar[1], A. Mosavi[1,*], A. R. Varkonyi-Koczy[1, 2]
[1]Institute of Automation, Kando Kalman Faculty of Electrical Engineering, ObudaUniversity, Becsi Str. 94-96, 1431 Budapest, Hungary, [2]Department of Mathematics and Informatics, J. Selye University, Elektrarenskacesta 2, 945 01 Komarno, Slovakia
[*]amir.mosavi@kvk.uni-obuda.hu

Reference evapotranspiration (ET0) was determinate using the FAO-56 Penman-Monteith equation based on the weather data collected from six sites in Serbia during the period of 1980-2010. In this study, an algorithm, integrated with particle swarm optimization (PSO) and principle component analysis (PCA), is utilized to estimate the ET0. The accuracy of the computational model is evaluated using four statistical tests including Pearson correlation coefficient (r), mean square error (MSE), root mean-square error (RMSE), and coefficient of determination (R2). The results show that the ET0 can be estimated with good accuracy by the combination of PCA and ANFIS. Moreover, the result indicated that the ANFIS model can be simplified whiteout or with little change in estimation accuracy by reduce dimension of input data of ANFIS using PCA and accordingly reduce of ANFIS membership parameters. Furthermore, the data that their dimensions are reduced can be stored in small space instead of original data that they need bigger space to store for future applications.

Keywords: Fuzzy algorithm; reference evapotranspiration; principle component analysis; particleswarm optimization.

Notes:

On the Role of Shaped Noise Visibility for Post-Compression Image Enhancement

Y. Osawa, K. Kato, D. M. Chandler*, and G. Ohashi
Department of Electrical and Electronic Engineering, Shizuoka University, 1-3-5 Johoku, Naka-Ku, Hamamatsu, Shizuoka, Japan 432-8561
*chandler.damon.michael@shizuoka.ac.jp

Overview: Transmission of digital images and video have seen explosive growth in recent times, particularly on mobile devices, for both consumer and industrial applications. To meet the ever-increasing demands for higher-quality content, image/video compression has been an active and intense area of signal-processing research. The mainstream approach in compression research has traditionally focused on intelligent encoding strategies to reduce statistical and perceptual redundancies. However, an alternative technique toward enabling higher-quality compression is to focus on the decoding side via restoration and/or enhancement strategies that attempt to reduce the visual impact of the compression distortions. Here, we present our work toward one such enhancement strategy.
Specifically, we have developed a new technique for enhancing compressed images via the addition of what we call "perceptually shaped noise." Previous studies have shown that adding white noise to blurred images can potentially make the images' textures appear sharper [1]. More recently, we have shown that the addition of noise with spectral and statistical matching can better improve the perceived sharpness/quality [2]. However, a key unknown in this noise-addition strategy is the correct amount of noise to add: If too much noise is added, although the texture does indeed appear sharper, it also appears noisy/grainy. On the other hand, if too little noise is added, no improvements can be seen.
Objective: We seek to automatically predict the optimal amount of perceptually-shaped noise to add on a per-texture basis (we call this amount the "noise contrast factor"). We hypothesize that one factor which determines the optimal noise contrast factor is the visibility of the noise within the texture. In this work, we present the results of a study designed to investigate the relationship between the optimal noise contrast factors and the contrast thresholds for visually detecting the noise.
Methods: 30 images of size 1080x720 or 720x1028 pixels served as the source images in the study. The images were manually segmented by the authors to identify the main textures and obtain segmentation maps. Square-sized samples of the textures were extracted and used as templates to create the perceptually shaped noises. The 30 images were then compressed by using HEVC/H.265 with quantization scaling factors from 35-45 (medium-to-low quality). Representative 256x256-pixel texture patches were then cropped from the compressed images to serve as (blurred) textures in the experiment. In the experiment, the goal was, for each blurred texture, to measure the contrast detection threshold for (i.e., the minimum contrast required to see) the noise added to that blurred texture. A three-alternative forced-choice procedure was used to measure the thresholds. Five males aged 20-25 served as subjects. In a separate experiment, optimal noise contrast scaling factors were measured for the same textures from the same subjects by using the method of adjustment.
Results and Conclusions: The experiments are currently in progress; thus far, 15 of the 30 images have been completed. Of these results, we compared the mean contrast detection thresholds with the mean contrast scaling factors for each texture. This analysis yielded a Pearson linear correlation coefficient of 0.63, indicating that the noise's optimal contrast scaling factor for a blurred texture is indeed related to the contrast detection threshold of that noise within the texture. However, some notable exceptions were observed, particularly for textures that were difficult to match via the noise. Overall, the key finding is that contrast detection threshold shows promise as one feature which might be used to help develop an automatic prediction algorithm for the optimal contrast scaling factors on a per-texture basis. We are currently developing this prediction algorithm, which will be reported at the conference.

Keywords: Image enhancement; image restoration; visual perception.

[1] Kayargadde and Martens, "Perceptual Characterization of Images Degraded by Blur and Noise: Experiments," J. Opt. Soc. Am. A, vol. 13, no. 6, pp. 1166–1177, 1996.
[2] Yaacob, Zhang, and Chandler, "On the Perceptual Factors Underlying the Quality of Post-Compression Enhancement of Textures," IS&T Human Vision & Electronic Imaging, 2017.

Notes:

TiO_2 Formation on Ti Substrate by Plasma Immersion Ion Implantation: Morphology, Photocatalytic and Optical Properties

A. Medvids[1,*], L. Grase[1], A. Mychko[1], S. Varnagiris[3], H. Mimura[2], D. Milčius[3], E. Letko[1], S. Gaidukovs[4], A. Pludons[5], P. Onufrijevs[1]

[1]*Institute of Technical Physics, Faculty of Materials Science and Applied Chemistry, Riga Technical University, P. Valdena 3/7, Riga LV-1048, Latvia*

[2]*Research Institute of Electronics, Shizuoka University, 3-5-1, Johoku, Naka-ku, Hamamatsu 432 8011 Japan*

[3]*Center for Hydrogen Energy Technologies, Lithuanian Energy Institute, 3 Breslaujos St., Kaunas, Lithuania*

[4]*Institute of Polymer Materials, Faculty of Materials Science and Applied Chemistry, Riga Technical University, P. Valdena 3/7, Riga LV-1048, Latvia*

[5]*Institute of Silicate Materials, Faculty of Materials Science and Applied Chemistry, Riga Technical University, P. Valdena 3/7, Riga LV-1048, Latvia*

[*]*medvids@latnet.lv*

Plasma Immersion Ion Implantation (PIII) was used to form TiO_2 layer on titanium substrate [1,2]. The influence of PIII treatment time from 1 to 3 hours on properties of TiO_2 layer structure was studied [3]. It was found that at longer treatment time anatase phase crystal concentration in TiO_2 film has increased. Crystalline phases and morphology of the obtained film were characterized by XRD, SEM, AFM and Raman spectroscopy. Photocatalytic decomposition ratio and surface energy in obtained TiO_2 films were evaluated. First order reaction constant increased from 3.2×10^{-3} min $^{-1}$ to 4.2×10^{-3} min^{-1} and surface free energy increased from 39.0 mN/m to 49.5 mN/m with increasing of PIII treatment time [4].

Keywords: Plasma Immersion Ion Implantation, TiO2, anatase phase, photocatalytic activity, surface free energy.

[1] P.K. Chu, Progress in direct-current plasma immersion ion implantation and recent applications of plasma immersion ion implantation and deposition, Surf. Coatings Technol. 229 (2013) 2– 11. doi:10.1016/j.surfcoat.2012.03.073.

[2] W. Jin, P.K. Chu, Surface functionalization of biomaterials by plasma and ion beam, Surf. Coatings Technol. 336 (2018) 2–8. doi:10.1016/j.surfcoat.2017.08.011.

[3] S. Mändl, D. Manova, Modification of metals by plasma immersion ion implantation, Surf. Coatings Technol. (2018). doi:10.1016/j.surfcoat.2018.04.039.

[4] T. Luttrell, S. Halpegamage, J. Tao, A. Kramer, E. Sutter, M. Batzill, Why is anatase a better photocatalyst than rutile? Model studies on epitaxial TiO2 films, Sci. Rep. 4 (2014) 4043. doi:10.1038/srep04043.

Notes:

A Comparison of an Execution Efficiency of the Use of a Skip List and Simple List in a .NET Application

I. Košt'ál*
University of Economics in Bratislava, Faculty of Economic Informatics, Dolnozemská cesta 1, 852 35 Bratislava, Slovakia,
*igor.kostal@euba.sk

A one-way linked list is a dynamic data structure that is used for storing data in applications. It uses the application's memory space very efficiently. The most used version of the one-way linked list is the single level linked list (a simple list). However, there are also multi-level linked lists (called skip lists) that are more complicated for creating, but searching for the required data elements in them is more efficient because they allow us to skip to the correct element in them. There is implementation of skip lists in C programs with simple, unstructured data in their data elements [1, 2]. We have created a C# object-oriented .NET application that uses both lists, a simple and skip list, but with structured data in their data elements. By using our C# application, we want to compare the execution efficiency of the use of these lists, therefore the same structured students' data is stored in the data elements of its simple and skip list. Our C# application is able to carry out basic operations with these data elements of a simple and skip list, such as searching for students (data elements) according to their points for accommodation, their year of birth, their surname and according to their ISIC in both lists, inserting of a new student (a data element) ordered into both lists etc., and simultaneously it is able to measure the execution times of particular operations. By comparing these times we have examined the execution efficiency of these operations in a simple list and in a skip list with different numbers of data elements in the same data set used in both lists. The use of a skip list in the .NET application should be more effective. The results and evaluation of this examination are listed in the paper.

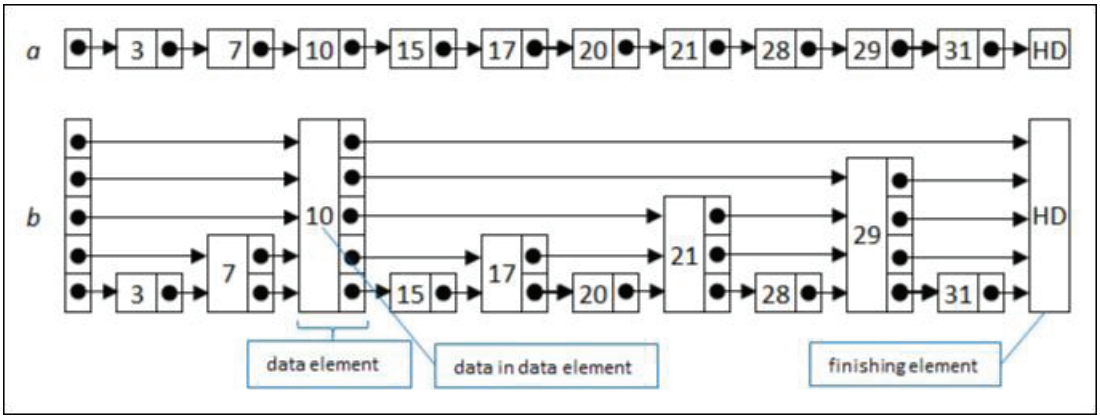

Fig. 1. The simple list (*a*) and the skip list (*b*) with simple, unstructured data in their data elements

Keywords: single level linked list; simple list; multi-level linked lists; skip list; data element.

[1] T. Niemann, "Sorting and Searching Algorithms" epaperpress.com (1999).
[2] W. Pugh, "Skip Lists: A Probabilistic Alternative to Balanced Trees" Communications of the ACM (1990), 33(6).

Notes:

Design and creation of metal-polymer absorbing metamaterials using the vacuum-plasma technologies

I. Semchenko[1,*], S. Khakhomov[1], A. Samofalov[1], D. Slepiankou[1],
V. Solodukha[2], A. Pyatlitski[2], N. Kovalchuk[2], A. Goncharenko[3], and G. Sinitsyn[3]
[1]*Francisk Skorina Gomel State University, Sovyetskaya Str. 104, 246019 Gomel, Belarus*
[2]*JSC "INTEGRAL", Korjenevsky Str. 12, 220108 Minsk, Belarus*
[3] *B.I. Stepanov Institute of Physics, Nezavisimosty Av. 68, 220072 Minsk, Belarus*
**isemchenko@gsu.by*

The paper aimed to create on the basis of three-dimensional bianisotropic elements new absorbing metamaterials and coatings that do not have a reflecting base and are "invisible" on the irradiated side; to study the patterns of interaction of electromagnetic radiation with such metamaterials [1-3].
The unusual properties of metamaterials were experimentally studied mainly in the MHz and GHz ranges, where the resonant metamaterial elements are of millimeter and centimeter sizes. In these cases it is fairly easy to form 3D elements and arrange them in the form of 3D arrays. Currently, there is a clear trend towards the development and investigation of THz metamaterials, since the THz technique is rapidly developing.
To obtain a matched metamaterial impedance, all resonators of a very large array must be tuned very accurately. Among the widely used techniques, only the conventional planar technology (which allows us to form planar elements and their layers) can provide the required sizes and accuracy. In principle, it is impossible to specify the properties of such a metamaterial consisting of planar elements in all three dimensions. Moreover, in most experiments the researchers have to be restricted to one layer of elements (i.e., metamaterial monolayer) because of the restrictions of the planar technology, which hinders the study of volumetric electromagnetic properties. At the same time, volumetric metamaterials with specified three-dimensional electromagnetic properties are necessary for almost all current metamaterial applications.
Another way of 3D metamaterial design is possible. Using planar technology you can create the planar elements and then make the 3D metamaterial from planar stripes. To find optimal parameters for placing rectangular omega elements in a cell and cells in a structural array, the finite element method was modeled on the properties of an absorbing low reflecting two-dimensional array at various distances between the rectangular omega elements in the cell and between cells in the structural array.
As a vacuum-plasma technique for depositing titanium on a substrate, the magnetron sputtering method was chosen. Omega elements of rectangular shape will be made of titanium applied to polyamide. The findings can be used for theoretical and experimental studies of artificial composite absorbing media with inclusions of various shapes, in the development of microwave absorbers with improved properties.

[1] I. V. Semchenko, S. A. Khakhomov, A.L. Samofalov, M. A. Podalov, V. A. Solodukha, A.N. Pyatlitski, N.S. Kovalchuk. Omega-Structured Substrate-Supported Metamaterial for the Transformation of Wave Polarization in THz Frequency Range. Recent Advances in Technology Research and Education. INTER-ACADEMIA 2017, Ed. by Luca D., Sirghi L., Costin C., Advances in Intelligent Systems and Computing, Vol. 660, Springer. – 2018. – P.72 – 80.
[2] I. V. Semchenko, S. A. Khakhomov, A.L. Samofalov, M.A. Podalov, Q. Songsong. The effective optimal parameters of metamaterial on the base of omega-elements, Recent Global Research and Education: Technological Challenges / Ed. by Ryszard Jablonski and Roman Szewczyk, Advances in Intelligent Systems and Computing, Vol. 519, Springer. – 2017. – P. 3 – 9.
[3] I. V. Semchenko, S. A. Khakhomov, V. S. Asadchy, S. V. Golod, E. V. Naumova, V. Ya. Prinz, A. M. Goncharenko, G. V. Sinitsyn, A. V. Lyakhnovich, V. L. Malevich. Investigation of electromagnetic properties of a high absorptive, weakly reflective metamaterial substrate system with compensated chirality, Journal of Applied Physics. 2017. V.121, №1. p. 015108.

Notes:

Investigation of X-ray attenuation properties in 3D printing materials used for development of head and neck phantom

J. Laurikaitienė[1,2,*], J. Puišo[1], E. Jaselskė[1,3]

[1]*Kaunas University of Technology, Faculty of Mathematics and Natural Sciences, Studentų g. 50, LT-51368 Kaunas, Lithuania*

[2]*Hospital of Oncology, Hospital of Lithuanian University of Health Sciences Kauno klinikos, Volungių g.16, LT-45433 Kaunas, Lithuania*

[3]*Hospital of Lithuanian University of Health Sciences Kauno klinikos, Eivenių g. 2, LT-50009 Kaunas, Lithuania*

[*]*jurgita.laurikaitiene@ktu.lt*

3D printing technologies became an integral part of the medical environment due to their ability to produce relevant copies of human organs and tissues. This feature can be used by developing of radiotherapy/radiology phantoms for patient dose verification thus providing an excellent possibility for individualization of irradiation procedure.

X-ray attenuation properties of four different 3D printing materials (PLA, ASA, PETG and HIPS) thought for phantom construction. Irradiation of samples printed in ZORTRAX300 3D printer was performed in X-ray therapy unit GULMAY D3225; peak voltage of 120 kV was applied. Multipurpose semiconductor detector BARACUDA was used for the assessment of X-ray attenuation in irradiated samples. Experimental results were verified with the results obtained using XCOM data based simulations. It was found, that X-ray attenuation properties of investigated materials were similar to those estimated for thyroid gland, brain, muscle and skin, however differed significantly from attenuation properties in bone and teeth, which are present in the head and neck region and play an important role in attenuation of X-rays in this anatomic region during irradiation procedure.

Keywords: 3D printing materials, Attenuation coefficients, Phantom.

Notes:

Application of artificial neural networks to the analysis of alcohol addiction

K. Urbaniak[1,*] and K. Lewenstein[2]
[1]*Politechnika Warszawska, Wydział Administracji i Nauk Społecznych, Warszawa, Polska*
[2]*Politechnika Warszawska, Wydział Mechatroniki, Warszawa, Polska*
[*]*k.urbaniak@ans.pw.edu.pl*

The article presents the preliminary results of research on the possibilities of using artificial neural networks in the diagnosis of alcohol disease based on the analysis of psychophysical features [1-6]. The research was undertaken in close cooperation with the medical community, including a psychiatry doctor specializing in the diagnosis and treatment of alcohol addiction. This resulted in a verified material that was prepared and described by a specialist physician characterizing the behavioral and physiological properties of people addicted to alcohol and healthy. Processed to digital form (mostly in bit form) were directly inserted into the artificial MLBP [7] neural network for its learning and testing. Initially, all features describing a given person, i.e. 64 parameters, were used to teach and test the MLBP neural network. The obtained test result at the level of 95%, consisting in classifying test cases to one of two classes (0 - no addiction, 1 - alcohol addiction) unambiguously indicates the linear separability of features and very good classification properties of neural networks.
Research is just beginning. The main objective of the study is to identify artificial neural networks as a tool to support the health status of addicts and alcohol abusers.
Traditional parameters will be analyzed and interpreted [5]. Further studies will focus on the process of optimizing the vector of features, ie, the process of selecting the characteristics best describing the particular condition of the patient [1-3]. The artificial neural networks such as MLBP will be used to evaluate feature vectors.

[1] O. Savola, O. Niemela, M. Hillbom Blood alcohol is the best indicator of hazardous alcohol drinking in young adults and working-age patients with trauma. Alcohol Alcohol. (2004); 39: 340–345.
[2] JP. Allen, RZ. Litten. The role of laboratory tests in alcoholism treatment. J. Subst. Abuse Treat. (2001); 20: 81–85.
[3] O. Niemela, Biomarkers in alcoholism. Clin. Chim. Acta (2007); 377: 39–49.
[4] F. Musshoff, Chromatographic methods for the determination of markers of chronic and acute alcohol consumption. J. Chromatogr. B Analyt. Techno. Biomem. Life Sc. 2002; 781: 457–480.
[5] BT. Woronowicz. Bez tajemnic o uzależnieniach i ich leczeniu. Warszawa: Instytut Psychiatrii i Neurologii, (2001).
[6] PC. Sharpe, Biochemical detection and monitoring of alcohol abuse and abstinence. Ann. Clin. Biochem. (2001); 38: 652–664.
[7] S. Osowski, Sieci neuronowe w ujęciu algorytmicznym. WNT (1996).

Notes:

Two-photon fluorescent microscopy for 3D dopant imaging in wide bandgap semiconductors

A. Al-Tabich[1,2], W. Inami[1], Y. Kawata[1] and R. Jablonski[2,*]
[1]*Graduate School of Engineering, Shizuoka University,3-5-1, Johoku, Naka, Hamamatsu 432-8561, Japan*
[2]*Faculty of Mechatronics, Warsaw University of Technology, Sw. A. Boboli 8, Warsaw 02-525, Poland*
[*]*r.jablonski@mchtr.pw.edu.pl*

This paper presents a method of three-dimensional imaging of dopants in wide band gap semiconductors by two-photon fluorescence microscopy. Tightly focused light beam radiated by titanium-doped sapphire laser is used to obtain two-photon excitation of selected area of the semiconductor sample. Photoluminescence intensity of a specific spectral range is selected by optical band pass filters and measured by photomultiplier tube. Reconstruction of specimen image is done by scanning the volume of interest by piezoelectric positioning stage and measuring the spectrally resolved photoluminescence intensity at each point.

Notes:

Ion Mobility Spectrometry detection of corona discharge decomposition of phthalates

B. Michalczuk, L. Moravský, and Š. Matejčík*
Comenius University, Faculty of Mathematics, Physics and Informatics, Bratislava, Slovakia
*matejcik@fmph.uniba.sk

For monitoring of plasma decomposition of VOC's detection of very low concentration of molecules is very important issue. Very promising technique appears Ion Mobility Spectrometry (IMS), which offers fast and ultrasensitive detection [1-6].
In present paper we demonstrate the ability of IMS to detect the dimethyl phthalate (DMP) and its isomers dimethyl isophthalate (DMIP) and dimethyl teraphthalate (DMTP) with very low vapor pressures of 0.304 Pa, 0.099 Pa and 0.01 Pa at 25°C respectively. IMS has fast response time (<1s) and sufficient spectral resolution to separate these isomers. These parameters make IMS a suitable instrument for online monitoring of these compounds. The phthalate vapors were mixed with ambient air at atmospheric pressure and this mixture was introduced in small experimental corona discharge (CD) reactor. Decomposition of DMP was carried out in CD reactor of wire to cylinder geometry, in positive polarity and U = 6.7kV, I = 350-650μA. The flow rate of the sample gas was 5 sccm. We are going to present the first results. Application of CD decomposition on the DMTP resulted in decrease of the DMP signal in IMS spectrum from the original amplitude for nontreated vapors (black) to lower amplitudes (red and green) for CD treated gas. The amplitudes correspond to the relative DMP concentrations in the range from 1 ppm to 100 ppb.

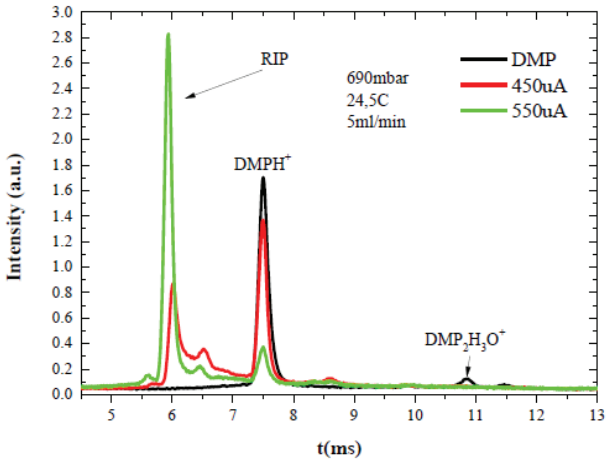

Fig. 1. IMS spectra of DMP after degradation by corona discharge at various discharge current

Acknowledgment: This work has been supported by European Union's Horizon 2020 research and innovation programme under the Marie Skłodowska-Curie grant agreement No 674911 and innovation programme under grant agreement No 692335, additionally Slovak Research and Development Agency Project Nr. APVV-15-0580 and the grant agency VEGA, project Nr. VEGA-15-089 support is acknowledget.

[1] S. J. Valentine, X. Y. Liu, M. D. Plasencia, A. E. Hilderbrand, R. T. Kurulugama, S. L. Koeniger, D. E. Clemmer, Expert Rev. Proteom. 2 (2005) 553–565.
[2] S. L. Koeniger, S. J. Valentine, S. Myung, M. Plasencia, Y. J. Lee, D. E. Clemmer, J. Proteome Res. 4 (2005) 25–35.
[3] R. A. Sowell, S. L. Koeniger, S. J. Valentine, M. H. Moon, D. E. Clemmer, J. Am. Soc. Mass Spectrom. 15 (2004) 1341–1353.
[4] C. Wu, W. F. Siems, J. Klasmeier, H. H. Hill,. Anal. Chem. 72 (2000) 391–395
[5] J. A. McLean, B. T. Ruotolo, K. J. Gillig, D. H. Russell, Int. J. Mass Spectrom. 240 (2005) 301–315.
[6] M.F. Jarrold, Annu.Rev.Phys. Chem. 51 (2000) 179–207.
Notes:

Thermal convection of a phase-changing fluid

Mashiko[1,*], Y. Inoue[1], Y. Sakurai[1], and I. Kumagai[2]
[1]*Shizuoka University, 3-5-1 Johoku, Naka-ku, Hamamatsu, Japan*
[2] *Meisei University, 2-1-1, Hodokubo, Hino, Tokyo, Japan*
[*]*mashiko.takashi@shizuoka.ac.jp*

Thermal convection, which arises in a fluid cooled from the top and heated from the bottom, has been studied for more than a century, from both the viewpoints of basic physics and application potentiality. Vast knowledge has been accumulated for simple model systems of a single-phase fluid; state transitions, heat transfer, flow structures, fluctuation properties, and so on. In real situations, however, thermal convection sometimes involves phase transition of the fluid, which interacts with and affects the convection behaviors [1]. Experimental studies have been done to investigate such systems, but are limited in number and to particular transitions like the one between ice and water [2]. Here we report a novel type of experiment, in which the transition characteristics are controllable and thus a systematical investigation of the effect of phase transition on thermal convection is enabled.

Our approach is to utilize a thermosensitive gel, which exhibits volume phase transition with changing temperature. To be specific, we use the fluid of the mixture of pure water and mashed gel of poly(N-Isopropyl-Acrylamide) (PNIPAM), which swells by absorbing water below a critical temperature T_c, while it contracts by discharging water above T_c. The key point is that the swelling ratio, as well as T_c, can be controlled by varying the conditions of PNIPAM synthesis, and thus we can conduct experiments using fluids with different degrees of phase transition.

The experimental apparatus to fill the fluid is a container of 20 cm × 20 cm × 1 cm, consisting of acrylic resin sidewalls and top and bottom copper plates (Fig. 1). The temperatures of the water-cooled top and electrically-heated bottom plates are kept at T_{top} and T_{bot}, respectively ($T_{top} < T_c < T_{bot}$). The flow is visualized by the use of a laser sheet, fluorescent particles mixed with the fluid, and a low-pass filter, so that particle image velocimetry (PIV) with high signal-to-noise ratio can be conducted.

We have so far observed some interesting phenomena such as the segregation of the fluid into high-velocity and low-velocity regions, being reminiscent of the mantle convection of the Earth. In the typical snapshot of the visualized flow and the corresponding velocity field obtained by PIV shown in Fig. 2, we notice some low-velocity regions such as an elliptical area in the top and a triangle area in the left, which are surrounded by high-velocity regions. These regions are spatially fixed and stable for a long time. This segregation presumably results from the multi-phase property of the fluid.

We are trying to interpret these observations in terms of the fluid properties such as the shearthinning behavior, which we found in rheological measurements. Also, we are beginning a series of experiments in which the degree of phase transition is systematically changed.

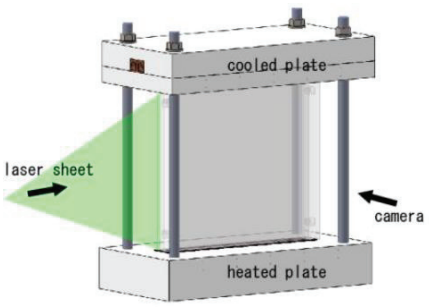

Fig. 1. Experimental apparatus

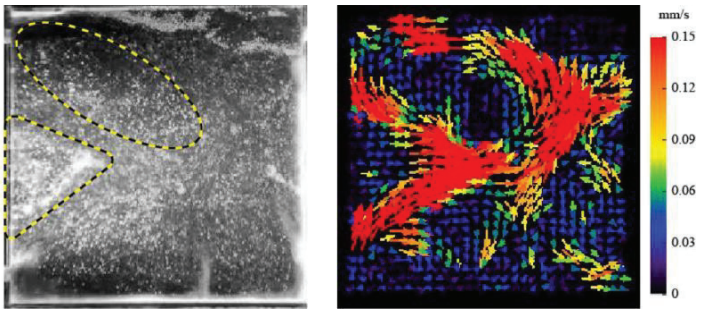

Fig. 2. Visualized flow (left) and velocity field (right)

Keywords: Thermal convection, Phase transition, Thermosensitive gel.

[1] P. Machetel and P. Weber, Nature 350 (1991), 55-57.
[2] R. S. Tankin and R. Farhadieh, Int. J. Heat Mass Transfer 14 (1971), 953-956.

Notes:

Automatic identification of the kidney shape in CT images

T. Les[1,*], T. Markiewicz[1,2], M. Dziekiewicz[2], M. Lorent[2]
[1]*Warsaw University of Technology, Warsaw, Poland*
[2]*Military Institute of Medicine, Warsaw, Poland*
**lest@ee.pw.edu.pl*

The article presents an innovative method of kidney recognition in computed tomography (CT) images. Kidney cancer is one of the most common causes of death. Over 300,000 people die per year from this disease. A fast and correct diagnosis of neoplastic lesions in computed tomography images allows to choose the proper method of treatment. This article presents an innovative and unique methods of kidney recognition in CT images. The proposed methods are based on morphological operations, shape analysis, geometrical coefficients calculations as well as the directional operation of flood fill with automatic selection of the stop criterion. The article presents also an innovative method of closing the boundary of an unrecognized kidney. Application of fast and effective algorithms for an automatic kidney shape recognition allows to make a 3D reconstruction of the kidney model. The use of algorithms to improve visualization of CT scans allows more accurate diagnosis by specialists. The system for supporting kidney cancer diagnosis presented in the article has been tested to assess the quality of kidney shape recognition. The recognition results of the shape of the kidney by the automatic system are comparable to the results obtained by a human expert and the accuracy of the diagnosis is at the level of 86%. Despite the difficult task, it was possible to obtain satisfactory results of the kidney shape recognition.

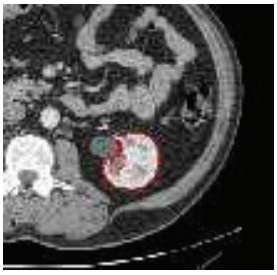

Fig. 1. An exemplary CT image illustrating the difficulty of the kidney diagnosis task

Keywords: Flood fill, shape analysis, geometrical coefficients, brightness correction.

[1] Lin D, Lei C, Hung S., "Computer-Aided Kidney Segmentation on Abdominal CT Images", IEEE transactions on information technology in biomedicine, vol. 10, no. 1, january 2006.
[2] D. Trevathan-Ramirez, "Innovations in breast disease diagnosis," Radiology Technol., vol. 70, no. 2, pp. 197–203, 1998.
[3] B. Tsagaan, A. Shimizu, H. Kobatake, and K. Miyakawa, "An automated segmentation method of kidney using statistical information," in Proc. Medical Image Computing and Computer Assisted Intervention, vol. 1, 2002, pp. 556–563.
[4] B. Tsagaan, A. Shimizu, H. Kobatake, K. Miyakawa, and Y. Hanzawa, "Segmentation of kidney by using a deformable model," in Int. Conf. Image Processing, vol. 3, Thessaloniki, Greece, 2001, pp. 1059–1062.
[5] Saii M, Kraitem Z. "Automatic Detection and Segmentation of Kidneys in Magnetic Resonance Images Using Image Processing Techniques", Biomedical Statistics and Informatics. Vol. 2, No. 1, 2017, pp. 22-26. doi: 10.11648/j.bsi.20170201.15.
[6] T. Les, T. Markiewicz, S. Osowski, W. Kozlowski, M. Jesiotr, "Fusion of FISH image analysis methods of HER2 status determination in breast cancer", Expert Systems with Applications Volume 61, 1 November 2016, Pages 78-85.

Notes:

The Flip-Side of Academic English (AE)

D. Chandler[2] B. V. Wilkinson[1,*] T. Mashiko[2]
Shizuoka University 1-3-5 Johoku, Naka-Ku Hamamatsu, Japan 432-8011
[*]vwilk@inf.shizuoka.ac.jp

When we presented "Flipping Out in Japan" at iA2017 in Iasi, Romania, we positively reported that the atmosphere in the work-shop "flipped classroom" was dynamic and awake. The student teams created conference style Poster Presentations in 4 three week cycles. The two groups, the electrical and the electronic engineering (EEE) group on Wednesday afternoon and Friday morning were designated as experimental and control. Among the questions raised while our paper was under review and at the presentation itself: Was there any empirical evidence of improvement of language? Were the two groups properly treated as control and experimental populations? The answer to both of these questions was subjective and impressionistic. What we did on Wednesday easily blended into the Friday class. The "coach/mentor" who was supposed to add a dimension to the experimental group was not entirely satisfactory. Our final exam results were unclear, and in one part of the test showed the control group to be more coherent than the Experimental group.

We have another chance to run the experiment, to teach required AE for 3rd year EEE students. We intuitively feel that we are on the right track, but we need to re-examine our premises and the goals of our research. We noted that many such AE classes rely on vocabulary learning strategies (VLS) and, as far as we were able to determine, such classes rely word recall rather than context mastery. The "flipped classroom" is all about context, the engineering mind-set, and the routine of creating poster presentations with a team. Since the control group did well on the final tests and the atmosphere of the class was altogether superior to the "traditional format" that we tried in 2016, we determined that we would treat the control in the basically the same manner as we did in 2017 with some tweaks in scheduling. We plan to make significant changes to the definitions and procedures in the experimental group. We keep the coach/mentor, a senior engineering student, to be the coach of the 12/13 team leaders in the experimental group. We plan to use vocabulary and principles from project based learning (PBL), utilizing the concepts of *group dynamics* and *group cohesion* from the theory of *group process*. We also utilize input from Jean Lave and Etienne Wenger "Situated Learning: Legitimate Peripheral Participation"[1] where the concept "Communities of Practice" (CoP) was also introduced. Finally, Paul Grice's "Cooperative Principle" [2], which developed in the linguistic domain of pragmatics, adds a dimension to the theory that the power of an orderly team engaged in work they choose and enjoy will result in strong performance in presentation skills, coherent teams, and we hope appropriate vocabulary for the task at hand.

Keywords: situated learning, group dynamics, project based learning, Cooperative Principle.

[1] Tuckman, Bruce W. "Developmental sequence in small groups," Psychological Bulletin #63 (1965).
[2] Lave, Jean and Etienne Wenger. Situated Learning: Legitimate Peripheral Participation. (1991).
[3] Grice, H. Paul. Logic and Conversation. [In: Syntax and Semantics, Vol. 3, Speech Acts, ed. by Peter Cole and Jerry L. Morgan. New York: Academic Press 1975, 41–58].

Notes:

ZnO/Me Sol-Gel Film for Solar Sells and Photodetectors

S.A. Khakhomov[1], A.V. Semchenko[1], V.V. Sidsky[1,*], V.V. Malyutina-Bronskaya[2], S.A. Soroka[2], V.B. Zalesskiy[2], N.S. Kovalchuk[3], A.N. Pyatlitski[3], V.A. Solodukha[3]
[1]*F. Skorina Gomel State University, Sovetskaya 104, Gomel, 246019, Belarus*
[2]*SSPA "Optics, optoelectronics and laser technology", Nezalezhnasti av. 68/1, Minsk, 220072, Belarus*
[3]*JSC "INTEGRAL", Korjenevsky str., 12, Minsk, 220108, Belarus*
**sidsky@gsu.by*

The numerous studies of thin films and nanomaterials based on ZnO obtained by various methods for use in optoelectronics, volumetric and other fields are investigated. In recent time the interest increased in the use of ZnO as material for optoelectronic devices with wide range of applications working in the visible and short-wave wavelength ranges. This material is already used in transparent thin-film transistors, photodetectors, light emitting diodes (LEDs) and laser diodes [1]. The attractive properties of zinc oxide, such as high transmittance in the visible spectral range and good electrical conductivity, are on the grounds of the stoichiometry of the film and the presence of internal crystal defects [2]. The introduction of various impurities into the crystal structure of the film leads to the change in both optical and electrical properties of the film.

The properties of ZnO:Me:RE^{3+} films synthesized by sol-gel method and ZnO:Me:RE^{3+} heterostructures on the substrate of single-crystal silicon and glass are presented. These structures are photosensitive to the IR and visible wavelength range. High photosensitivity confirms the prospects of their use in optoelectronic devices, in particular for the creation of active layers of solar cells.

Measurements of the current-voltage characteristics (VAC) on an E7-20 immittance meter at room temperature were made. The I-V measurements were carried out both in the dark and under illumination with an incandescent lamp and an IR source.

The maximum photosensitivity for the ZnO:Me:RE^{3+}/Si structure appears for all films in the presence of bias voltage. The maximum sensitivity to IR radiation was observed for the ZnO:Al:Er^{3+}/Si structures, and to the visible region for ZnO:Ag:Eu^{3+}/Si structures. This effect can be attributed to the fact that the trivalent Eu^{3+} ions cause the luminescence in the visible range due to optical transitions, and the trivalent Er^{3+} ions in the infrared region of the spectrum.

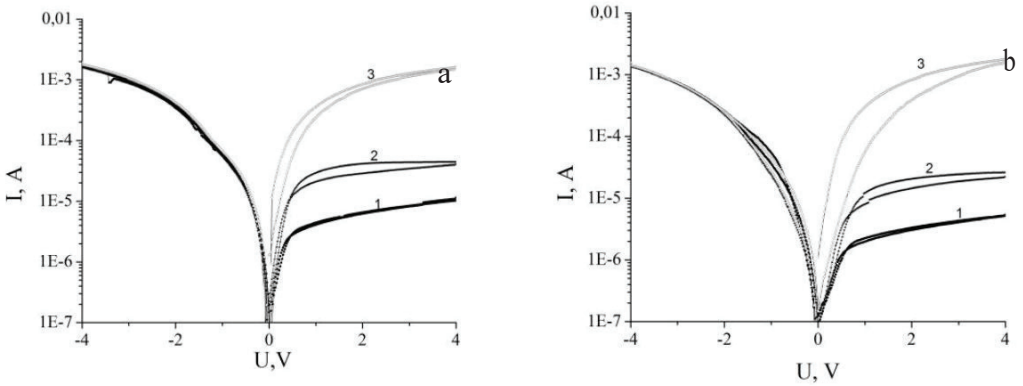

Fig. 1. Volt-ampere characteristic of ZnO: Al: Eu^{3+} (a) and ZnO: Ag: Eu^{3+} (b) films on silicon substrate. Light sources: 1- without lighting (dark), 2-IR source, 3-incandescent lamp

Keywords: sol-gel, current-voltage characteristics, transparent conductive ZnO:Me –films, hydrophobic properties, photosensitivity.

[1] Ü. Özgür, Ya.I.Alivov, C.Liu. J. Appl. Phys. 98 (2005), 041301.
[2] D. Sahu, B. S. Acharya, N. R. Panda. AIP Conference Proceedings 1728 (2016), 020165.

Notes:

iA2018 - Conference Programme

Monday, September 24			Tuesday, September 25			Wednesday, September 26		Thursday, September 27
	Hall 1	Hall 2		Hall 1	Hall 2		Hall1	
8:00-9:00	Registration							9:00-20:00 Conference Excursion
9:00-9:30	Opening Ceremony		9:00-9:30	Registration		9:00-9:30	Registration	
9:30-10:00	**MO-1** H. Mimura		9:30-10:00	**TU-1** V. Marozas		9:30-10:00	**WE-1** K. Murakami	
10:00-10:30	**MO-2** R. Raišutis		10:00-10:30	**TU-2** D. Adlienė		10:00-10:30	**WE-2** A. Galdikas	
10:30-10:50	*Coffee break*		10:30-10:50	*Coffee break*		10:30-10:50	*Coffee break*	
10:50-11:10	**MO-3** K. Hara	**MO-8** J. Kondoh	10:50-11:10	**TU-3** Y.Oya	**TU-8** Y.Okano	10:50-12:30	Special Poster Session for iA Young Researchers (iAY) – 5 min oral communication	
11:10-11:30	**MO-4** A.Medvids	**MO-9** B.Rakos	11:10-11:30	**TU-4** M. M. Sychov	**TU-9** S.Matsuda			
11:30-11:50	**MO-5** M.Dobromir	**MO-10** A. Mosavi	11:30-11:50	**TU-5** M.Zhao	**TU-10** N. Kh. Gomidze			
11:50-12:10	**MO-6** K.Zelenska	**MO-11** M. F.Kashif	11:50-12:10	**TU-6** C. Jin	**TU-11** G.Ilewicz			
12:10-12:30	**MO-7** S.Meenachi-sundaram	**MO-12** A.Makiuchi	12:10-12:30	**TU-7** S. Wang	**TU-12** T. Miyake			
12:30-12:35	**Conference photo**							
12:35-13:30	*Lunch*		12:30-13:30	*Lunch*		12:30-13:30	*Lunch*	
13:30-13:50	**MO-13** Y. Ono	**MO-17** H. Ikeda	13:30-13:50	**TU-13** D. Moraru	**TU-16** V. A. Wilkinson	13:30-15:30	Poster session (Hotel lobby)	
13:50-14:10	**MO-14** S. Tripathi	**MO-18** V. Gnatyuk	13:50-14:10	**TU-14** A. Mykytiuk	**TU-17** C. Pascual			
14:10-14:30	**MO-15** D. Moraru	**MO-19** P.Onufrijevs	14:10-14:30	**TU-15** M. Dobromir	**TU-18** B. Tusor			
14:30-14:50	**MO-16** M.Murugan-than	**MO-20** J. Mruk						
14:50-15:00	*Bus*		14:30-15:00	*Bus*				
15:00-17:30	*Excursion to SANTAKA Integrated Science, Studies and Business Centre (Valley)*		15:00-19:00	*Excursion Kaunas at a glance*		15:30-16:00	Conference closing	
						16:00-17:00	iA Committee Meeting	
18:00-20:00	*Dinner*		19:00-21:00	*Dinner*		19:00-22:00	*Gala Dinner*	